AD-A160 707 ESTIMATING RADIATED THERMAL ENVIRONMENTS FROM ALUMINUM-LOX (LIQUID OXYGEN..(U) SCIENCE AND ENGINEERING ASSOCIATES INC SALEM MA B S CHAMBERS

UNCLASSIFIED 15 DEC 84 SEA-62-00-Q:01 DNA-TR-85-3 F/G 20/13 NL

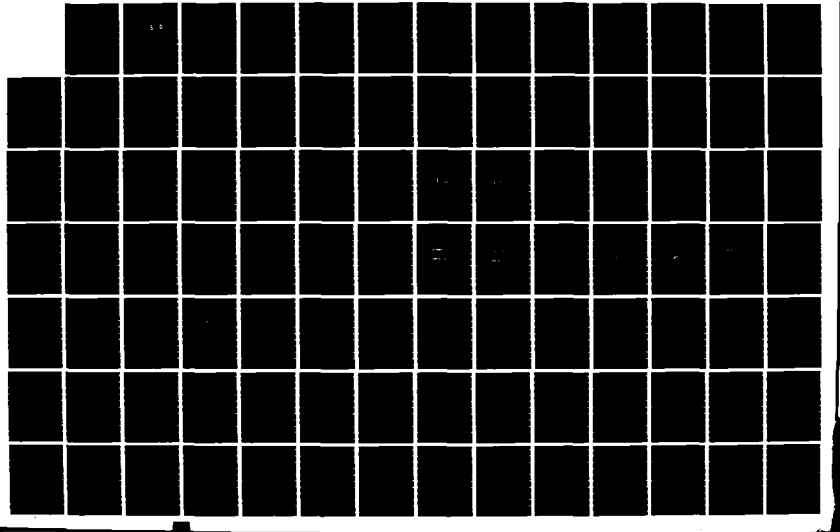

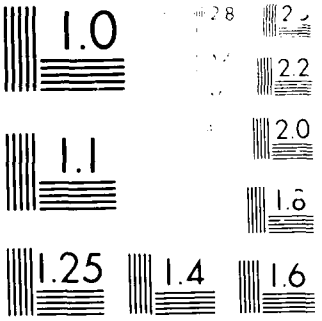
1.0
2.8
2.2
2.0
1.1
1.8
1.25
1.4
1.6

DNA-TR-85-3

(12)

ESTIMATING RADIATED THERMAL ENVIRONMENTS FROM ALUMINUM-LOX THERMAL RADIATION SIMULATORS

Burton S. Chambers III
Science and Engineering Associates, Inc.
76 Lafayette Street
Salem, MA 01970

15 December 1984

Technical Report

CONTRACT No. DNA 001-81-C-0020

Approved for public release;
distribution is unlimited.

THIS WORK WAS SPONSORED BY THE DEFENSE NUCLEAR AGENCY
UNDER RDT&E RMSS CODE B345081466 G54AAXYX00001 H2590D

Prepared for
Director
DEFENSE NUCLEAR AGENCY
Washington, DC 20305-1000

UNCLASSIFIED
SECURITY CLASSIFICATION OF THIS PAGE

REPORT DOCUMENTATION PAGE

Form Approved
OMB No. 0704-0188
Exp. Date: Jun 30, 1986

1a REPORT SECURITY CLASSIFICATION UNCLASSIFIED	1b RESTRICTIVE MARKINGS
2a SECURITY CLASSIFICATION AUTHORITY	3 DISTRIBUTION / AVAILABILITY OF REPORT Approved for public release; distribution is unlimited.
2b DECLASSIFICATION / DOWNGRADING SCHEDULE N/A since UNCLASSIFIED	
4 PERFORMING ORGANIZATION REPORT NUMBER(S) SEA 62-00-Q:01	5 MONITORING ORGANIZATION REPORT NUMBER(S) DNA-TR-85-3
6a NAME OF PERFORMING ORGANIZATION Science and Engineering Associates, Inc. 6b OFFICE SYMBOL (If applicable)	7a NAME OF MONITORING ORGANIZATION Director Defense Nuclear Agency
6c ADDRESS (City, State, and ZIP Code) 76 Lafayette Street Salem, MA 01970	7b ADDRESS (City, State, and ZIP Code) Washington, DC 20305-1000
8a NAME OF FUNDING / SPONSORING ORGANIZATION 8b OFFICE SYMBOL (If applicable)	9 PROCUREMENT INSTRUMENT IDENTIFICATION NUMBER DNA 001-81-C-0020
8c ADDRESS (City, State, and ZIP Code)	10 SOURCE OF FUNDING NUMBERS

PROGRAM ELEMENT NO	PROJECT NO	TASK NO	WORK UNIT ACCESSION NO
62715H	G54AAXY	X	DH005106

11 TITLE (Include Security Classification)
ESTIMATING RADIATED THERMAL ENVIRONMENTS FROM ALUMINUM-LOX THERMAL RADIATION SIMULATORS

12 PERSONAL AUTHOR(S)
Burton S. Chambers III

13a TYPE OF REPORT	13b TIME COVERED	14 DATE OF REPORT (Year, Month, Day)	15 PAGE COUNT
Technical	FROM 801020 TO 820813	1984, December 15	190

16 SUPPLEMENTARY NOTATION
This work was sponsored by the Defense Nuclear Agency under RDT&E RMSS Code B345081466 G54AAXYX00001 H2590D.

17 COSATI CODES			18 SUBJECT TERMS (Continue on reverse if necessary and identify by block number)	
FIELD	GROUP	SUB-GROUP		
14	2		Nuclear Weapons Effects	TRS Free-Field Data
20	13		Thermal Radiation Simulators(TRS)	MILL RACE
			Simulation of Thermal Radiation	Airblast/TRS Interference

19 ABSTRACT (Continue on reverse if necessary and identify by block number)

This report describes the early modeling work done to estimate the radiated thermal environment generated by Aluminum-LOX thermal radiation simulators. The ability to calculate the environment produced by these simulators is necessary to effectively plan combined airblast/thermal simulations of nuclear weapon effects. Included are: (1) an overview of the modeling effort and how a model is calibrated, (2) comparisons with MILL RACE results, (3) the models, and (4) preliminary work on airblast/TRS interference. The primary result of the effort was the development of a model that potentially can accurately predict the environment from a TRS. It was also concluded that much more effort must go into making repeatable and reliable TRS simulators, and a significant calibration program is then warranted.

20 DISTRIBUTION / AVAILABILITY OF ABSTRACT	21 ABSTRACT SECURITY CLASSIFICATION
☐ UNCLASSIFIED/UNLIMITED ☒ SAME AS RPT ☐ DTIC USERS	UNCLASSIFIED

22a NAME OF RESPONSIBLE INDIVIDUAL	22b TELEPHONE (Include Area Code)	22c OFFICE SYMBOL
Betty L. Fox	(202) 325-7042	DNA/STTI

DD FORM 1473, 84 MAR 83 APR edition may be used until exhausted
All other editions are obsolete

SECURITY CLASSIFICATION OF THIS PAGE
UNCLASSIFIED

6a. NAME OF PERFORMING ORGANIZATION (Continued)

Under purchase order (No. 15-840006 65) from:

Science Applications Intl Corp.

6c. ADDRESS (Continued)

P.O. Box 1303
McLean, VA 22102-1303

18. SUBJECT TERMS (Continued)

Modeling of Simulated Environments
Airblast/Thermal Synergistic Effects

SUMMARY

The work reported herein was conducted in support of the use of thermal radiation simulators (TRS) on the Defense Nuclear Agency (DNA) high explosive (HE) event MILL RACE. The type of TRS used on MILL RACE was the so-called flame or torch TRS, which consists of a set of nozzles each burning aluminum powder in sprayed liquid oxygen (LOX).

Guidance and technical assistance were provided to DNA Field Command and in turn to any MILL RACE experimenters, who would be utilizing the TRS. Models of the thermal radiation were developed and then estimates were made of the expected thermal environments at various locations. New TRS data were incorporated into a data base which was then used to improve the model predictions. Recommendations were made indicating where calorimeters should be placed in order to best support the modeling effort. Unfortunately, other requirements, such as the determination of proper operating conditions for the TRS nozzles, generally precluded use of the recommendations concerning data collection for improving the models.

In addition to the estimation of thermal environments, this effort contained a task to investigate interference to the HE-generated air blast from thermal effects generated by the TRS units. Of primary concern were effects that would adversely affect planned air blast loading. If the interference effects were considered to be significant, suggested alternative approaches were to be made toward meeting the objectives of the combined thermal-air blast experiments.

Finally, the models were again refined as a part of this effort, after the MILL RACE event occurred. The objective of this latter task was to improve the model developed earlier by incorporating two modifications: (1) represent each flame as an inverted cone rather than a right circular cylinder, and (2) account for the change in view angle resulting from flame obscuration.

This effort produced a number of results and conclusions during the course of estimating the radiated thermal environments from aluminum-liquid oxygen (LOX) thermal radiation simulators (TRS). Most importantly, it produced models of TRS generated peak flux that represent those same environments in the field. The inverted cone model is the best developed to date when flame obscuration and an accurate treatment of view angle are included.

It is now possible to use one calibration of the inverted cone model to represent all nozzle arrangements used thus far. Consequently, the data base may now be of sufficient size to allow certain statistical inferences to be made about the inherent variability of using the TRS in the field.

In the area of TRS-Air Blast interference, the results are less clear. The effort conducted is largely incomplete, and additional work is required to resolve the issues. Calculations indicate that incipient blowoff of ground material was probable on MILL RACE. Other calculations have also indicated that incipient ground blowoff is probable at the DNA TRS site at Kirtland Air Force Base (KAFB) in Albuquerque, New Mexico. What looks like the "steam porch" phase of ground blowoff has been seen in the photographs taken at the TRS site. The effect of any resultant hot thermal layer immediately above the ground on air blast propagation was not investigated.

It was also concluded that modeling a TRS flame as merely a hot clean flame, i.e. one containing no particulates, will not accurately simulate results from MISERS BLUFF. During MISERS BLUFF the overpressure was reduced on one of the targets placed immediately behind the TRS units. Numerical calculations performed for overpressures up to 10 psi and for flame widths up to two meters wide demonstrated that other effects will need to be considered. Additional work is recommended to quantitatively understand the influence of particulates on the effect seen during MISERS BLUFF.

Our recommendations in the area of TRS modeling are that much experimental work and some modeling work need to be done. In the area of TRS-airblast interference, our recommendation is to determine how well the current

interference mitigation techniques will find acceptance in the nuclear survivability and vulnerability community. The current technique is to fire the TRS early enough to allow the flame and its combustion products to rise above the target so that they will not interfere with the air blast. For some nuclear scenarios, this approach will introduce a significant cooling period before air blast arrival.

A substantially more exhaustive and careful effort to obtain calorimeter data needs to be performed. This recommendation is made with the knowledge that the data base essentially doubled during September 1982 when DNA and SAI conducted a Calibration Program of the DNA TRS site at Kirtland AFB. Even with those data, significant additional data obtained under more controlled conditions is necessary if the community is to be expected to place great reliance on modeled results.

More thorough data interpretation and analysis is recommended. At least four individuals have read the "peak" flux off oscilliscope traces that have been entered into the DNA data base. Now that these data are being recorded digitally, the detailed temporal waveforms can be made available for meaningful data analysis. There has been no consistent approach applied to evaluating these data. In some cases data were withheld as not being representative.

The TRS development to date has been geared toward improving the flame generation. Little emphasis has been given to evaluating reliability or repeatability. We strongly recommend that one design be fixed for future use in the DNA HE program, and that that design be calibrated under realistic field conditions.

Finally, we regretably observe that much difficulty in accessing the DNA-provided computational facilities at KAFB made it virtually impossible to continue the investigation of TRS-air blast interference. It is recommended that DNA, not a contractor, more closely monitor difficulties that contractors are having when using government furnished equipment. Whether this would lead to any improvement in throughput is debatable; nevertheless, we feel it is

important to improve this communication of the problems we have been having, so that DNA management might have representative information available when decisions are made.

PREFACE

The work reported herein was performed by Science Applications, Inc. (SAI) for Defense Nuclear Agency (DNA) under DNA contract No. 001-81-C-0020 during the period 20 October 1980 to 13 August 1982. The SAI principal investigator was Mr. Burton S. Chambers, III.

This work was conducted for the Shock Physics Test Division (SPTD) at Headquarters, DNA, in support of the MILL RACE High Explosive (HE) Event. It included both a pretest and posttest phase, and was coordinated with Field Command, DNA (FCDNA) at Kirtland AFB, New Mexico, as well as with some of the MILL RACE TRS experimenters.

Mr. R. C. Webb was the DNA Contracting Officer's Representative (COR) until his transfer to BMDSCOM in December 1980. LTC Robert Flory, United States Army, was the COR during the remainder of the effort. Lt. Col. Ronald Bousek, United States Air Force, was the point of contact at FCDNA.

The author thanks LTC Flory, Mr. Webb, and Lt. Col. Bousek for their useful guidance and suggestions during the technical effort. The continuing interest of Mr. Tom Kennedy, Director of SPTD, is also most appreciated.

Finally, the author would like to express his appreciation for the many fruitful technical discussions with Mr. John Dishon, Dr. Richard Miller, and Mr. Jerry Lattery of the Radiation Effects Division of SAI. These many discussions substantially helped the author in formulating simple descriptive modeling algorithms, which represent the radiated environment from the DNA TRS simulators in the field.

TABLE OF CONTENTS

LIST OF ILLUSTRATIONS

LIST OF ILLUSTRATIONS (Continued)

LIST OF TABLES

SECTION I

INTRODUCTION

The effort reported herein was conducted in support of TRS experiments on MILL RACE and consisted of a pretest and posttest phase. The objectives for the pretest phase were: (1) to provide guidance and technical assistance to DNA Field Command and the MILL RACE TRS experimenters, and (2) investigate possible interference of the TRS units with the MILL RACE air blast, and then to suggest alternative approaches for meeting experimental objectives, if interference effects were expected to be significant. The objective of the posttest phase was to improve the modeling of the TRS radiated environment, where flames partially obscure one another, by modifying the earlier obscuration model as follows: (1) represent the flame as an inverted cone rather than a right cylinder, and (2) account for the change in view angle resulting from flame obscuration.

1-1 THE DNA THERMAL SIMULATION PROGRAM.

An important difference between explosions of nuclear weapons and chemical high explosives (HE) is the fraction of energy released in the electromagnetic spectrum. Since a nuclear explosion starts at a much higher energy state, the transport, absorption, and reradiation of this energy becomes quite significant (Reference 1). The chemical HE, on the other hand, releases most of its energy in mechanical form, ie. air blast.

During the nuclear explosion a large amount of energy is reradiated from the X-ray generated fireball in the form of light and heat; both forms are commonly referred to as thermal radiation. This thermal radiation, generally arriving before the shock wave, can precondition an exposed weapon system, so that its response to air blast may be modified from what it would

be to air blast alone.

The combination of air blast and thermal radiation loading can cause synergistic effects (ones more severe than what would be expected from both loadings operating independently). These synergistic effects have been observed on various military equipment (Reference 2). Until fairly recently, however, these effects have been impossible to generate in the field, without above-ground nuclear testing, due to the lack of thermal simulators that produce significant radiative output over large areas.

DNA has been providing simulated nuclear weapon environments with HE events to investigate various nuclear weapon-related effects. The simulated environments provided have been air blast and ground motion. The HE events have been conducted for many years to support the United States military services, and in some cases, our allies. More recently, the Shock Physics Test Division (SPTD) at DNA has been supporting research that is identifying various ways to simulate intense thermal radiation, characteristic of nuclear weapons, in order to study both synergistic thermal-air blast effects and thermal-only effects.

DNA is sponsoring both the development of large area thermal irradiation simulators to allow observation of full scale effects and the development of smaller laboratory thermal simulators that provide better simulation fidelity. Effective use of both types of these facilities should allow significant advances in our knowledge of nuclear weapon thermal effects and synergistic thermal-air blast effects.

The first significant large area irradiation system, initiated seven years ago, was the so-called bag system developed by Dishon and Lattery of Science Applications, Inc. (SAI) for DNA. The bag system consisted of an ensemble of mylar bags, each bag being a cylinder, hemispherically capped at both ends, about 6 meters high with a diameter of 1.5 meters. Each bag was filled with pure gaseous oxygen into which was sprayed aluminum powder. This mixture was then ignited with a device resembling a common railroad flare.

The bag system was fielded during the late seventies at a site used by DNA on Kirtland AFB. Various targets of military significance were exposed to thermal-only environments. These tests allowed qualitative assessments of the effects induced from large area irradiation onto targets of significant size. Effects such as aircraft panel buckling, which would be hard to obtain on small tests, were observed. This type of data was felt to be useful for validating large complex structural analysis computer codes.

One ensemble of TRS bags was fielded on DNA HE event MISERS BLUFF where it became obvious that the use of the TRS actually interferred with the air blast loads delivered to the exposed U.S. Army S-280 hardened shelter. The bag system had been placed in close proximity to the shelter, between it and the HE. When the air blast propagated through the hot combustion products of the bags, its peak overpressure was significantly reduced. This experiment provided some of the motivation for seeking an improved way of burning the aluminum powder.

A significant advancement in simulators was achieved when Dishon and his co-workers at SAI successfully developed the flame TRS system under DNA sponsorship. The flame system is now recognized as a significant improvement over the bag system, not surprisingly since it was designed to avoid many of the undesirable features of its predecessor.

The flame system consists of a set of nozzles, vaguely similar to rocket engines, but directed upwards, that burn aluminum powder in an oxygen rich environment. The aluminum powder is fluidized in nitrogen gas to facilitate flow through the plumbing from supply to nozzle. Liquid oxygen (LOX) is also sprayed into this mixture in the nozzle. The resulting combustible mixture is ignited with a flame that is burning outside the nozzle. This outside flame is lighted before the aluminum and liquid oxygen mixture is flowing, and its fuel is usually propane. After the aluminum and oxygen mixture is ignited, a bright flame is produced that can burn until the materials being injected are exhausted.

Due to the time taken for the burning of the aluminum particles, the

initial momentum associated with the spray, and buoyancy forces, the flame from each nozzle typically reaches a significant height of three to eight meters depending on how rapidly aluminum is introduced into the system. The radiating part of each flame, for a 5 kilogram per second burn of aluminum, appears approximately as an inverted cone of height about 6 meters and diameter of 5 meters at the cone's "base" (the nozzle is at the cone's apex).

This latter simulator, the Al-LOX flame system, was fielded on MILL RACE, and is the system that has been modeled during this effort.

1-2 THE DNA THERMAL SIMULATION MODELING PROGRAM.

DNA has also been sponsoring research on calibrating these Al-LOX flame sources to allow their use in the field, either as stand-alone systems or in conjunction with large HE events. The experimental calibration programs have been complemented with modeling efforts to allow interpolation, and in some cases extrapolation, of the environments.

In preparation for the MILL RACE experiment, the effort reported herein was initiated to provide guidance and technical assistance to DNA Field Command and to the MILL RACE experimenters who would be utilizing the Al-LOX flame source. Specifically, estimates were made of the thermal environments expected from the TRS units at various experiment locations and then provided to FCDNA for planning the use of the TRS units.

The estimates were based on early models of the bag system, that had been developed from a very limited data base. As data generated under another DNA contract were made available, they were incorporated into the DNA TRS data base and were used to expand and improve the existing models.

When the test bed configuration was altered, or when significantly different (and better) estimates of the Al-LOX TRS environment became available, updated estimates were provided to FCDNA and these were in turn given

to the MILL RACE experimenters. Recommendations were also made, on a limited basis, where calorimeters should be placed in order to improve the modeling effort. Other requirements, however, generally precluded use of these recommendations by the TRS developers.

1-3 THE DNA THERMAL-AIR BLAST INTERFERENCE PROGRAM.

In addition to the estimation of thermal environments, this effort included a task to investigate possible modifications to (or interference with) the HE-generated air blast by thermally induced effects generated by the TRS units. Of primary concern were adverse effects on planned air blast loading, as was seen on MISERS BLUFF (Reference 2). If the interference effects were considered significant, suggested alternative approaches for meeting the objectives of the combined thermal-air blast experiments were to be made.

It is necessary to place the flames relatively close to the targets to be irradiated since the thermal output of even these powerful TRS simulators is small in comparison to that of a nuclear burst (approximately five orders of magnitude below a kiloton of energy). This arrangement produces combined air blast and thermal effects under certain conditions. These effects can approximate those that would be seen during an actual nuclear explosion. However, if the TRS simulator is not sufficiently strong to allow its placement far enough away from the irradiated target, it is possible that the combined effects generated may only fortuitously simulate real ones.

An example was the experience on MISERS BLUFF where an S-280 U.S. Army Shelter was exposed to both thermal and air blast (Reference 2). The only available large scale simulator for MISERS BLUFF was the bag TRS. It had to be placed very close to the target in order to be able to deliver the required environment. Because the timing between the onset of thermal irradiation and air blast arrival was set to simulate a particular nuclear scenario with this MISERS BLUFF experiment, the air blast arrived while the TRS-generated

fireball was still in front of the shelter. When the air blast passed through this hot region, which was essentially touching the target surface, the received air blast overpressure was appreciably reduced. This effect was considered undesirable by the U.S. Army.

On MILL RACE, however, an attempt was made to mitigate the direct influence of the flame on the air blast peak overpressure by allowing sufficient time for the flame to just rise out of the way before air blast arrival. The length of time necessary for this to occur was determined during a series of small yield HE shots at the TRS test site at Kirtland AFB. This modest HE test program, called the Pentolite series, also determined if the air blast would be modified by passage through the region of space previously occupied by the flame. This approach of avoiding thermal "interference" with air blast takes advantage of the expected time delay in the real world case and is the current planned approach for use of TRS units during future HE tests.

However, careful consideration of the consequences of this approach are advisable since its use could lead to other problems of interpretation. For example, if the target cools too much before air blast arrival, the test may not meaningfully represent the worst possible effects. One might incorrectly conclude that some system is less vulnerable to combined effects than it really is.

1-4 TRS UNITS FIELDED AT MILL RACE.

Four flame systems were eventually fielded for the DNA HE event, MILL RACE (Reference 3). Throughout this report, the systems are referred to as: (1) UK-1, (2) UK-2, (3) BRL, and (4) Navy. Each of the four TRS systems consisted of one line of equally spaced nozzles. The UK-1 system, fielded for the use of the United Kingdom experimenters, consisted of eight nozzles of seven feet separation. The UK-2 system, also for the United Kingdom, consisted of four nozzles spaced at the same seven foot interval. The BRL system, fielded primarily for use by the U. S. Army Hardened Army Tactical

Shelter (HATS) program, consisted of four nozzles spaced three and one-half feet apart. Finally, the Navy system, fielded for various U.S. Navy experiments, consisted of four nozzles spaced ten and one-half feet apart.

1-5 REPORT OUTLINE.

The principal product of this effort has been the development of models that describe the radiated thermal environment in the field from Al-LOX TRS systems burning at the rate of 5 kilograms of aluminum per second. Although numerous calculations were performed that were useful in helping DNA site the TRS experiments on MILL RACE, none of these are difficult nor expensive to replicate, and therefore, there is little reason to document them beyond the numerous technical memoranda that have already been generated. It is worthwhile, however, to present what has been learned during the modeling effort, since this will have lasting value to those who will use the TRS on future HE tests and in large shock tubes.

Therefore, the bulk of the report discusses the models of TRS generated environments. Section 2 presents an overview of the modeling effort and discusses how a model is calibrated before being used. Section 3 presents comparisons of results with MILL RACE. Section 4 presents the models and algorithms that were developed. Section 5 summarizes the work done on TRS interference with air blast. The results given are preliminary in nature, since not all of the issues have been resolved. Finally, Sections 6 and 7 present our conclusions and recommendations.

SECTION 2

MODELING TRS RADIATED ENVIRONMENT

This section presents an overview of the modeling activity and the goals for this effort. A more detailed presentation of the actual models used to estimate the thermal environments produced by the DNA Al-LOX TRS is given in Section 4.

All of the various versions of the models discussed here have historically been referred to as ALFGEE, which is an acroymn for Aluminum-LOX Field Generated Environment Estimator. Basically, ALFGEE is simply a numerical simulation that represents the current capability to estimate TRS-generated thermal environments.

In the early attempts to model TRS radiated environments, the goal was to develop ways of estimating these data within some acceptable accuracy. Consistency of model parameters with the physical observables was desirable but not essential. Later it became apparent that more reliance would be placed on the modeling capability because of the costs associated with measurement, and therefore the goal shifted to developing a more universal model, one that agreed better with the physical observables.

The most important motivation for improving the models was due to their use in HE events. Model predictions are used to lay out experiment locations. Inadequacies in estimation can translate into experimental requirements being compromised.

2-1 MODELING FLUX.

When the TRS units are ignited the radiated power rises rapidly to

its peak in a few tenths of a second. The power from the flames then remains at the peak for a duration close to the burn time, typically a second or so, and then decays rapidly. Usually, the result is that most of the received energy comes from the flames while they are radiating at their peak power.

The resultant environment, that has been modeled during this and earlier efforts, is the flux received at a surface placed in the field facing the flames. The flux is modeled in calories per square centimeter per second. Furthermore, this modeling has been restricted to times when the flame has stabilized in shape and power corresponding to when the flux is at or near its peak value.

A suggested alternate approach is to model fluence measured in calories per square centimeter. However, we have chosen to not explicitly model the fluence. Instead, it is calculated as the product of the burn time and the modeled peak flux. This only approximates the fluence since the flame dimensions depend on time. Errors associated with the chosen approach have not been evaluated yet for a variety of reasons. Furthermore, the need to independently model the fluence has not been urgent, since the TRS units have normally been used to generate relatively long pulses.

While advantages may exist to model the fluence, reasons exist to prefer modeling the flux, if a choice has to be made. First, modeling fluence requires the time dependency of all the parameters; otherwise the burn time would have to be included in the model in a complicated way. Second, any smoke generated during an experiment could corrupt the late time flux, and hence the fluence, in a way that greatly complicates the analysis. Sufficient photographic data do not exist to establish which calorimeters have been obscured by smoke, hence past data may have limited value. Third, the data taken early in the program suffered from a thermal effect on the calorimeter test stands. The poles, holding the calorimeters, would tip back as they were irradiated as a result of asymmetrical thermal stress. The diameters of the poles used in the early tests were too small. This latter effect was studied and a summary is presented as Appendix A.

All of the effects listed above tend to alter the flux data especially at later times. Therefore, we chose to include the early time (peak at earliest time) data in the modeling data base expecting that this would be sufficient for our needs. Modeling the rest of the effects, that may be needed some day, was not considered a reasonable approach for the initial phase of the modeling effort. At that time few data existed anyway, so little benefit would have resulted.

2-2 INTRODUCTION TO THE ALFGEE MODELS.

An ALFGEE model consists of relationships and parameters that determine the received thermal radiation at some detector given additional information about the number of nozzles, their spacing, and such. An example of a relationship is the way the radiated power per unit height varies as a function of height. An example of a parameter is the height of the radiating part of the flame. A relationship is typically described by an equation and one or more parameters. A parameter is described by a single numerical value.

The calculation of the received environment in the field is straightforward once the geometrical shape of a TRS flame has been established, if its radiance is known. The irradiance is calculated at desired positions in the field upon some imaginary surface, the normal of which is oriented in some specified direction, by simply integrating over the radiating elements, accounting for the viewing angles to both the detector and each element. Atmospheric attenuation is insignificant for most of the energy for the distances involved, and therefore, is not included.

A number of approaches have been used during the modeling effort to represent the geometrical nature of the flames when calculating irradiance. The first representation was a linear array of point sources each radiating with constant power. Initially, it was easy to modify parameters to produce adequate agreement with the limited data. This was especially true because many tests were conducted with the same calorimeter layout, which although providing a measure of how well the TRS development was proceeding, did not

yield information at other locations needed to stress the modeling task. Many combinations of parameters can produce good agreement.

The first refinement, motivated by the eventual taking of data at other heights, was to use the same linear array of point sources as in the first representation but with a linear falloff in power with height. This second model served the community well until interest existed in placing calorimeters off to the side of the TRS units. It subsequently became clear that the model needed to account for the effect of flames obscuring a detector's view of other flames. A cursory analysis indicated that considering this obscuration would substantially improve agreement.

The radiating right circular cylinder shape was selected as the third representation for its simplicity in dealing with obscuration. It proved to be quite acceptable until data became available for the early test firings of the MILL RACE nozzles. Before those events, all the data had been taken for a nozzle spacing of 3.5 feet. With the early test firing data available (two sets of 7 feet spacing and one set of 10.5 feet spacing), it became clear that it would be necessary to adjust model parameters for each nozzle spacing.

Further study, however, suggested that it might be possible to avoid recalibrations for each spacing by changing the representation of the flame's geometrical shape. Consequently, additional work was performed to improve the agreement between data and models subsequent to the MILL RACE event. This additional work resulted in the fourth representation that was designed to approximate the actual flame shape. Video and photographic records show flames that look like inverted cones with dense clouds of combustion products above them. Therefore the final representation was patterned as a radiating inverted cone capped with an opaque right cylinder. The power per unit length relationship was modified to reflect this newer geometry.

The use of the inverted cone representation has been found to adequately replicate the experimental data. It appears that a single calibration of the model provides reasonable agreement with the data base for a nozzle that burns 5 kilograms of aluminum per second for many nozzle

spacings. Since the inverted cone model was the best one developed during this effort, it is described in more detail in the following subsections.

An additional point must be presented before proceeding to the discussion of the inverted cone model. As a result of our review of the data, we conclude that there is reason to believe that each TRS unit, by itself, is reproducible if fired under the same operating conditions and characteristics. There is much variability in the data, however, and some of this we suspect is due to differences among the TRS units, for example, nozzle design.

2-3 INTRODUCTION TO THE INVERTED CONE MODEL.

After MILL RACE the inverted cone model was developed and algorithms for flame obscuration effects were included. Each flame was treated as a radiating inverted cone capped by an opaque cylinder, consistent with available photographic data. The radiating portion is considered to be a diffuse source. Capping the flame with the opaque cylinder approximates the influence from smoke generated by the flames. In addition, the effect due to change in view angle resulting from flames obscuring one another was considered and added to the model. The energy incident on any flame is modeled as being fully absorbed with no appreciable effect on the flame's radiating characteristics.

In the model each flame is represented as an ensemble of point sources above the nozzle, along its axis of symmetry. This is adequate as long as enough points are included on the axis to allow an accurate integration, and if the effect from flame-flame obscuration is properly estimated.

The parameters of the inverted cone model are: (1) flame strength or power, measured in calories per second, (2) flame width or diameter (at the "base" of the inverted cone), measured in centimeters, (3) flame height at the point where significant radiation seems to end, also in centimeters, (4) and (5) two adjustable parameters that quantitatively represent the height

variation of power per unit length divided by the radius of the flame at that height, and (6) the ground's albedo. These six parameters are discussed more fully in Section 4.

2-4 CALIBRATING ALFGEE MODELS.

In practice, before any ALFGEE model is used, it is calibrated to the data. A calibration is defined as the set of six parameters that best represent the data being modeled, where this set will probably be different from the set for another physical representation of the flame's geometry. The right cylinder representation was the one most widely used during this effort. It was also the one used to predict the environments for MILL RACE. The more recent inverted cone model had not been exercised much during this effort.

The process of model calibration generally proceeds as follows. A set of parameters are chosen, usually based on past experience. Calculations for points where data exist are performed and these compared with the experimentally measured values. The difference between the predicted and experimental values is also computed and is called the residual. The absolute strength parameter of the flame model is adjusted to give a zero residual sum. The model's measure of goodness is defined to be the smallness of the sum of the variations, where a variation is computed as the residual squared.

The entire TRS data base should not necessarily be used when calibrating a model. A subset should be chosen, for example, excluding measurements made with defective calorimeters, or measurements where the aluminum and LOX flow rates are largely different from current practice. The resultant calibrations can be compared to see how well they represent the data base. It is important to inspect individual comparisons to be sure differences are random rather than biased.

Since ALFGEE is a six parameter model, any subset must contain at least six perfect data points to determine a unique model. Since the data taken in the field are subject to variability, much more data must be

available to provide a statistically meaningful sampling.

The best model is not necessarily that with a zero residual sum and the lowest sum of variations, even though it has been our practice to select our parameters on that basis. For example, if a comparison of the data with a calibrated model showed consistently lower flux close in to the flames and consistently higher flux farther out, another calibrated model might be preferable even if its residual sum was nonzero and it had a larger sum of variations. Forcing the residual sum to be zero and using the sum of variations as the measure of a model's ability to represent some data base subset, is an appropriate technique when the data show no biases.

2-5 EXAMPLES OF CALIBRATIONS.

This subsection presents results of four different calibration studies, out of many, that have been performed during this effort. These are examples of results generated with plausible model parameters. They were not produced with the intent to derive the optimum calibration. Instead, when someone needed a prediction within a short time constraint and only a meager set of data existed, we would run the necessary calculations to quickly arrive at a better calibration, and then provide revised model estimates.

Table I shows comparisons for different calibrations of the right circular cylinder model. The table consists of seven columns of data. The first column is the power of the TRS unit (ABS.STR) in calories per second. The second (F.DIAM) is the flame diameter in centimeters. The third (F.HGT) is the height of the flame's radiating portion, also in centimeters. The fourth (BK-HGT) and fifth (BK-STR) are coefficients, described later, that affect the variation of the power per unit length (height) of flame with its height. Both coefficients are non-dimensional. The sixth column is the ground albedo, another model parameter. Finally, the seventh column is the sum of the variation that serves as our measure of a model's goodness of fit. The lower this number, the better the agreement.

Table 1. Variation study for Navy TRS (no passive calorimeters).

VARIATION STUDY FOR NAVY TRS (NO PASSIVE CALORIMETERS)

19-APR-82 IS LAST UPDATE DNA TRS B. CHAMBERS

ABS.STR	F.DIAM	F.HGT	BK-HGT	BK-STR	ALBEDO	SUM-VAR
23390100	160.00	755.70	0.20	1.00	0.00	103
23390100	160.00	755.70	0.20	1.00	0.00	103
23697200	160.00	755.70	0.20	0.80	0.00	103
23999600	160.00	755.70	0.20	0.60	0.00	104
24297100	160.00	755.70	0.20	0.40	0.00	104
24589800	160.00	755.70	0.20	0.20	0.00	105
24878100	160.00	755.70	0.20	0.00	0.00	106
23390100	160.00	755.70	0.20	1.00	0.00	103
21887000	160.00	755.70	0.40	1.00	0.00	105
20660300	160.00	755.70	0.60	1.00	0.00	113
19948000	160.00	755.70	0.80	1.00	0.00	124
19775500	160.00	755.70	1.00	1.00	0.00	128
24873900	160.00	755.70	0.00	1.00	0.00	106
23390100	160.00	755.70	0.20	1.00	0.00	103
19775500	160.00	755.70	1.00	1.00	0.00	128

For the chosen subset, representative of the Navy MILL RACE TRS unit, large variations in some of the model parameters, as illustrated in Table 1, did not make much difference. Specifically, it shows that the sum of the variances is insensitive to the details of the relationship describing how the power from the flame depends on normalized height. The two parameters, BK-HGT and BK-STR, quantify this relationship. The interpretation that best fits this case is that the models are equally inadequate.

In the above example, the chosen data base consisted of nineteen measurements made with the calorimeters from pre-MILL RACE test firings and the active ones from MILL RACE. Nine of the measurements were taken at the test firings and were read by Miller of SAI. The nozzles during that firing were 1.75 meters above ground. Ten of the measurements were made on MILL RACE. Four of these were read by the author. Six were calculated by Bousek of FCDNA from the fluence divided by 2.4, the burn time. The sum of the flux measurements for the nineteen points was 297 calories per square centimeter per second.

Table 2 shows the results for the same Navy TRS unit and the same nineteen point data base subset, but using the inverted cone model. The columns are the same as in Table 1, except for two parameters that describe the power per unit flame length with height relatonship. The two new parameters are the luminosity limit, a height normalized by the flame height (LUM.LIM), and the power at the nozzle (P@NOZZ), which is relative to the power per unit height at the flame height (defined as unity). This latter parameter is normalized to conserve energy within the model.

In Table 2 the sum of the variation is much more sensitive to variations in the model parameters. The inverted cone model reduces the sum of variances by fourteen percent, and therefore could be considered a better model of these data.

Table 3 compares various calibrations of the inverted cone model to another subset of the data base. Here the effect of adding the passive calorimeter data was considered. Twenty two additional measurements were

Table 2. Variation study for Navy TRS (does not include passive calors).

VARIATION STUDY FOR NAVY TRS (DOES NOT INCLUDE PASSIVE CALORS)

21-APR-82 IS LAST UPDATE DNA TRS B. CHAMBERS

ABS.STR	F.DIAM	F.HGT	LUM.LIM	P@NOZZ	ALBEDO	SUM-VAR
30427800	480.06	640.08	1.00	1.00	0.00	129
37174700	480.06	640.08	1.00	0.00	0.00	243
32798800	480.06	640.08	1.00	0.50	0.00	160
30427800	480.06	640.08	1.00	1.00	0.00	129
27920100	480.06	640.08	1.00	2.00	0.00	105
25807700	480.06	640.08	1.00	4.00	0.00	93
24003900	480.06	640.08	1.00	10.00	0.00	89
23111200	480.06	640.08	1.00	25.00	0.00	89
22618100	480.06	640.08	1.00	100.00	0.00	90
30427800	480.06	640.08	1.00	1.00	0.00	129
28408500	480.06	640.08	1.00	1.00	0.20	198
26640800	480.06	640.08	1.00	1.00	0.40	275
25080200	480.06	640.08	1.00	1.00	0.60	356
23692300	480.06	640.08	1.00	1.00	0.80	439
22450000	480.06	640.08	1.00	1.00	1.00	521
30427800	480.06	640.08	1.00	1.00	0.00	129
34731200	480.06	640.08	1.20	1.00	0.00	155
38761700	480.06	640.08	1.40	1.00	0.00	182
50809200	480.06	640.08	2.00	1.00	0.00	255
91850900	480.06	640.08	4.00	1.00	0.00	382
29115100	400.00	640.08	1.00	1.00	0.00	135
30427800	480.06	640.08	1.00	1.00	0.00	129
33724300	600.00	640.08	1.00	1.00	0.00	147
28636400	480.06	600.00	1.00	1.00	0.00	112
30427800	480.06	640.08	1.00	1.00	0.00	129
38487500	480.06	800.00	1.00	1.00	0.00	219
18165500	480.06	400.00	1.00	25.00	0.00	153
19939300	480.06	500.00	1.00	25.00	0.00	112
22137400	480.06	600.00	1.00	25.00	0.00	92
23111200	480.06	640.08	1.00	25.00	0.00	89
24664700	480.06	700.00	1.00	25.00	0.00	90
27452000	480.06	800.00	1.00	25.00	0.00	102

Table 3. Variation study for Navy TRS (includes passive calorimeters).

VARIATION STUDY FOR NAVY TRS (INCLUDES PASSIVE CALORIMETERS)

18-APR-82 IS LAST UPDATE DNA TRS B. CHAMBERS

ABS.STR	F.DIAM	F.HGT	LUM.LIM	P@NOZZ	ALBEDO	SUM-VAR
28073100	480.06	640.08	1.00	1.00	0.00	1215
33556300	480.06	640.08	1.00	0.00	0.00	1870
30027600	480.06	640.08	1.00	0.50	0.00	1409
28073100	480.06	640.08	1.00	1.00	0.00	1215
25972000	480.06	640.08	1.00	2.00	0.00	1056
24176300	480.06	640.08	1.00	4.00	0.00	960
22622000	480.06	640.08	1.00	10.00	0.00	907
21845900	480.06	640.08	1.00	25.00	0.00	891
21415100	480.06	640.08	1.00	100.00	0.00	885
28073100	480.06	640.08	1.00	1.00	0.00	1215
26001800	480.06	640.08	1.00	1.00	0.20	1165
24215200	480.06	640.08	1.00	1.00	0.40	1159
22658300	480.06	640.08	1.00	1.00	0.60	1183
21289500	480.06	640.08	1.00	1.00	0.80	1226
20076700	480.06	640.08	1.00	1.00	1.00	1281
28073100	480.06	640.08	1.00	1.00	0.00	1215
31733800	480.06	640.08	1.20	1.00	0.00	1323
35081500	480.06	640.08	1.40	1.00	0.00	1370
45327400	480.06	640.08	2.00	1.00	0.00	1546
81808900	480.06	640.08	4.00	1.00	0.00	1792
26763100	400.00	640.08	1.00	1.00	0.00	1254
39983700	800.00	640.08	1.00	1.00	0.00	916
23188900	480.06	500.00	1.00	1.00	0.00	972
34628200	480.06	800.00	1.00	1.00	0.00	1552

added and then some of the calibrations in the previous table were redone. The variability of these additional data, as measured by the sum of the variations divided by the number of points, increased. The variability is increased by adding the passive calorimeter data. The added data were calculated from the measured fluence by Bousek of FCDNA. The approach of using measured fluences to determine flux can be misleading in the opinion of this writer.

Table 4 presents calibrations to data taken from two sets of nozzles using the inverted cone model. The two sets were lumped together because they were both spaced seven feet apart. The two sets were the UK-1 and UK-2 MILL RACE nozzles. UK-1 was an eight nozzle array and UK-2 was a four nozzle array. The data consisted of thirty three measurements: ten were the UK-1 pre-MILL RACE test firings for UK-1 and were read by Miller of SAI; eleven were from the pre-MILL RACE test firings for UK-2 and were read by Lattery of SAI; eight were the UK-1 MILL RACE results read by this writer; and four were the UK-2 MILL RACE results also read by this writer. The sum of the measured values was 794 calories per square centimeter per second. The lowest sum of variances was 323 in flux squared units. This result was not much different from the one obtained by using the best modeling for the Navy unit (Table 2), the latter shown at the bottom of Table 4 for the UK data. The residual is 29 calories per square centimeter per second, and is non-zero because the parameters were deliberately not changed. This latter comparison led us to believe that it is possible to build a unified model, that is, one with parameters that are independent of nozzle spacing.

2-6 DNA TRS DATA BASE.

A data base has been compiled from the experimental measurements recorded during the recent years of TRS firings. Any subset of the data base can potentially be used to calibrate any ALFGEE model, e.g. cylindrical or inverted cone. Depending upon the success achieved in replicating the experimental data, appropriate subsets of the data base can provide an indication of the overall variability of the data. Whether any variation has been caused by experimental error or instead by lack of repeatability is not

Table 4. Variation study for UK's TRS (does not include passive calors).

VARIATION STUDY FOR UK'S TRS (DOES NOT INCLUDE PASSIVE CALORS)

26-APR-82 IS LAST UPDATE DNA TRS B. CHAMBERS

ABS.STR	F.DIAM	F.HGT	LUM.LIM	P@NOZZ	ALBEDO	SUM-VAR
24311200	480.06	640.08	1.00	25.00	0.00	371
20369200	480.06	350.00	1.00	25.00	0.00	858
20596000	480.06	400.00	1.00	25.00	0.00	670
21073600	480.06	450.00	1.00	25.00	0.00	536
21724500	480.06	500.00	1.00	25.00	0.00	447
23445900	480.06	600.00	1.00	25.00	0.00	379
25754100	480.06	700.00	1.00	25.00	0.00	368
28395300	480.06	800.00	1.00	25.00	0.00	395
33920700	480.06	640.08	1.00	1.00	0.00	620
25426300	480.06	640.08	1.00	10.00	0.00	381
24311200	480.06	640.08	1.00	25.00	0.00	371
23701300	480.06	640.08	1.00	100.00	0.00	368
24311200	480.06	640.08	1.00	25.00	0.00	371
23069900	480.06	640.08	1.00	25.00	0.20	424
21949300	480.06	640.08	1.00	25.00	0.40	491
21370600	300.00	640.08	1.00	25.00	0.00	334
22019700	350.00	640.08	1.00	25.00	0.00	342
22835100	400.00	640.08	1.00	25.00	0.00	339
23728800	450.00	640.08	1.00	25.00	0.00	360
24311200	480.06	640.08	1.00	25.00	0.00	371
27017000	600.00	640.08	1.00	25.00	0.00	374
24311200	480.06	640.08	1.00	25.00	0.00	371
25351200	480.06	640.08	1.50	25.00	0.00	354
26441300	480.06	640.08	2.00	25.00	0.00	342
29064100	480.06	640.08	3.00	25.00	0.00	348
31615000	480.06	640.08	4.00	25.00	0.00	340
24828600	400.00	640.08	2.00	25.00	0.00	323
23111200	480.06	640.08	1.00	25.00	0.00	391
* NOTE: THIS IS A SPECIAL CASE (10.5) SUM OF RESIDUAL>						29

easily deduced.

Subsets of the data base have been chosen (and used to establish different calibrations) as statistically meaningful collections representing either: (1) a particular type of event, such as the collection of all multi-nozzle events wherein the nozzles are separated by 7 feet, or (2) where certain suspect measurements have been removed for example for the 3.5 feet nozzle separation data. The most suspicious data, those obtained from early experiments performed with different reactant flow rates, were removed in an attempt to avoid skewing the data.

Appendix B presents some of the peak flux data taken during the development program, as reported to this author, along with comparisons of an early model based on the right cylinder. The recorded peak value has been found to depend on who is reading the oscilliscope traces, primarily due to the interpretation of what is peak flux. Some take the absolute peak, they don't average over the rapid oscillations. Others use a faired curve through the data removing the high frequencies (kiloHertz and above). Therefore, the appendix includes more comparisons than would otherwise be needed.

2-7 CALORIMETER LOCATIONS.

Figures 1 through 6 illustrate where the calorimeters have been located relative to the flames. Each calorimeter is represented by a small circle, which is connected to its projection on the ground. The circle is drawn slightly to the calorimeter's right. The flames are pictorally shown as four straight lines always starting at the nozzle. Each of these figures are projections; they are perspective only for an eye position infinitely far away. The coordinate scale is shown in the upper left hand corner and is in centimeters. This scale refers to the distance at the end of each coordinate axis. Each axis is subdivided into ten intervals, each interval bounded by tic marks.

Note that the pre MILL RACE test firings of both the UK-1 eight nozzle array and the Navy four nozzle array were positioned above the ground

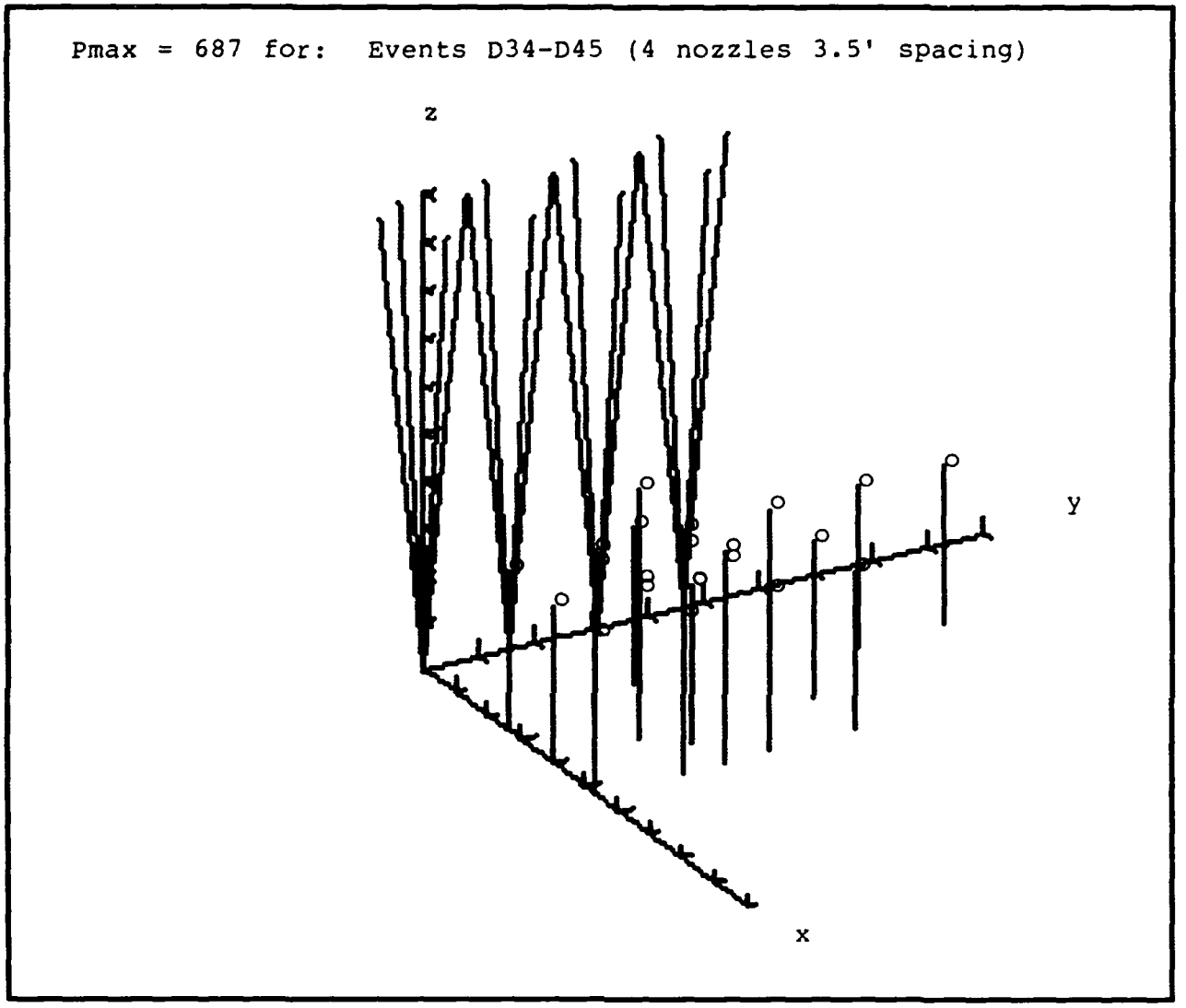

Figure 1. Calorimeter locations: events D34 to D45.

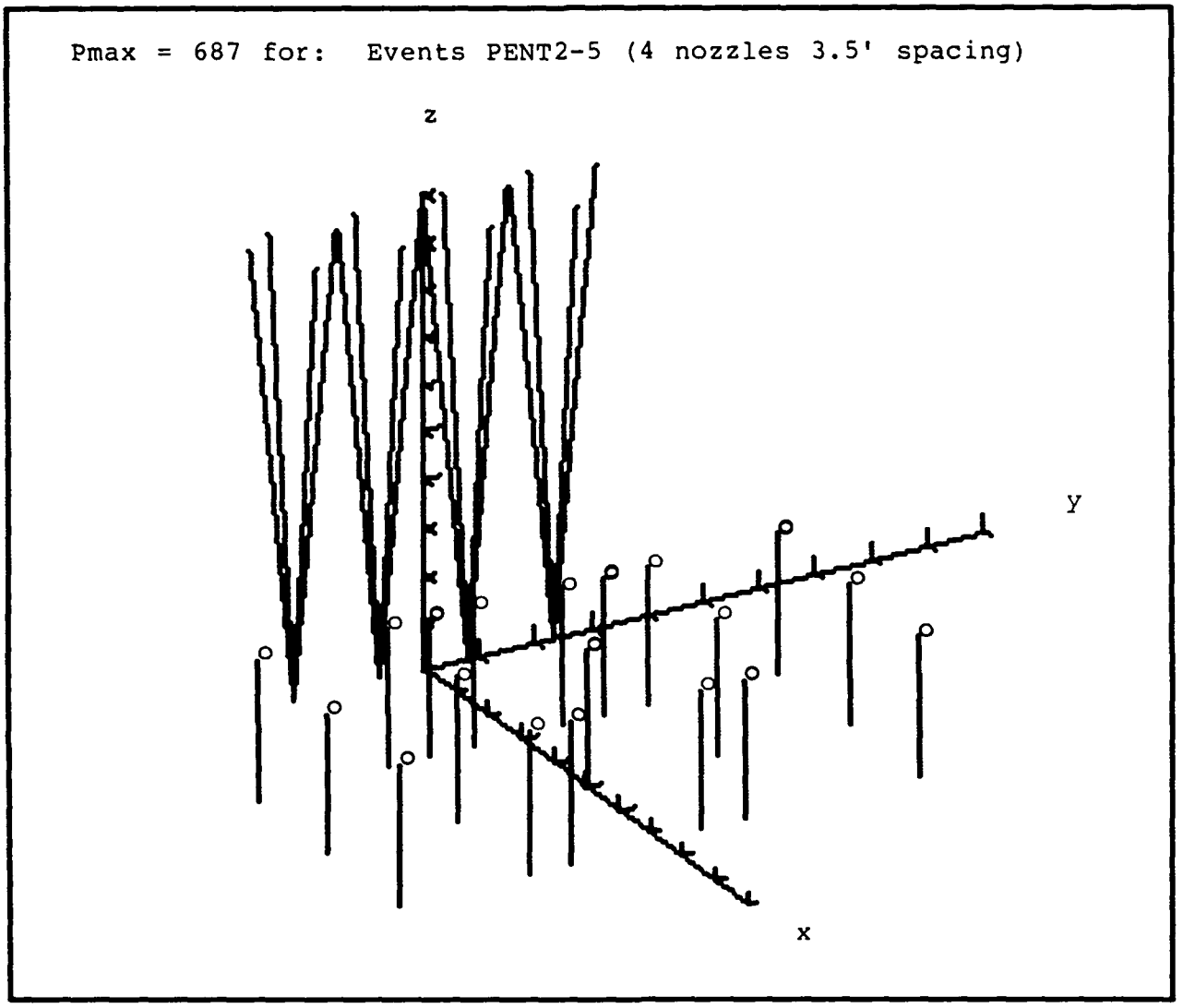

Figure 2. Calorimeter locations: events pentolite 2 to 5.

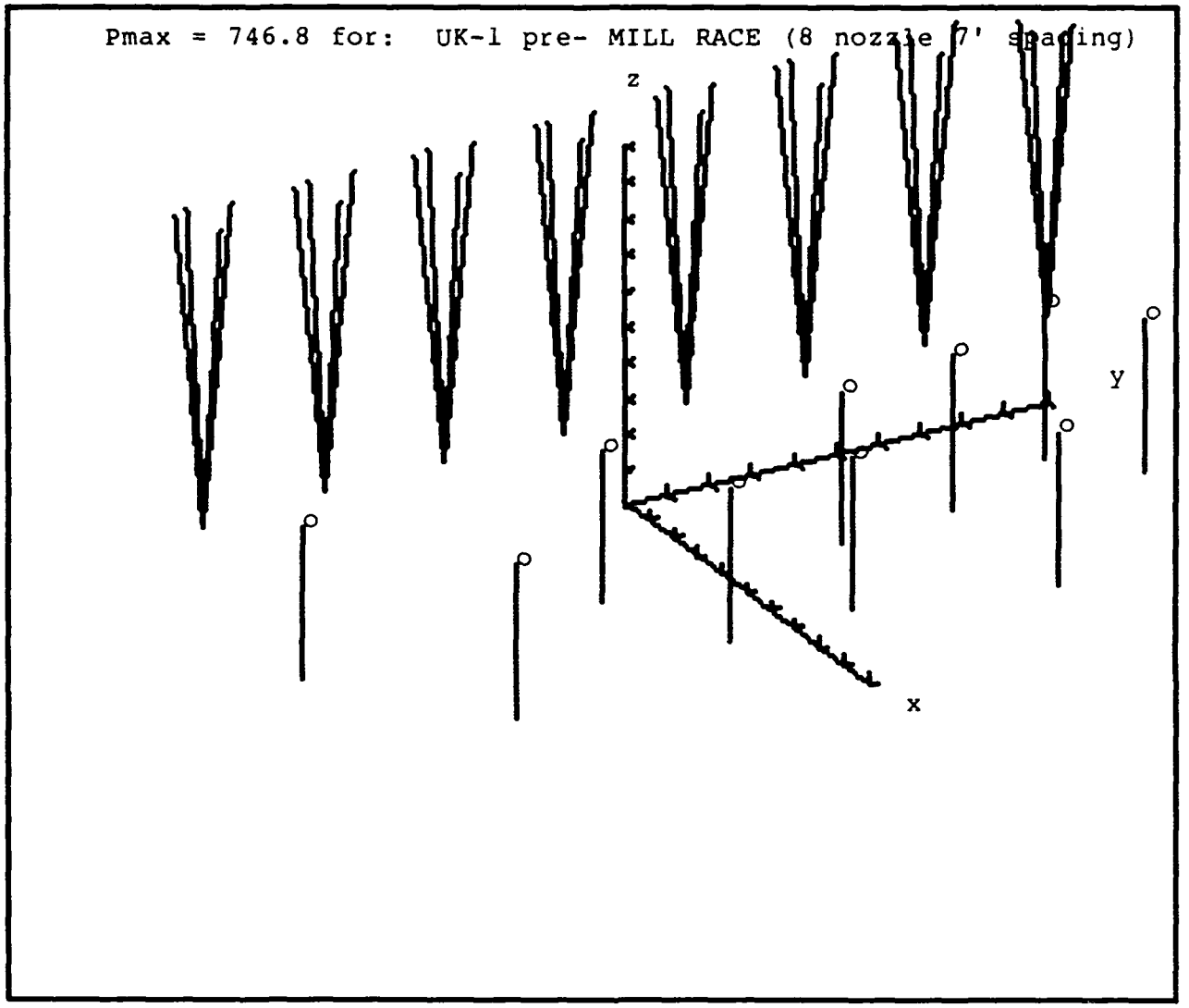

Figure 3. Calorimeter locations: event pre-MILL RACE UK-1.

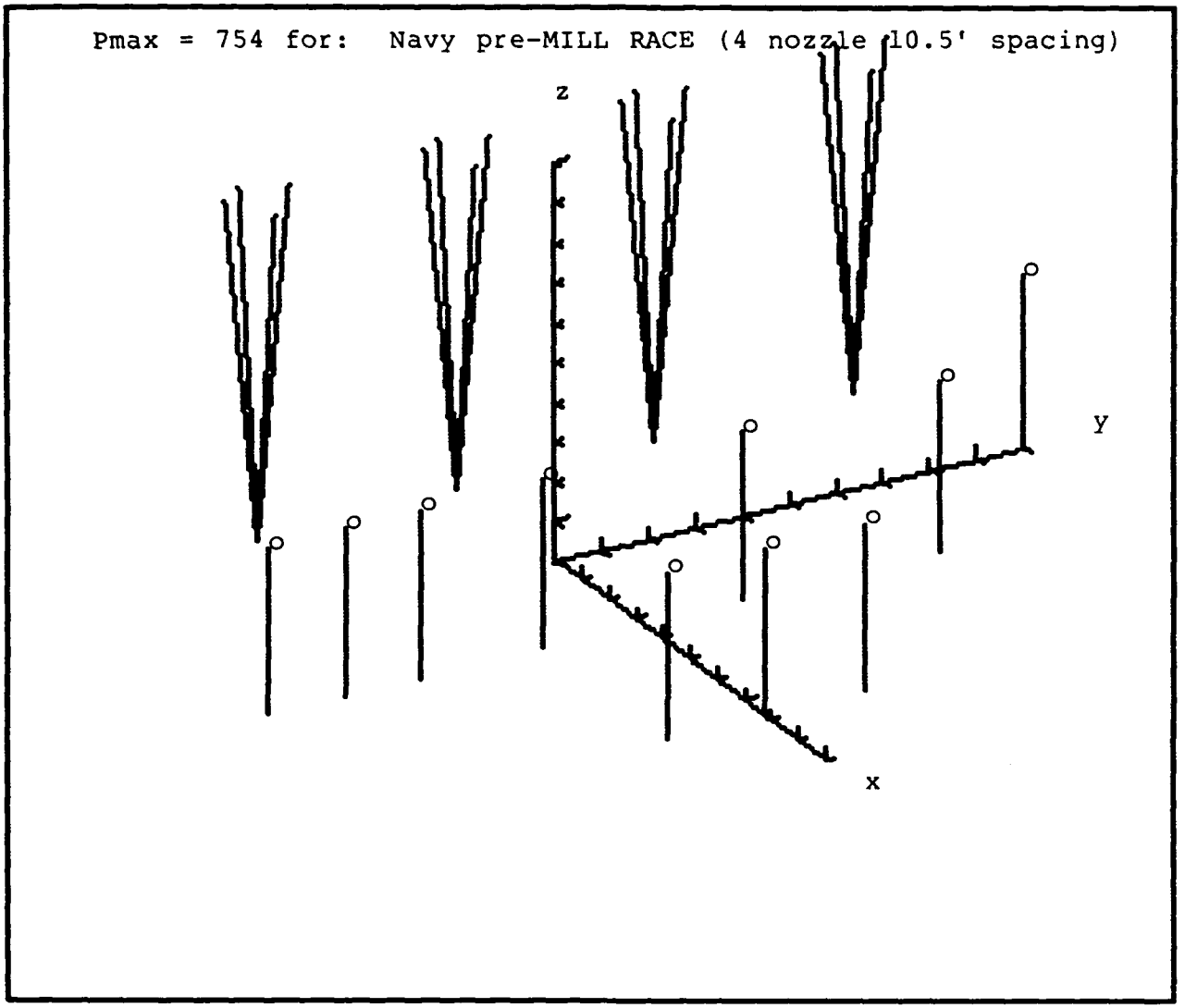

Figure 4. Calorimeter locations: event pre-MILL RACE Navy.

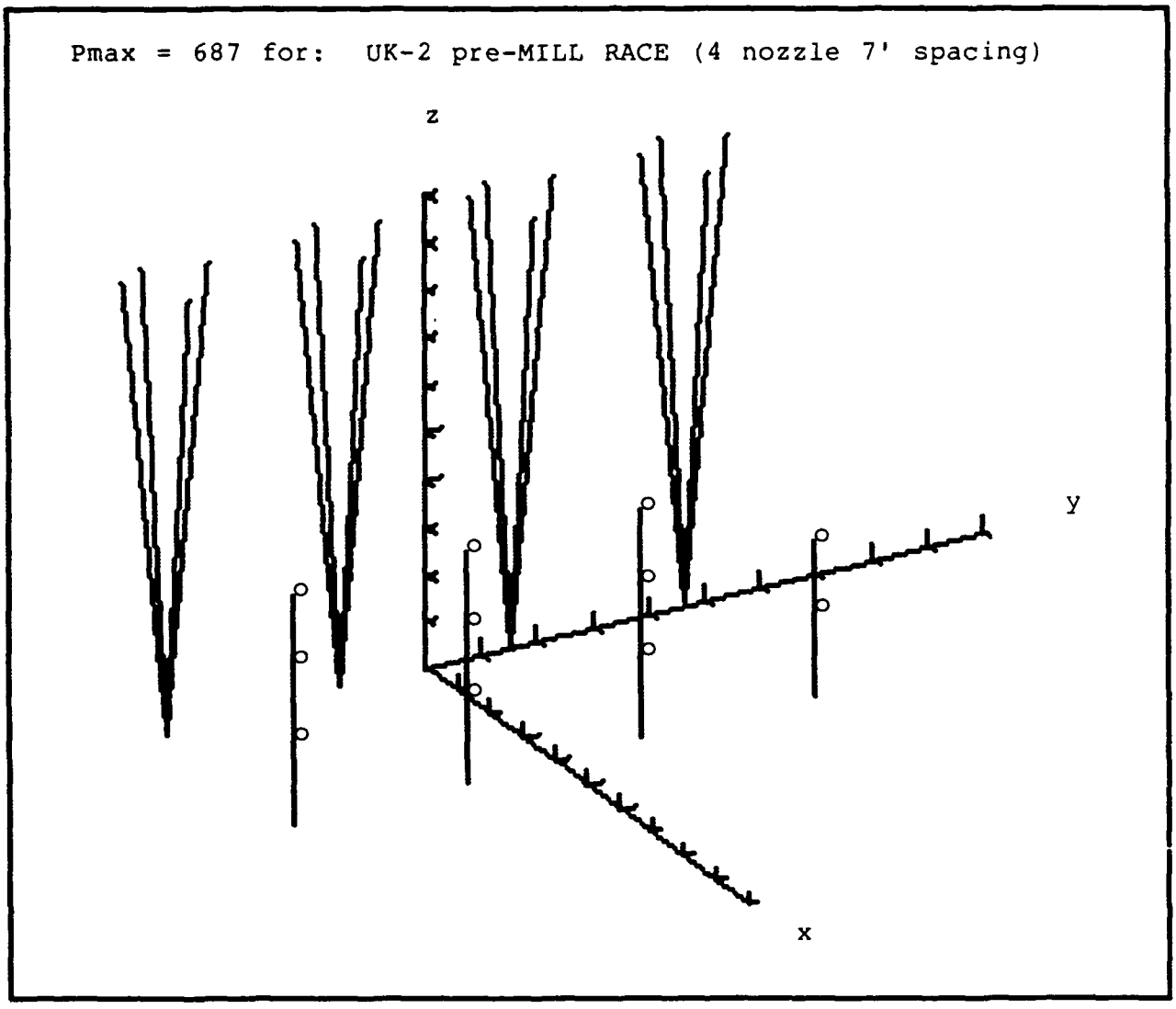

Figure 5. Calorimeter locations: event pre-MILL RACE UK-2.

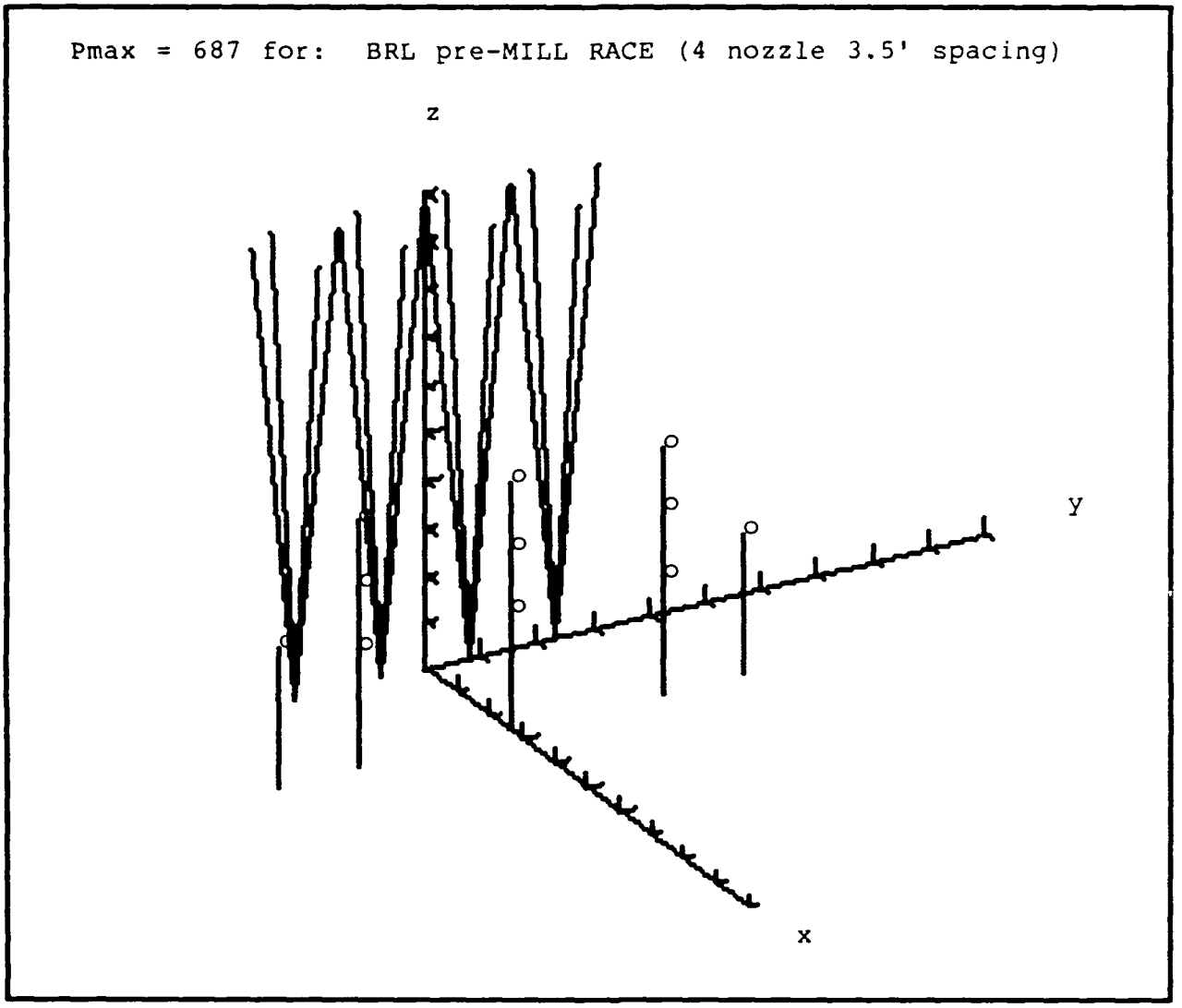

Figure 6. Calorimeter locations: event pre-MILL RACE BRL.

since both arrays were too long to fit in the TRS pit at the KAFB site. The nozzles were above the y-axis in the figures and were at a height of 1.75 meters. Referring to Figure 4, this height of 1.75 meters when divided by the coordinate scale, 7.54 meters, produces a value of 0.232, which corresponds to 2.32 tic marks up the z axis. This illustrates how to use the coordinate scale.

2-8 BIAS OF DATA BASE WITH EVENT.

One of the better calibrations was chosen to be compared with all the data available in the data base (including MILL RACE diagnostic calorimeters) to find any evidence of bias. The parameters for the chosen model are shown above in Table 4 as the last entry. That calibration was to the Navy data, which did not include the passive calorimeters.

The ratio of each experimental datum over the model value was computed and stored in a list along with its x (range) and z (height) coordinates. Each calorimeter and event identification was also included. Appendix C contains two tables that present this information, which is based on the data available to this writer up to and including MILL RACE, in two different orders. The first table shows the list in chronological order. The second table shows this list sorted on the value of the result ratio. It is included as Appendix C for reference.

Figures 7 and 8 show the variation of the ratio of measured values to calculated ones for two sets of data. The first set is for the TRS unit at the DNA site at KAFB. Initially this consisted of two nozzles, or one half of a normal unit, but later was modified to include two more nozzles. The second is for the four sets of TRS units built specifically for use on MILL RACE. There does not seem to be any discernible bias with event nor with time. However, there is clearly considerable variation in how well the data agree.

The distribution of variability with ratio is shown as Figure 9. In general since the ratio is used, figures of this type are more useful when the

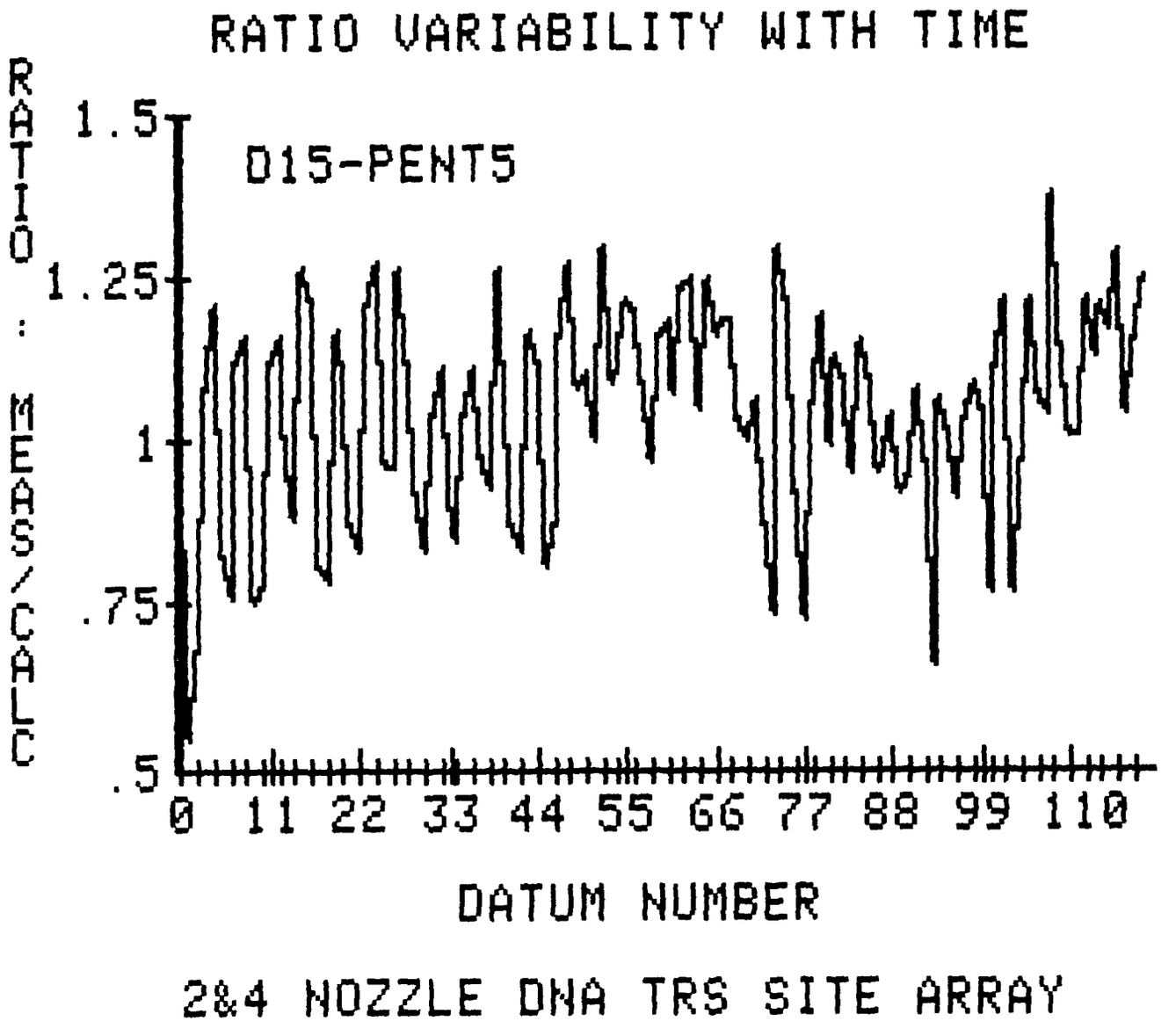

Figure 7. Variation of ratio: DNA TRS site nozzles.

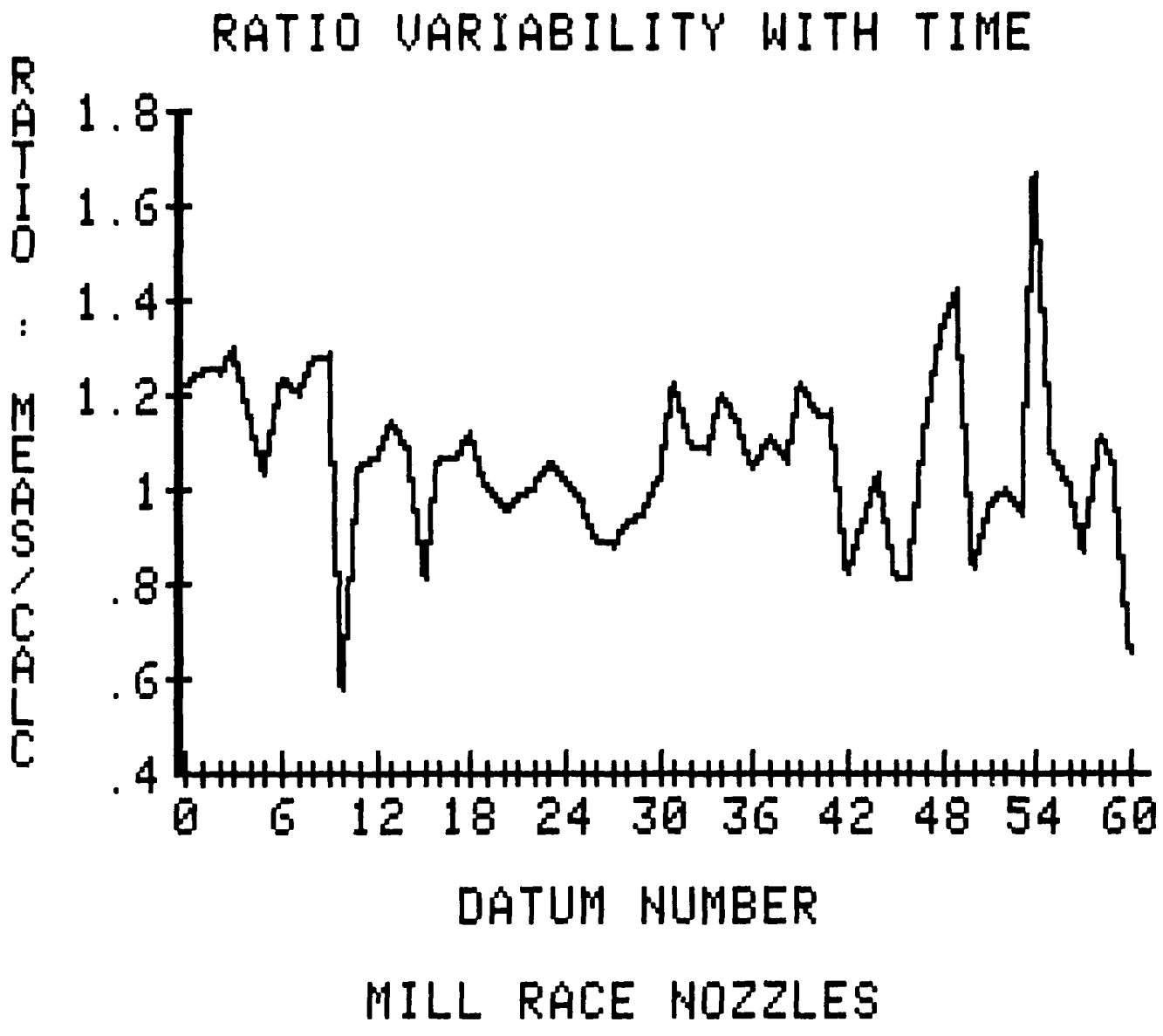

Figure 8. Variations of ratio: MILL RACE nozzles.

```
INC = .05

 .5>N *
 0.55 *
 0.60
 0.65 ***
 0.70 **
 0.75 ******
 0.80 ***********
 0.85 **********
 0.90 ********
 0.95 ****************
 1.00 ***********************
 1.05 ***************************
 1.10 ********************
 1.15 ******************
 1.20 ****************
 1.25 ************
 1.30 ***
 1.35 **
 1.40 *
 1.45
 1.50
 1.55
 1.60
 1.65 *
 1.70
```

Figure 9. Distribution of ratio differences.

log of the ratio is shown. The information to be gained, however, did not seem significant enough to replot the data. What this figure does show is that in general the spread in data appears almost normally distributed.

Taking the data shown in Figures 7 and 8, subtracting one from the ratio and then accumulating the result as datum number increases, Figures 10 and 11 are generated. If there was no bias with time, these figures would oscillate about zero. Where there is a positive or negative slope over a number of data points, an event is indicated which on average is higher or lower, respectively, than the model calculations. One such dominant slope region is on Figure 10 from datum number 45 to 66. This region corresponds exactly to Events D-30, D-31, D-32, D-33, D-34, and D-35. Whether this same region may have been seen in Figure 7 is debatable. The region is quite discernible in Figure 10, which makes the latter type of presentation useful for data analysis. The trend is also seen in Figure 11 for the UK-1 and BRL MILL RACE pretest firings.

2-9 BIAS OF DATA BASE WITH RANGE AND HEIGHT.

In order to establish whether there existed a bias with calorimeter field position, the figures within this subsection were prepared. All the active calorimeter data were separated into two groups. One group was for the DNA TRS site unit, and the other group were all the MILL RACE units. Three figures were prepared for each set. The first shows the projection of the locations of each calorimeter on the range-height plane. The second shows the ratio of the measured value to the computed one for the calibration used in the preceding subsections as a function of range. The third shows this same ratio as a function of height.

For the DNA TRS site unit, all data from Events D-15 to Pentolite 5 are shown in figures 12 through 14. The first thing that should be noticed is that the field has only been modestly covered. However, the nozzles have been near the ground in all cases. The second thing to be noticed is that there does not appear to be a clear bias of the variability with range.

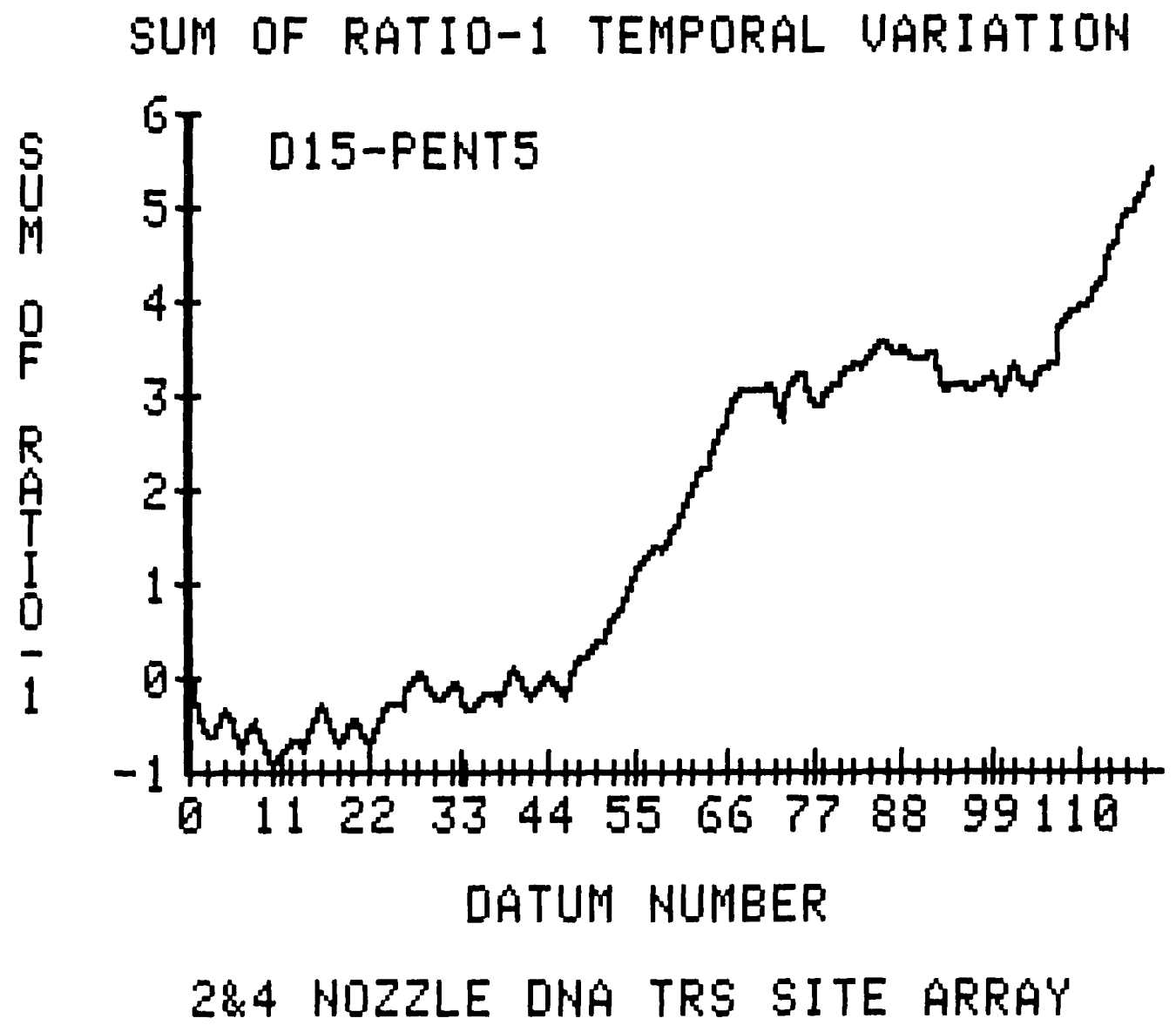

Figure 10. Cumulative value of (ratio-1): DNA TRS site nozzles.

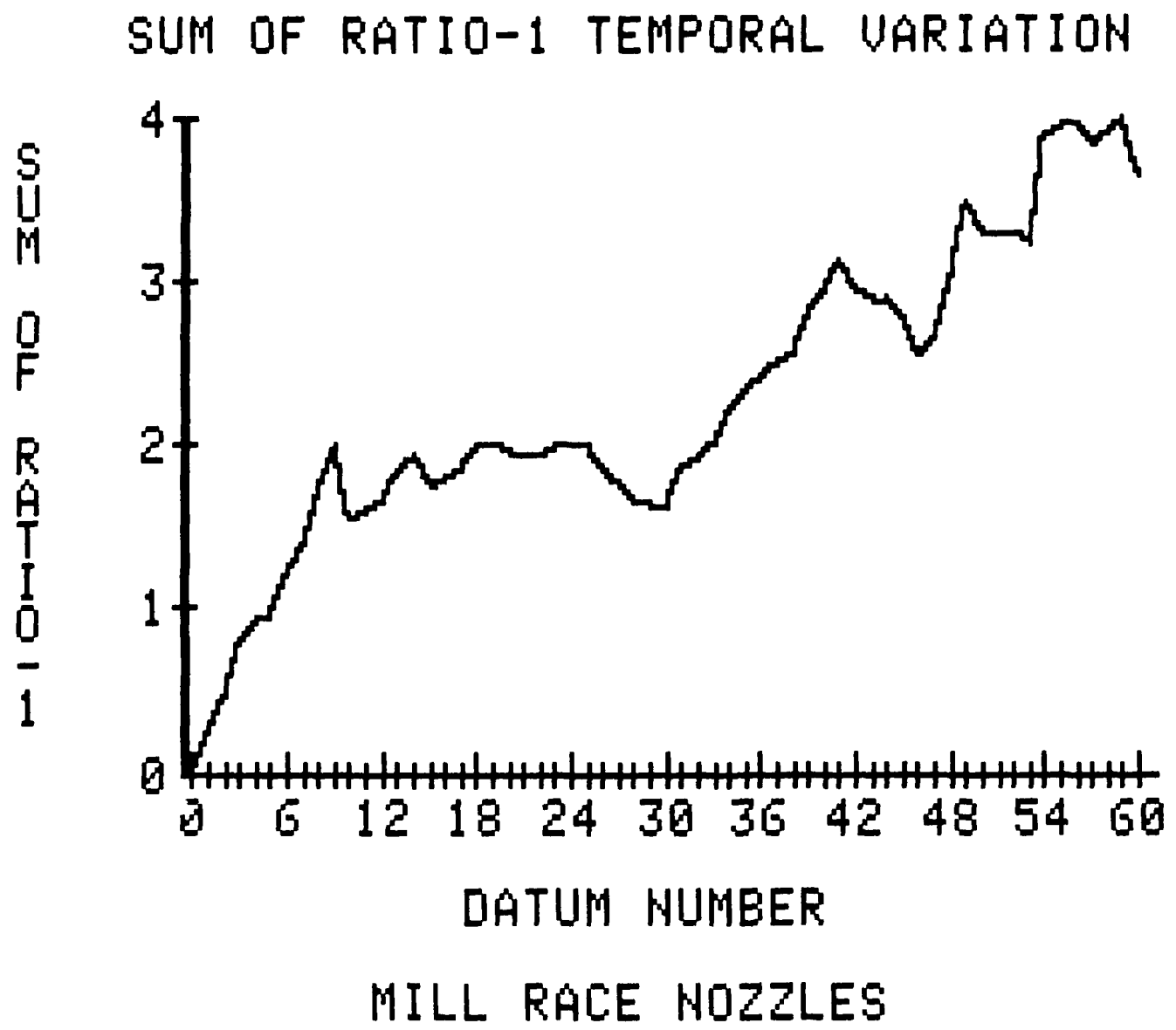

Figure 11. Cumulative value of (ratio-1): MILL RACE nozzles.

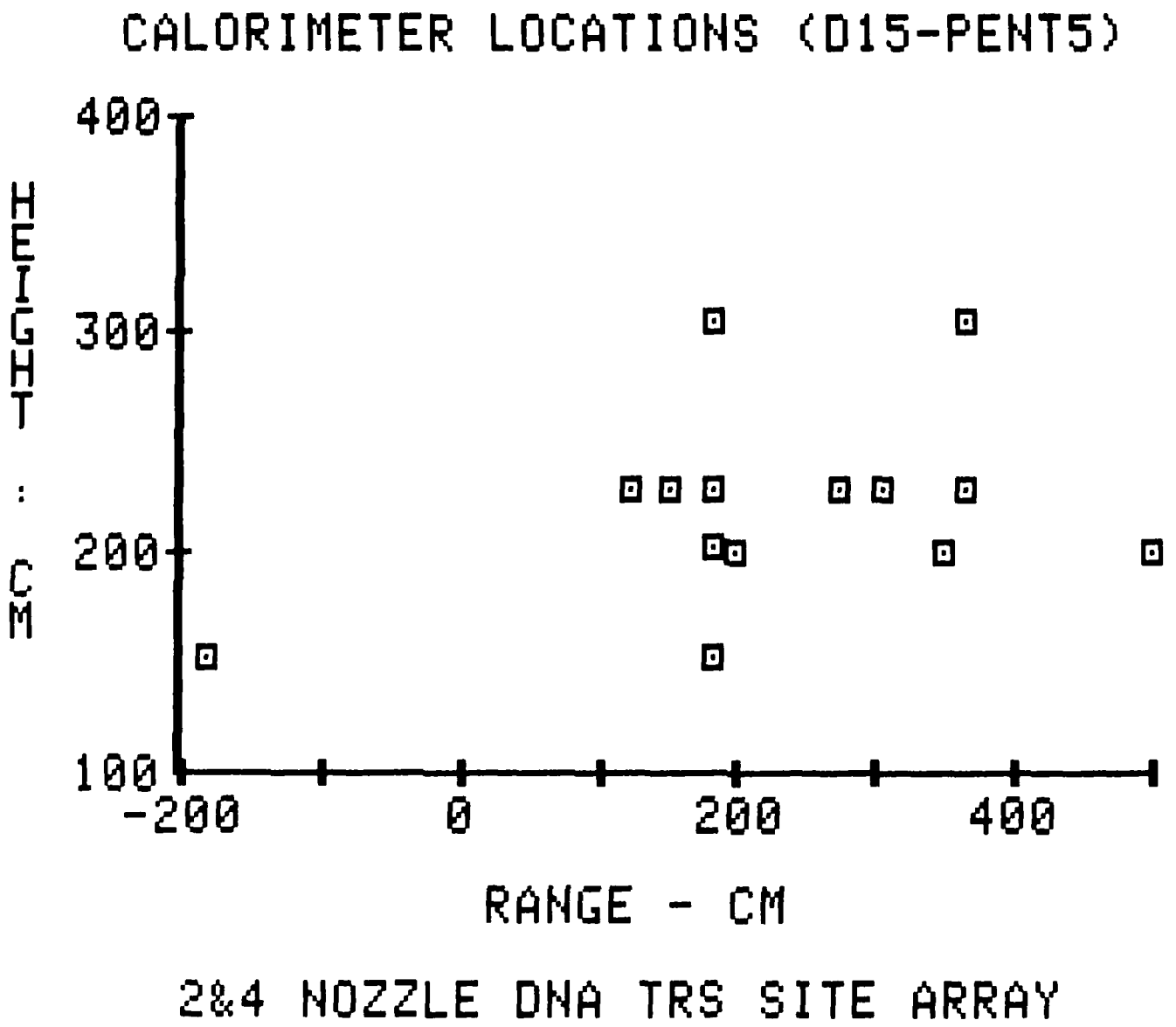

Figure 12. Calorimeter location: DNA TRS site nozzles.

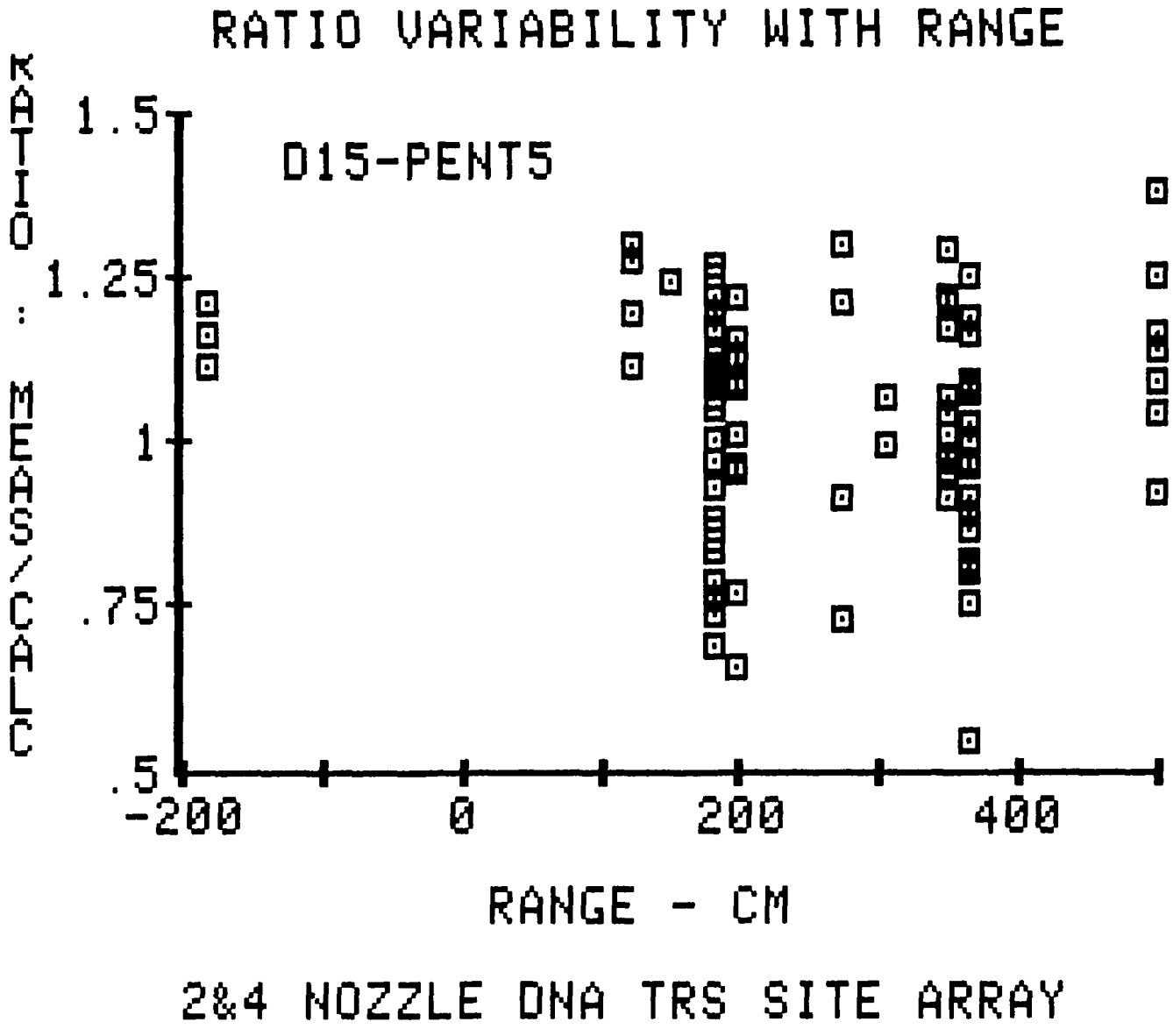

Figure 13. Ratio variability with range: DNA TRS site nozzles.

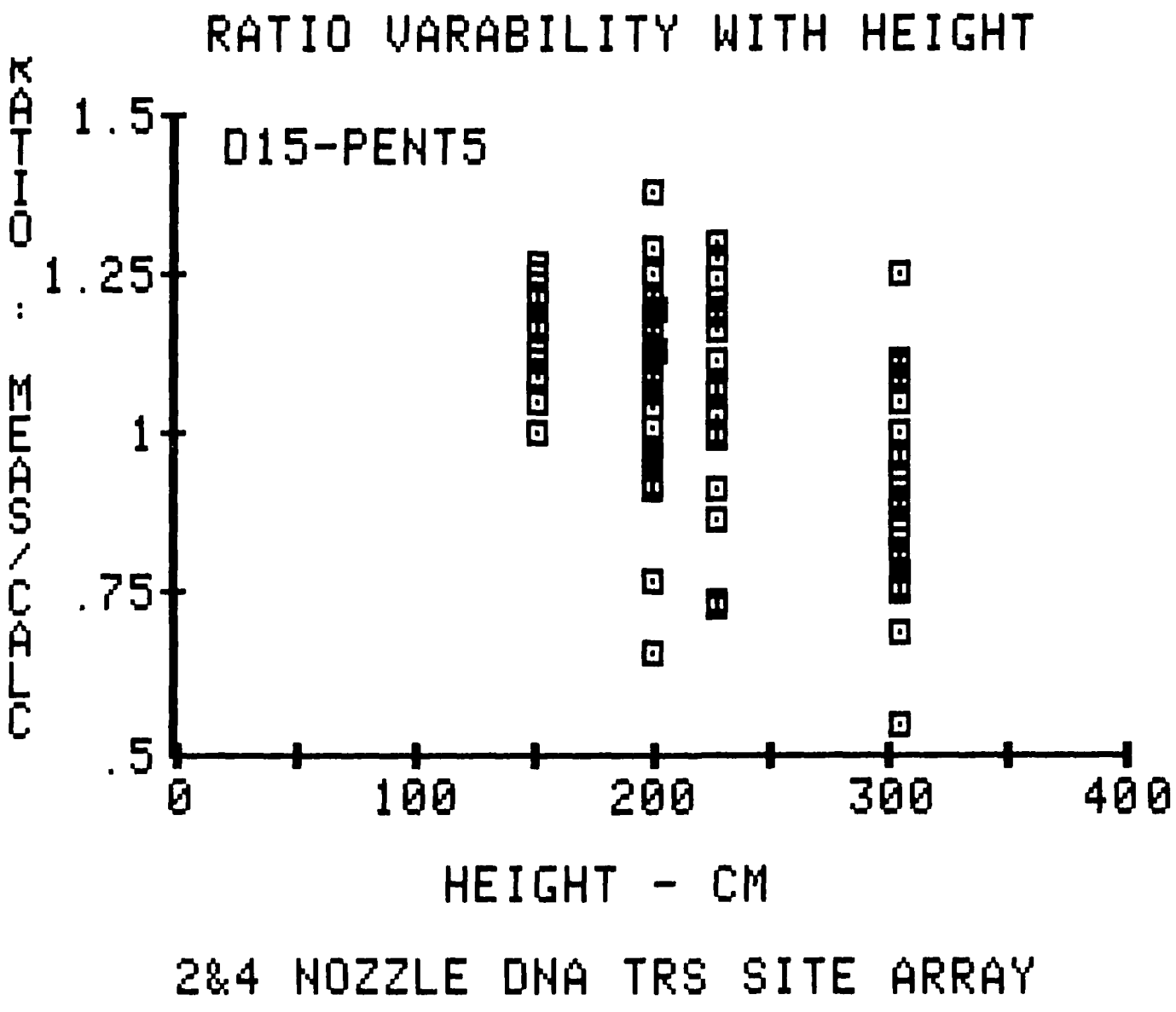

Figure 14. Ratio variability with height: DNA TRS site nozzles.

However, there does appear to be a slight bias as a function of calorimeter height. This bias with height is looked at more closely in the following subsection.

Figures 15 through 17 show similar data, but instead for the MILL RACE nozzles. Here again there does not appear to be any overall bias, neither with range nor with height. The interpretation in this case is not as straightforward, because during two of the pretest firings, the nozzles were 1.75 meters above the ground.

2-10 A CLOSER LOOK AT BIAS OF DATA BASE WITH HEIGHT.

Some of the data presented in the previous subsection showed an apparent bias of the ratio as a function of height. In this subsection, smaller samples of the data base are presented that were analyzed to see if the height bias can be made more visible, or if it is a function of event, or equivalently, time.

Figure 18 shows a plot of ratio versus height for all the data earlier than the Pentolite series, that is, Events D-15 to D-45. A slightly better hint of a height bias is seen. The alternative plot style also makes it clear where the points are really located. Subdividing these data further into two subsets, yields Figures 19 and 20. The choice of Event D-26 as the break point was somewhat arbitrary. Nevertheless, we see that the height bias is very clear for the very early data, whereas it is not clear that a bias exists for the later data.

During the early testing, considerable work was being done to improve the flame output. In fact, the reason the data earlier than D-15 has not been used in the modeling effort is that reasonable operating characteristics had not been established.

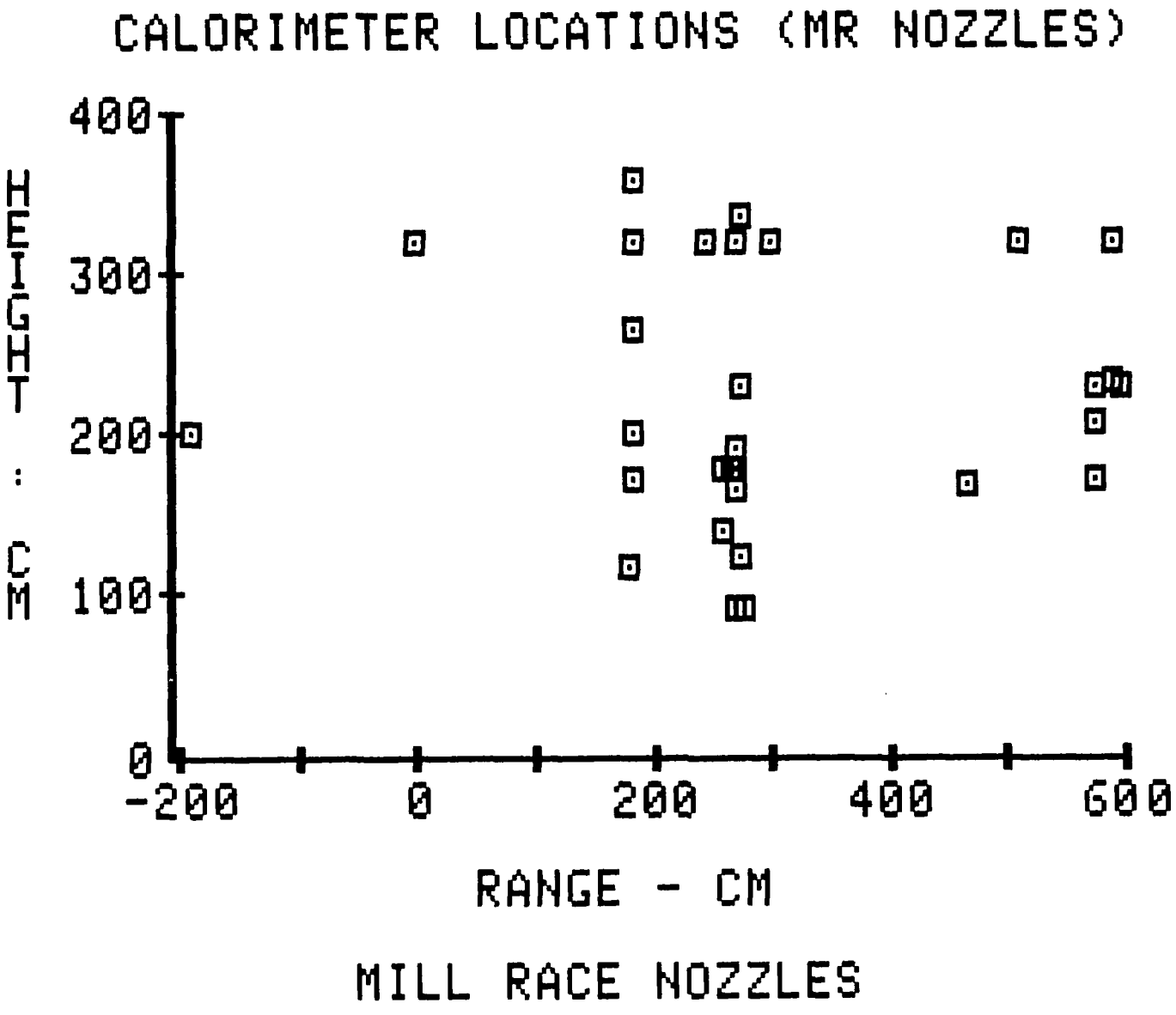

Figure 15. Calorimeter location: MILL RACE nozzles.

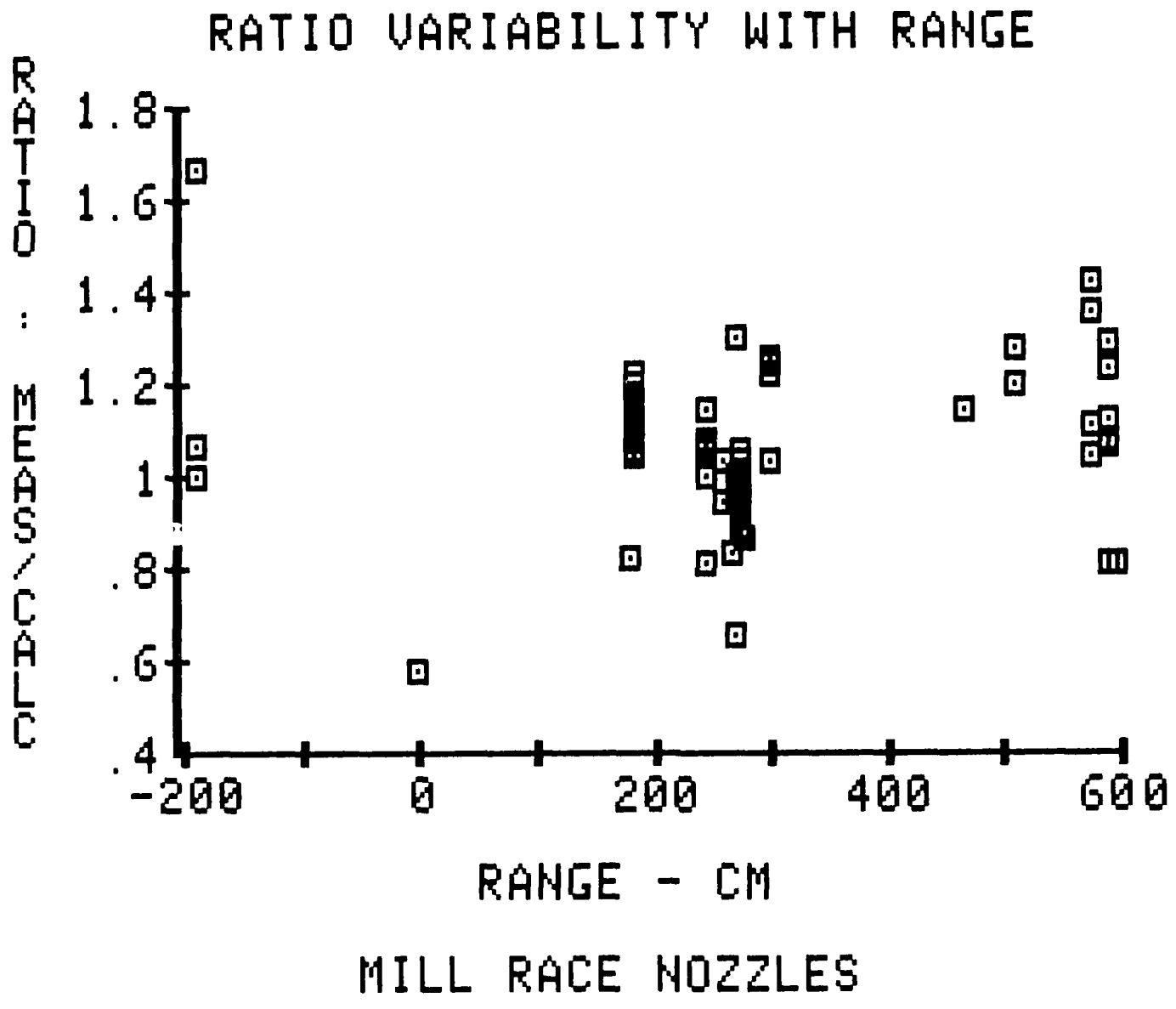

Figure 16. Ratio variability with range: MILL RACE nozzles.

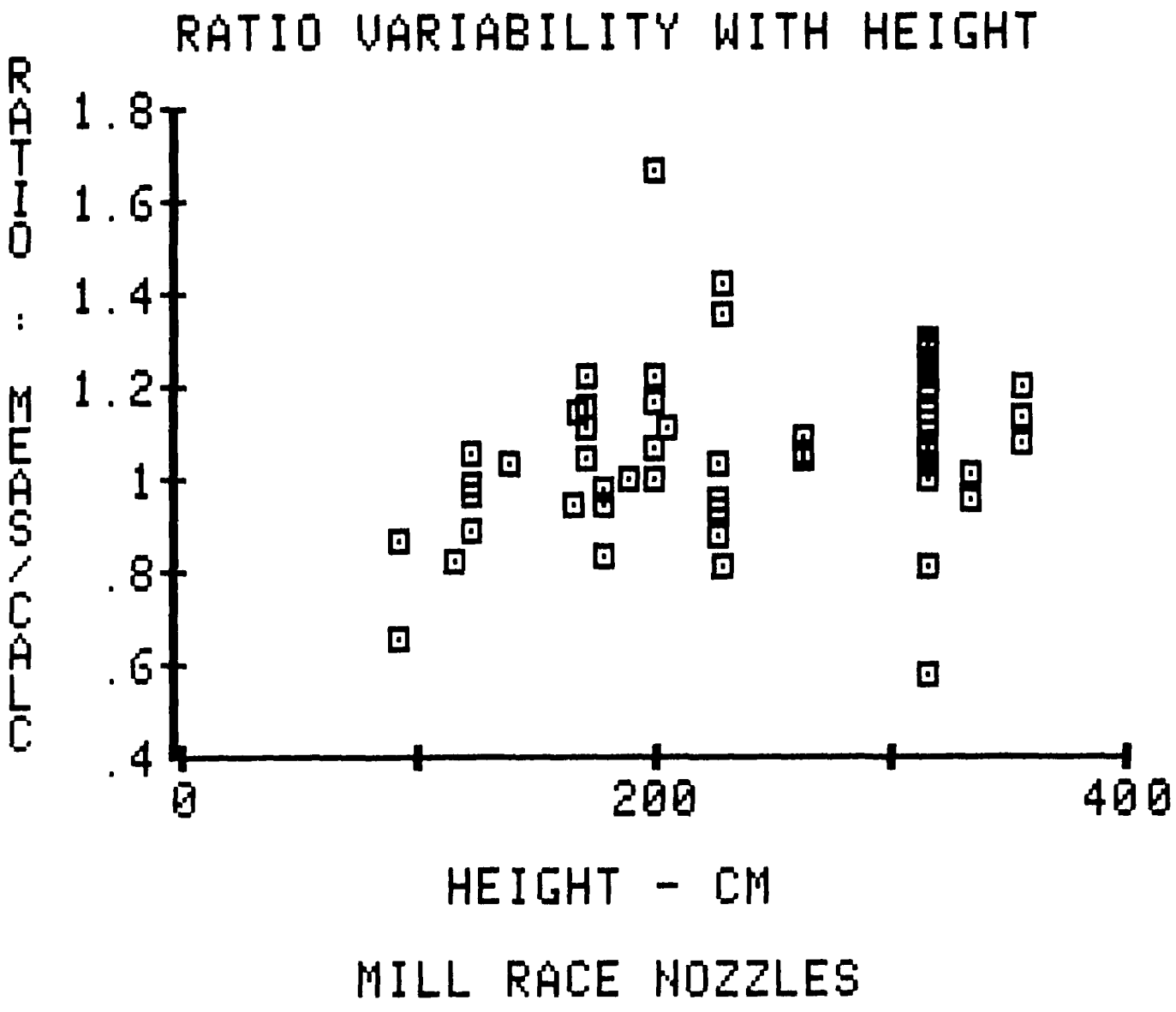

Figure 17. Ratio variability with height: MILL RACE nozzles.

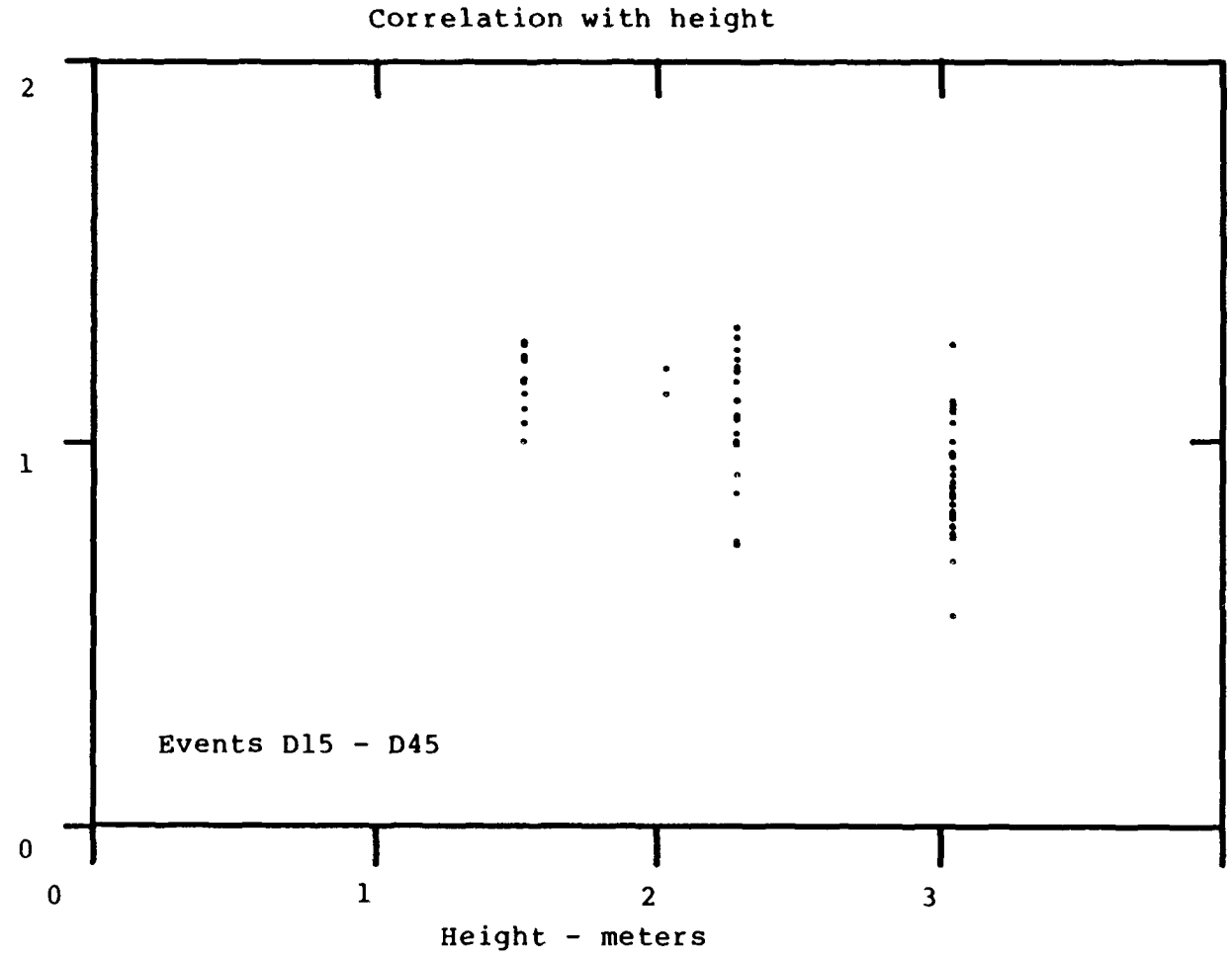

Figure 18. Ratio variability with height: events D15 to D45.

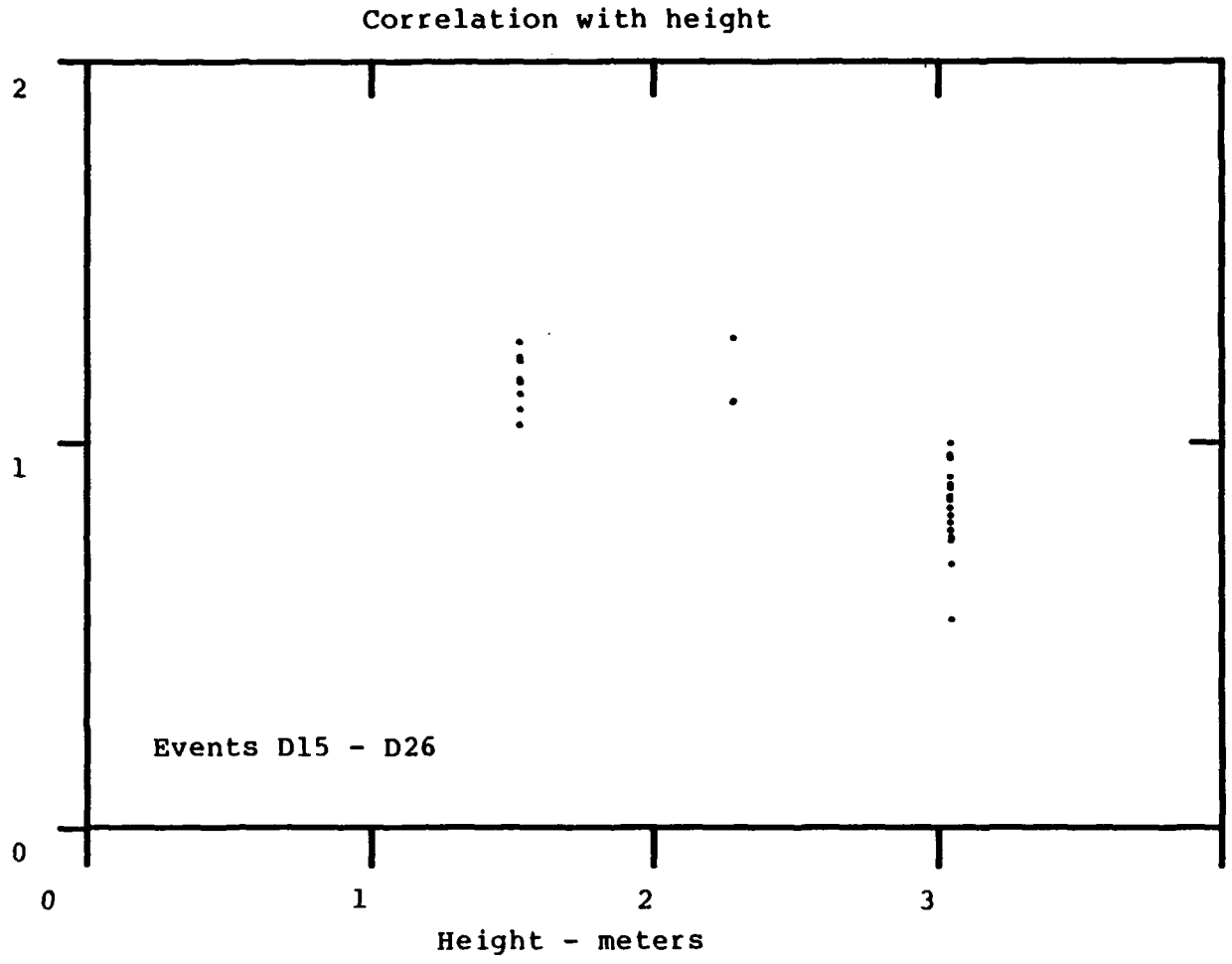

Figure 19. Ratio variability with height: events D15 to D26.

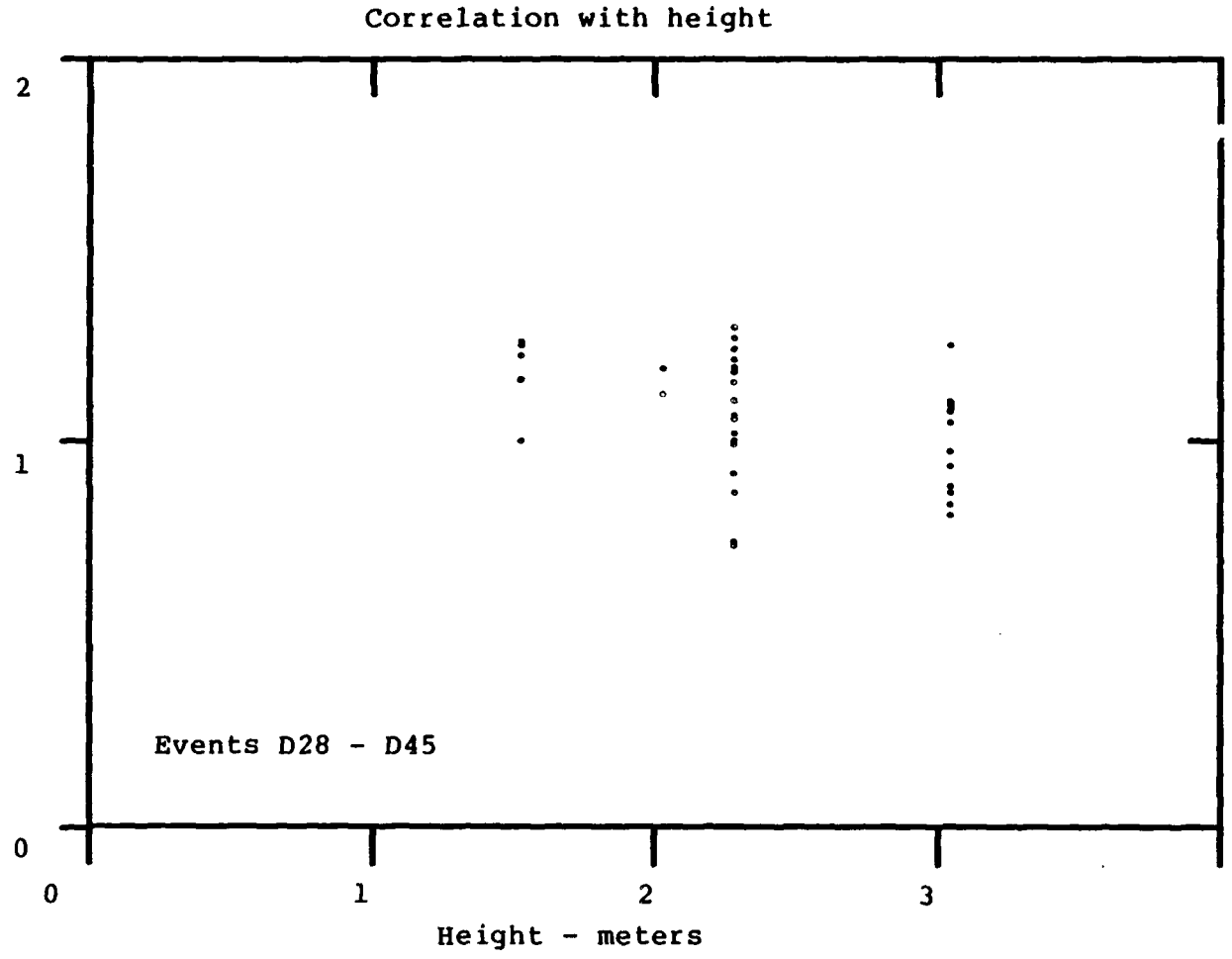

Figure 20. Ratio variability with height: events D28 to D45.

2-11 A CLOSER LOOK AT REPRODUCIBILITY.

After having inspected the entire data base taken up through MILL RACE, having gained a certain confidence in the data, and having finished the time urgent work for MILL RACE, we went back to look at the flux data to see if we could arrive at some measure of reproducibility. The most readily comparable data to establish this, as it turns out, are the early data. They are unique in that the calorimeters were never moved, except for FX-1 after it was established that both sides of the TRS unit generated nearly identical flux levels at the same range. Furthermore, the TRS unit consisted of the same two nozzles.

Figures 21 through 24 show the peak flux measurements for the four calorimeters that were available in the early test program. The calorimeters were labeled as FX-1, FX-2, FX-3 and FX-4. The position for calorimeter FX-1 changes immediately after event D-21. Clearly, the data recorded for event D-27 is anomalous.

Replotting these data, leaving out event D-27 and splitting the plot for FX-1 to reflect the two positions, more clearly reflects the true nature of the data. These are shown as Figures 25 through 29. The mean for FX-1 for events D-15 through D-21 is 41.3 calories per square centimeter per second. The corresponding unbiased standard deviation, s, is 1.39 in flux units. This compares quite well with the mean for FX-4 for events D-15 through D-31 with D-27 removed. The mean for FX-4 is 40.9 and its unbiased standard deviation is 2.90.

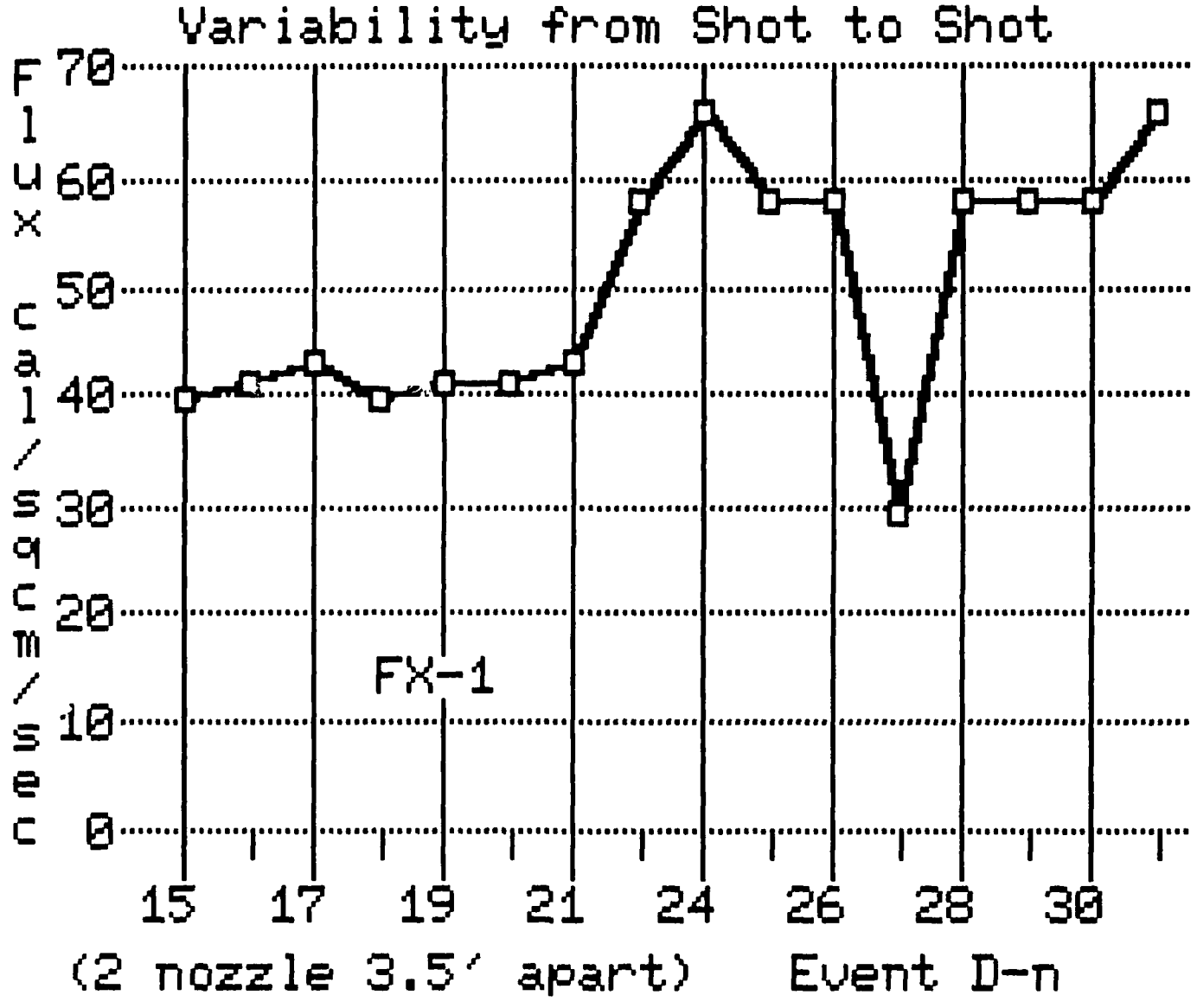

Figure 21. Early shot to shot variability: calorimeter FX-1.

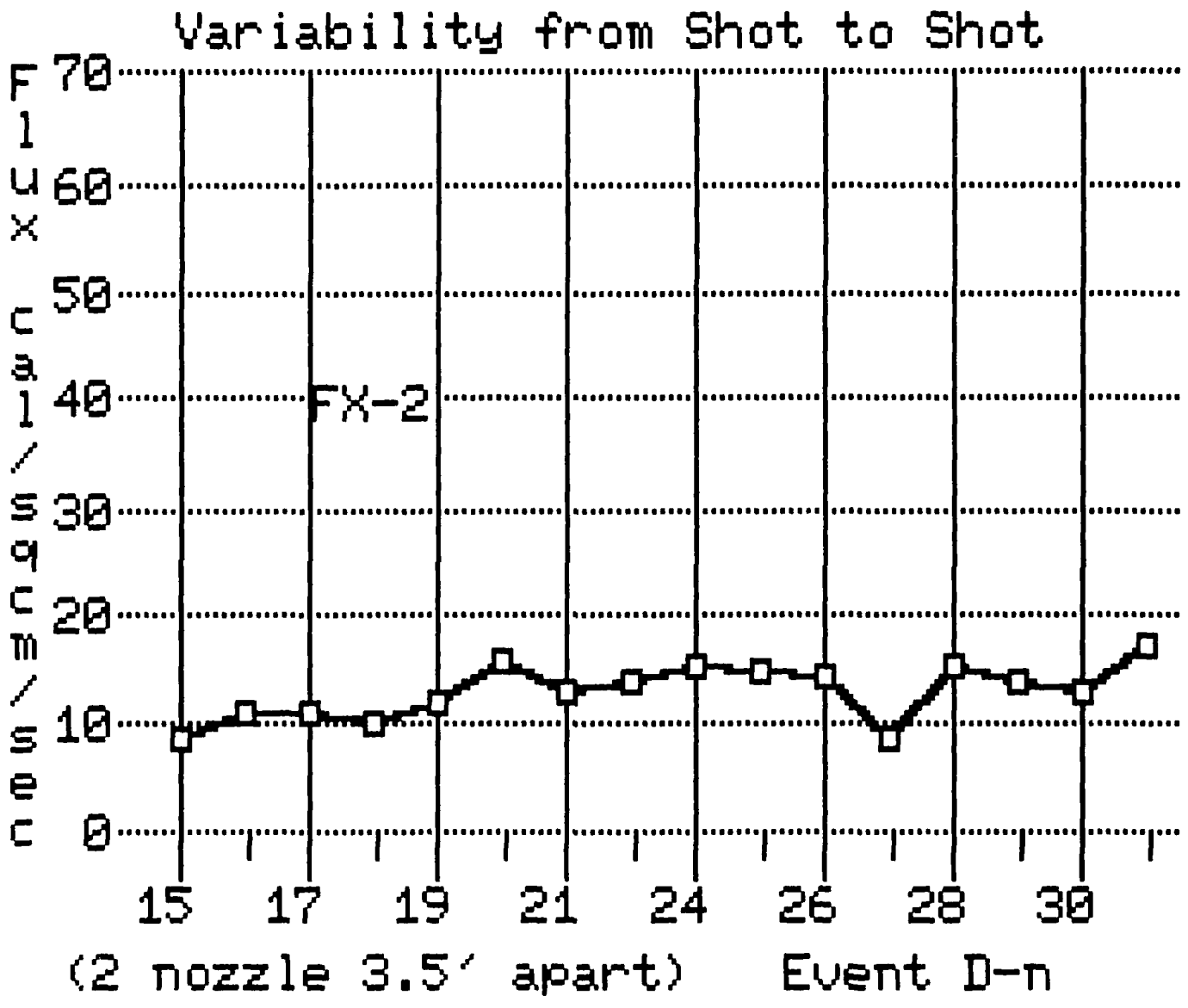

Figure 22. Early shot to shot variability: calorimeter FX-2.

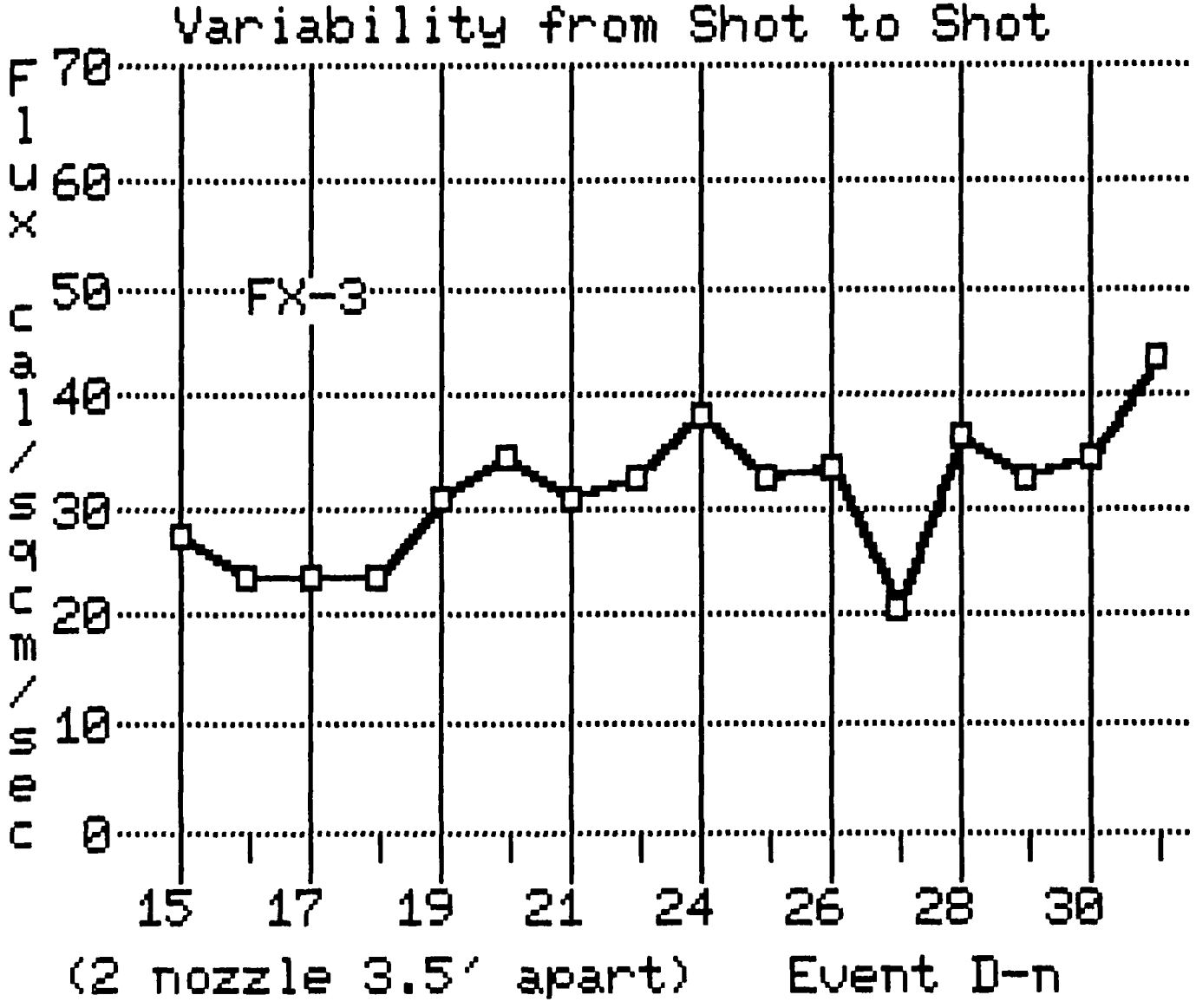

Figure 23. Early shot to shot variability: calorimeter FX-3.

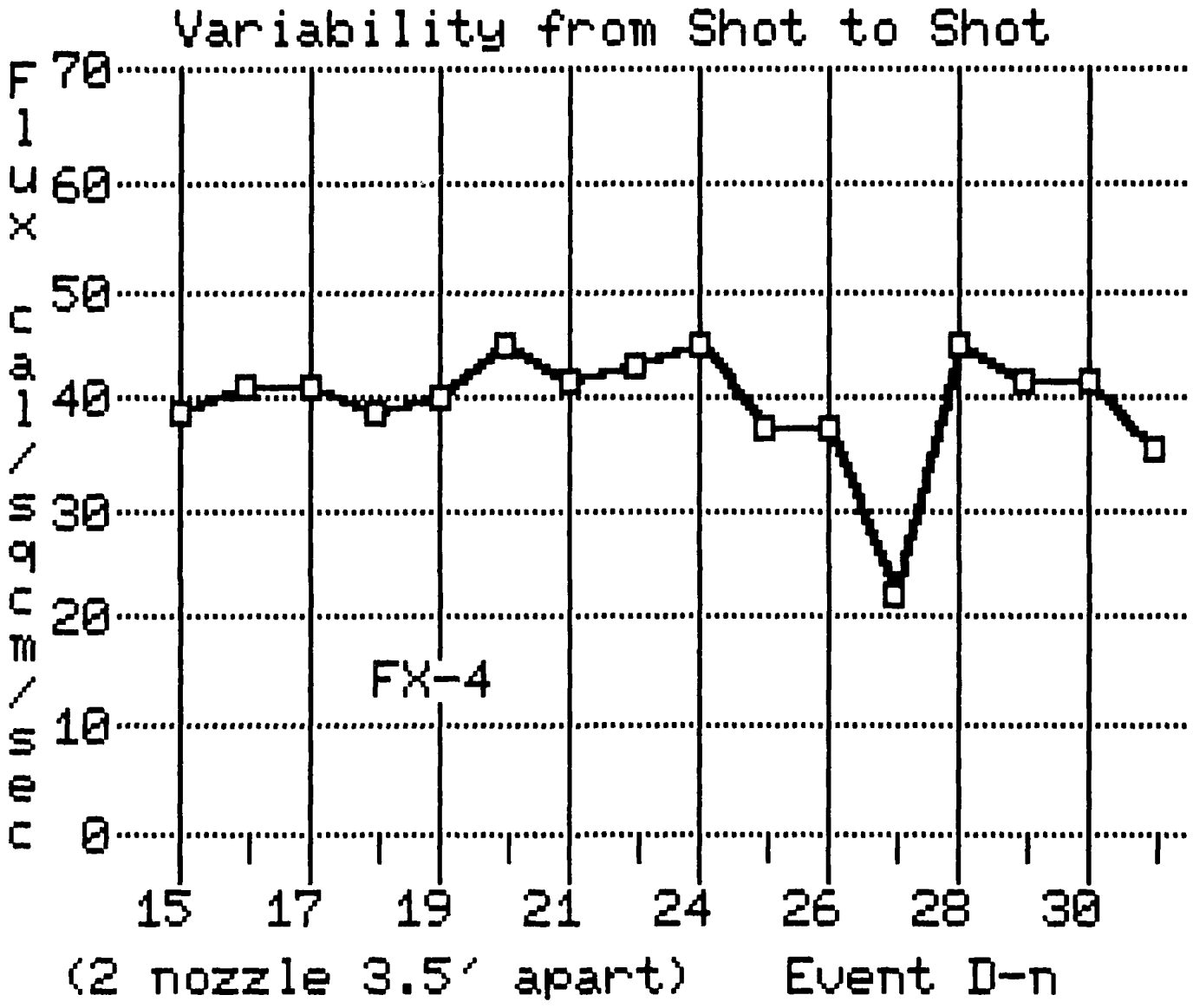

Figure 24. Early shot to shot variability: calorimeter: FX-4.

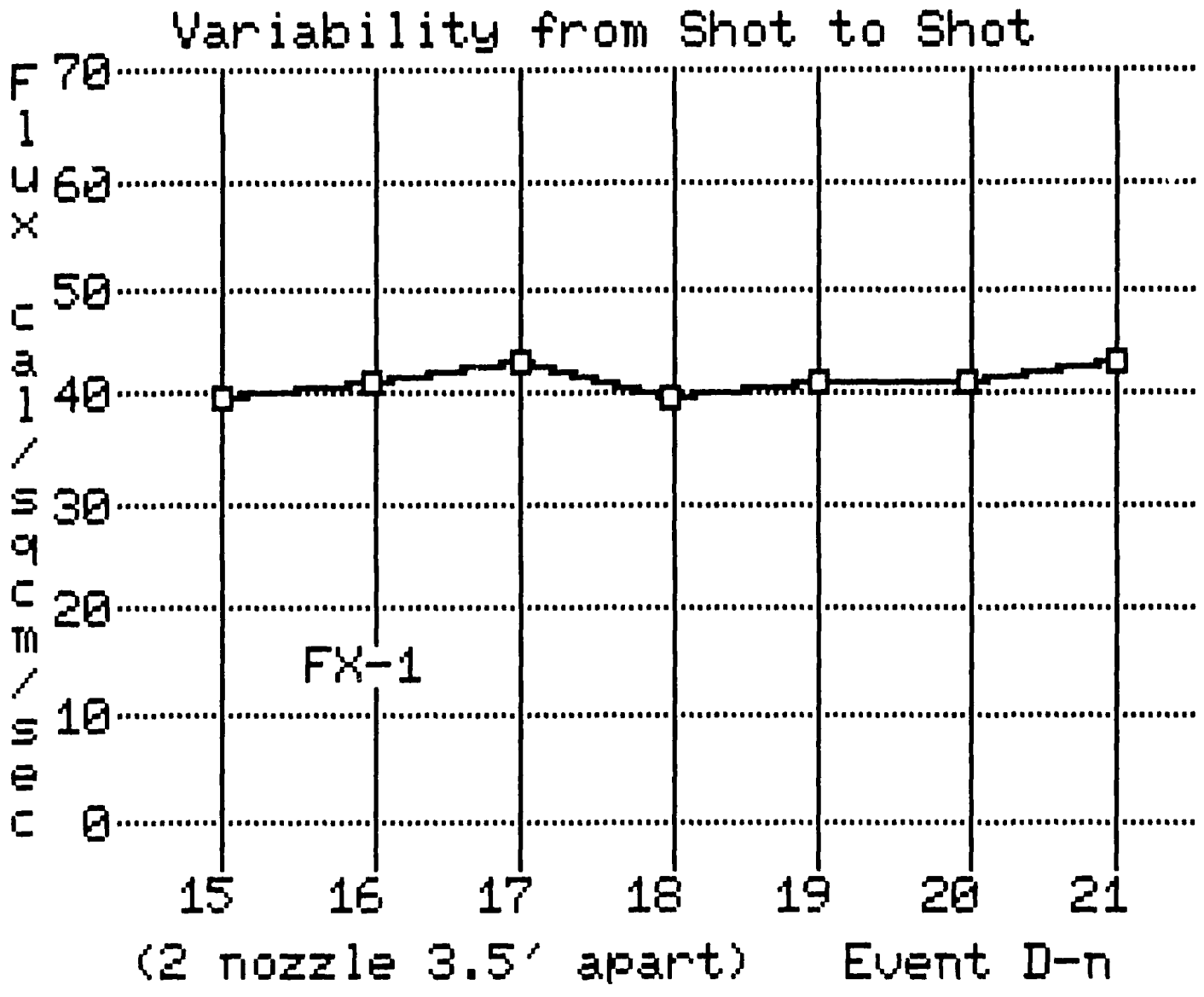

Figure 25. Shot to shot variability: FX-1 events D15 to D21.

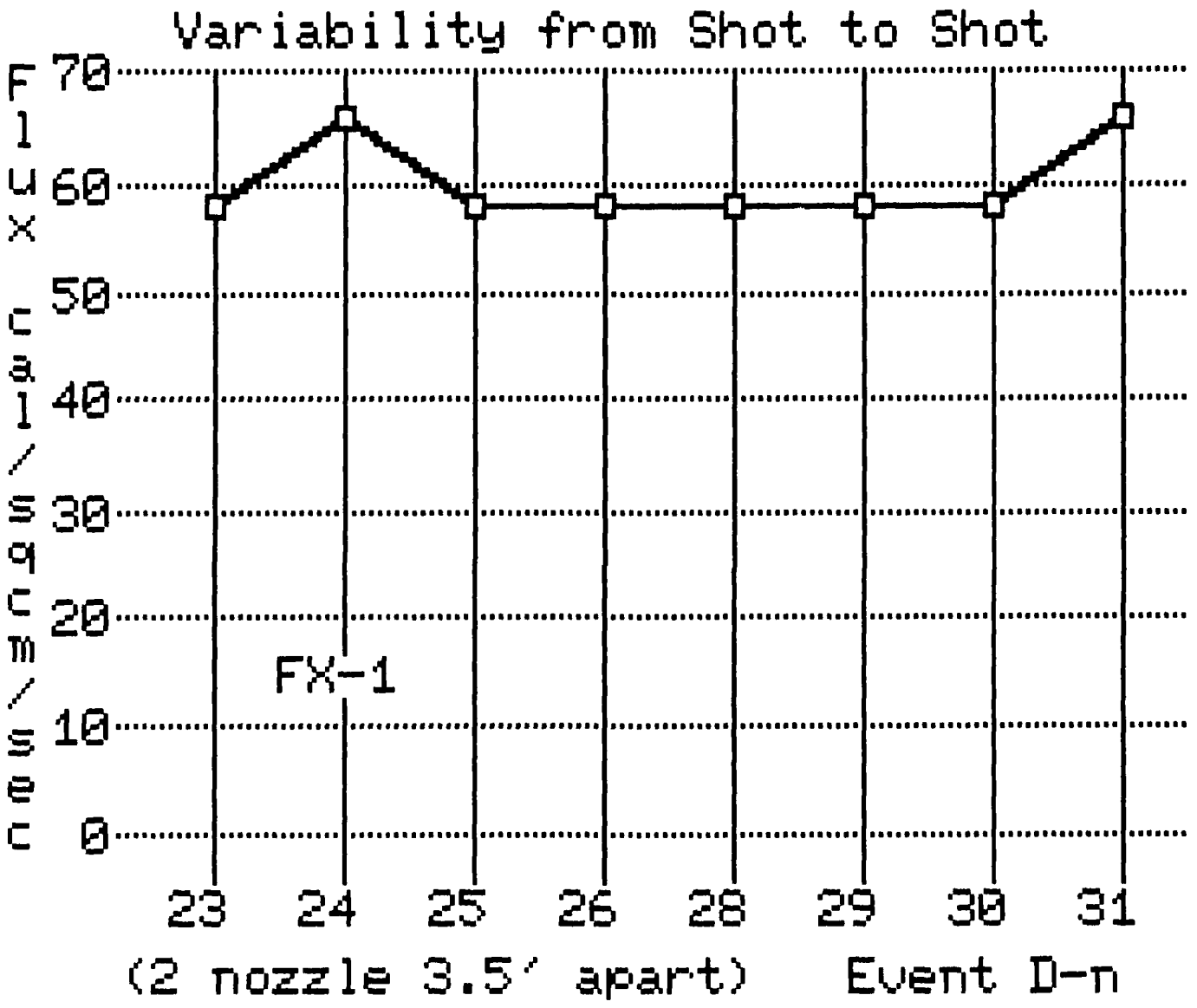

Figure 26. Shot to shot variability: FX-1 events D23 to D31.

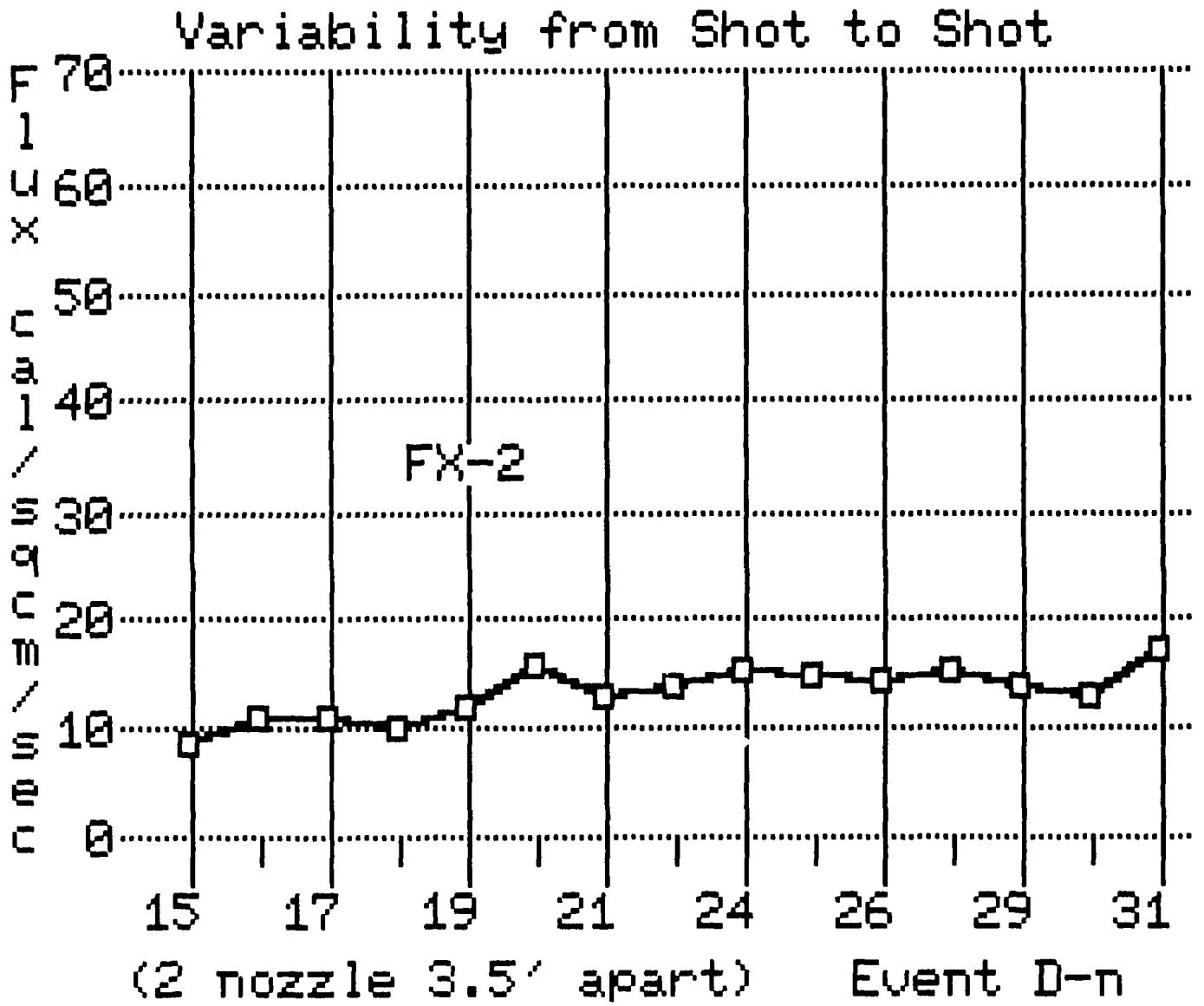

Figure 27. Shot to shot variability FX-2 events D15 to D31.

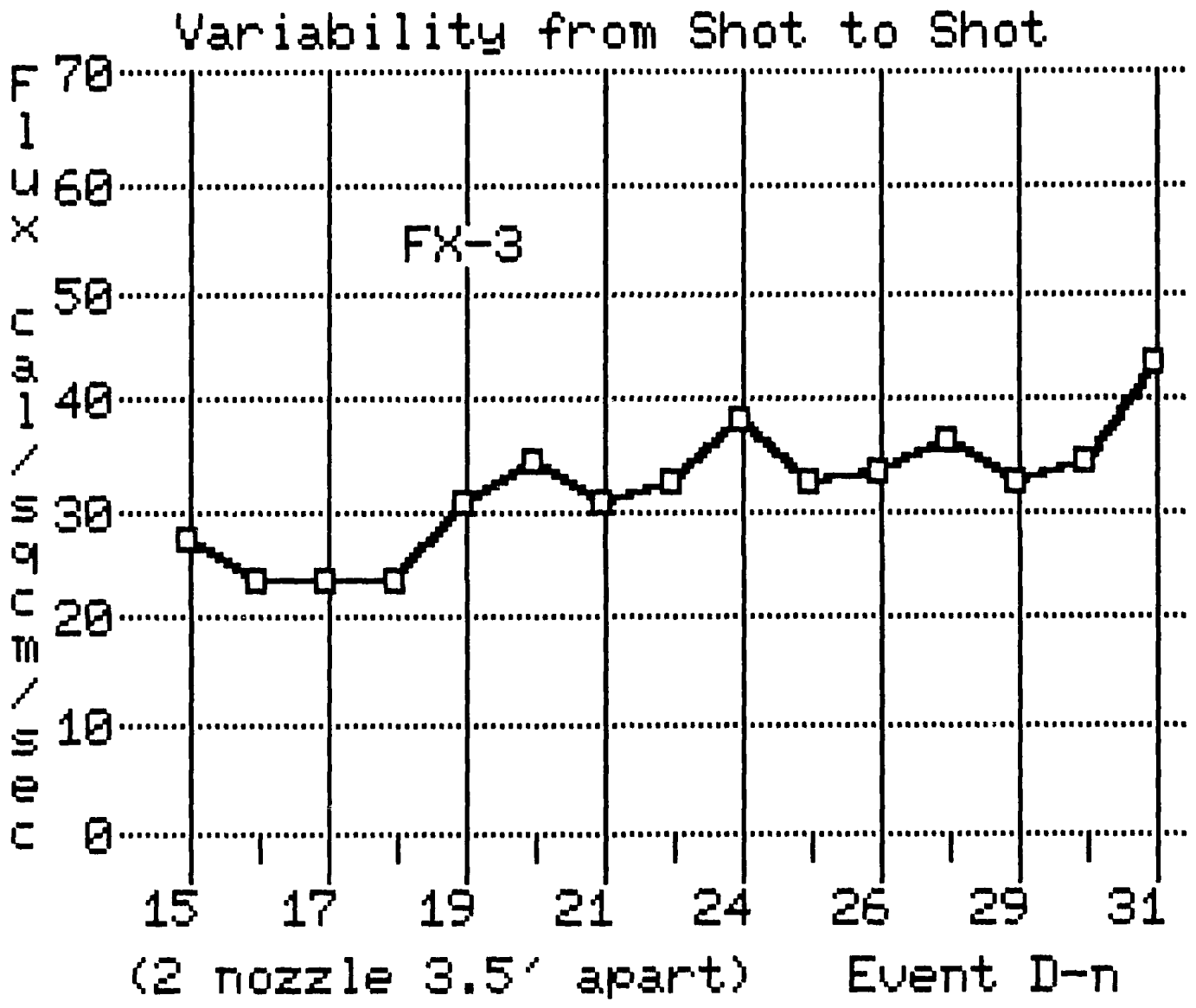

Figure 28. Shot to shot variability FX-3 events D15 to D31.

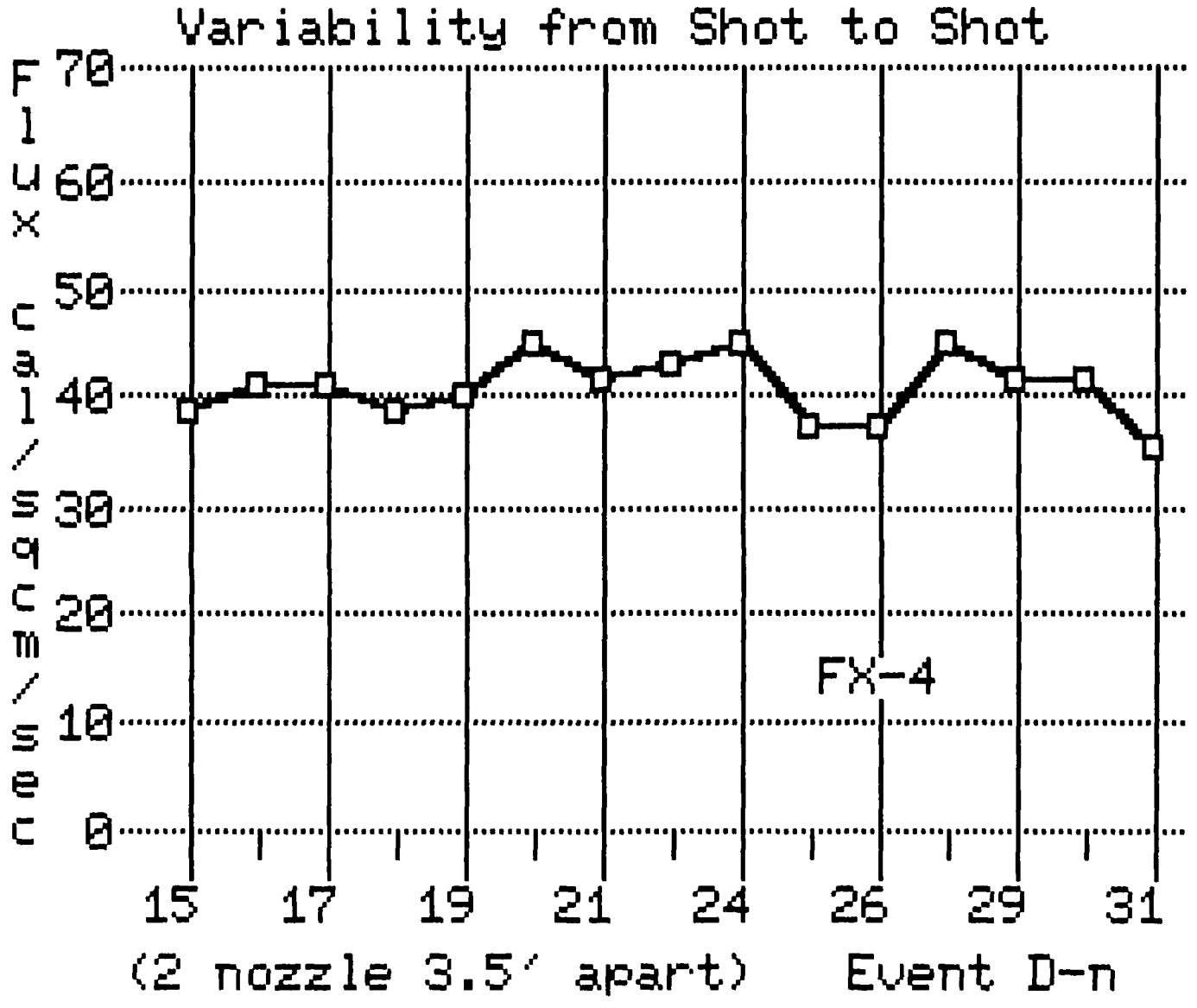

Figure 29. Shot to shot variability FX-4 events D15 to D31.

Statistics for Events D-15 through D-31

Calorimeter	Height (ft)	Event Start	Event End	Mean m	Standard Deviation	s/m
FX-1	5.0	D-15	D-21	41.3	1.39	0.03
FX-1	7.5	D-23	D-31	59.9	3.84	0.06
FX-2	10.0	D-15	D-31	13.5	2.37	0.18
FX-3	10.0	D-15	D-31	31.9	5.44	0.17
FX-4	5.0	D-15	D-31	40.9	2.90	0.07

The flux varies the most at the higher calorimeters. This is where the effects of wind will be most pronounced. From these data we get an indication that the shot to shot repeatability will depend on where the measurement is being made. Within the limited volume of space where the data were taken, the data suggest that the standard deviation is about 7 percent below 5 feet (1.52 meters) in height for ranges within 6 feet (1.83 meters) of the nozzles, and is 18 percent at 10 feet (3.05 meters) height within a range of 6 feet (1.83 meters) to 12 feet (3.66 meters).

SECTION 3

COMPARISONS WITH MILL RACE

This section presents comparisons of various ALFGEE models with calorimeter data taken on MILL RACE. These comparisons illustrate the size of the differences that can be expected as a result of calibrating ALFGEE to limited data. Twenty diagnostic calorimeters were fielded by Ballistics Research Laboratory (BRL) for DNA. One of the calorimeters failed to produce any data. About half of the rest agreed very well with the model predictions. Two calorimeters gave very different values from what was expected. One of them was about 50 percent too high and the other was about 50 percent too low. On the whole, the modeling provided a reasonably accurate prediction capability.

Not all of the TRS units burned as had been hoped. One in particular, UK-1, had two nozzles that did not ignite, because a jammed flow valve stopped aluminum flow. Furthermore, another nozzle on this same unit apparently did not burn well due to a faulty pilot flame. Based on performance of the TRS units on MILL RACE, experimenters should consider possible deviations from planned environments, especially at locations where little experimental data exist upon which to base the modeling.

3-1 ALFGEE MILL RACE COMPARISONS (CYLINDRICAL).

The comparisons of the peak flux data taken on the BRL/HDL HATS TRS is summarized first since its nozzle separation was the same as all the data taken prior to the pretest firings of the MILL RACE TRS units. Its nozzles were spaced 3.5 feet apart. The agreement with the model, as it existed prior to MILL RACE, is shown in Table 5 (Model A cylindrical). Only three out of four diagnostic calorimeters yielded data for this four nozzle burn. Only two

Table 5. Comparisons of BRL TRS at MILL RACE with DNA ALFGEE model.

Peak Flux (cal/cm/cm/s)

	Mill Race	Model-A	Model-B	Model-82
F-1	62.0	39.8	39.6	41.0
F-2	50.6	55.6	52.2	54.8
F-3	No data	55.9	52.5	55.1
F-4	37.6	40.7	40.4	41.8

Note: Model-A is best model used prior to MILL RACE.
Model-B is recalibration to 162 point data base.
Model-X is inverted cone 3.5' calibration.

of these calorimeter records were consistent with the expected environments. The cylindrical model was calibrated to the meager data obtained during the BRL TRS unit pretest firings. This calibration improves the agreement of model and MILL RACE data. We assert that these comparisons show that the data from calorimeter F-1 is highly suspicious.

The results for UK-2 are shown in Table 6, where the calibration based on the sparse eleven point 7 feet spacing data base yields the best agreement. Calorimeter F-1 is the only one that disagrees by more than three per cent from the expected environment.

The results for UK-1, the only 8 nozzle system (7' spacing), was unique in that two nozzles, numbers 3 and 4, did not inject any aluminum into the air. Not only did these nozzles fail to contribute any flux to the environment, but the fact that they did not ignite makes it difficult to select an appropriate calibration with which to measure the performance of the TRS system. Furthermore, the films of the BRL TRS shown during the MILL RACE symposium show that nozzle 7 burned in an unusual manner and may have contributed significantly less flux than otherwise would have been expected.

Because the effect of the nozzles either not firing or misfiring was uncertain, a number of calculations with different models were performed with the intent to estimate the magnitude of the possible effects. The results, summarized in Table 7, show that the calibration to the 11 point 7' spacing data again yielded the best overall agreement but only when nozzles 3 and 4 are turned off. No evaluation of the effect of additionally turning off nozzle 7 has been made.

Finally, the 10.5' spacing Navy 4 nozzle TRS results are summarized in Table 8. A study was performed to determine whether any use of the data obtained during the experimental calibration of the Navy TRS could be made for calibrating a model based on a cylindrical flame. It was possible to substantially improve the agreement for the two calorimeters that were placed farthest out. However, the results for the two close-in calorimeters were degraded.

Table 6. Comparisons of UK-2 TRS at MILL RACE with DNA ALFGEE model.

Peak Flux (cal/cm/cm/s)

	Mill Race	Model-A	Model-C	Model-82
F-1	12.5	14.4	14.3	14.7
F-2	30.3	28.9	29.5	30.8
F-3	32.0	29.9	31.7	32.0
F-4	21.7	21.7	21.6	23.0

Note: Model-A is model used prior to MILL RACE
Model-C is recalibration to 11 point 7' data base.
Model-Y is inverted 7' calibration.

Table 7. Comparisons of UK-1 TRS at MILL RACE with DNA ALFGEE model.

Peak Flux (cal/cm/cm/s)

	Mill Race	Model-A	Model-S1	Model-C	Model-S2	Model-82
F-1	16.5	22.0	19.3	20.0	19.3	22.2
F-2	22.5	22.3	22.2	29.1	22.0	23.8
F-3	12.7	14.4	13.2	32.2	12.7	14.1
F-4	7.2	8.4	9.7	14.0	9.2	8.3
F-5	6.8	9.5	11.3	19.4	9.5	9.2
F-6	13.6	13.9	15.1	23.7	11.2	13.7
F-7	14.4	13.2	15.5	19.3	11.0	13.2
F-8	11.5	10.8	12.8	14.0	10.2	10.8

Note: Model-A is 3.5' model used prior to MILL RACE
Model-S1 is recalibration to 11 point 7' data base (N 3&4 OFF).
Model-C is recalibration to 11 point 7' data base (N 3&4 ON).
Model-S2 is recalibration to 11 point 7' data base (N 3&4&6 OFF - should have been 3&4&7).
Model-82 is with Nozzles 3 & 4 off.

Table 8. Comparisons of NAVY TRS at MILL RACE with DNA ALFGEE model.

Peak Flux (cal/cm/cm/s)

	Mill Race	Model-A	Model-C	Model-D	Model-Z	Model-82
F-1	13.2	15.4	14.3	16.5	15.2	15.4
F-2	13.2	9.7	11.4	13.2	11.9	10.0
F-3	12.0	9.7	11.1	12.8	11.6	10.0
F-4	12.0	18.8	17.4	20.1	18.5	18.9

Note: Model-A is model used prior to MILL RACE
Model-C is recalibration to 11 point 7' data base.
Model-D is recalibration to 9 point 10.5' data base.
Model-Z is Inverted calibration to 19 pt 10.5' data.

It should be mentioned that the calibration shot performed on the Navy TRS unfortunately included only calorimeters placed at the same height of 3.2 meters. That particular arrangement makes it very difficult to calibrate any model with any degree of confidence.

3-2 USE OF INVERTED CONE MODEL WITH TRS DATA BASE.

Predictions based on the new inverted cone model with the changed view angle algorithms were compared with the entire TRS data base to determine whether it is indeed an improvement, and what are the best parameters to model the experimental results. The conclusion thus far seems to be that all of the recent data could be represented with one calibration, instead of having to resort to a different calibration for each nozzle spacing. In other words, it may be possible to explain the effects of greater nozzle separation on geometric and obscuration considerations. If in fact this conclusion is finally supported, a possibly sound basis for better quantifying the shot to shot variability may now exist.

As further testimony to the apparent improvement gained with the new inverted cone model, we would like to mention that two of the model parameters were taken directly from cursory measurements on still pictures of flames at a time of peak flux. This latter fact greatly improves our confidence that the newest model may approximate very well the TRS flame thermal radiation environment.

3-3 COMPARING CALIBRATIONS FOR MILL RACE.

A number of comparisons between pairs of calibrations were performed to evaluate the sensitivity of the agreement with the MILL RACE data to model parameters. Some of the comparisons were useful; many were not. In order to acquaint the reader with the relative changes made with different model parameters, the following comparison is presented.

Table 9 is one example of the comparisons made between different models. This table shows four calibrations and compares the results of each model prediction for the set of data that includes both the UK-1 and UK-2 units pre MILL RACE test firings and the MILL RACE firings. Since two of the nozzles did not fire for the UK-1 unit on MILL RACE, their source strength was set to zero in the model predictions. No account, however, was taken for the badly fired nozzle, since we had no way of knowing what its strength was on the test.

Overall the comparisons presented here show that the cylindrical model gave slightly better results than the three calibrations to the inverted cone model. While this will sometimes be the result for these types of comparisons, the general result has been that the inverted cone model can more consistently agree with experimental data. This particular comparison illustrates that choosing the best geometrical representation for modeling is not necessarily straightforward.

3-4 COMPARING FLUX FIELD MAPS.

Substantial differences can exist between the predictions of one model over another at some locations. Less often, this can even be true if both were calibrated to similar data. It happens quite frequently, however, when the models have to be used in regions where the results must be extrapolated.

The following tables, 10 through 13, show some comparisons between pairs of two models that shed some light on where biases can be significant. For example, the comparison of model A and model D for the Navy MILL RACE TRS unit shows similar results at the ground, but model D predicts a significantly higher flux (about 40 percent) at 3 meters height.

These types of comparisons can be important for planning HE tests because they illustrate the uncertainties in model predictions. When these uncertainties are large and when this is important to the experimenter, he

Table 9. Comparisons of models for UK-1 & 2.

26-APR-82 COMPARISONS OF MODELS FOR UK-1&2

OLD MODEL		NEW MODEL			
18973000		POWER	21370600	31615000	24828600
160.00		DIAM	300.00	480.06	400.00
687.00		HGT	640.08	640.08	640.08
1.00	BRKHGT	LUM-LIM	1.00	4.00	2.00
1.00	BRKSTR	POW@NOZ	25.00	25.00	25.00
0.20		ALBEDO	0.00	0.00	0.00
1.11		UK-1 FX-1	1.19	1.17	1.17
1.10		UK-1 FX-2	1.18	1.20	1.18
1.09		UK-1 FX-3	1.17	1.19	1.17
1.12		UK-1 CA-4	1.23	1.25	1.24
0.96		UK-1 CA-6	1.10	1.10	1.10
0.93		UK-1 FX-4	1.00	0.98	0.98
1.10		UK-1 CA-1	1.15	1.12	1.13
1.06		UK-1 CA-2	1.11	1.10	1.11
1.12		UK-1 CA-3	1.17	1.17	1.17
1.14		UK-1 CA-5	1.19	1.17	1.17
1.07			1.15	1.15	1.14
1.07		UK-2 CA-1	0.89	0.91	0.90
0.80		UK-2 CA-2	0.97	0.95	0.96
1.09		UK-2 CA-3	0.92	0.97	0.95
0.84		UK-2 CA-4	1.03	1.00	1.02
1.09		UK-2 CA-5	0.92	0.97	0.94
0.76		UK-2 CA-6	0.94	0.92	0.93
0.72		UK-2 CA-7	0.88	0.85	0.87
0.86		UK-2 FX-1	0.85	0.84	0.85
0.89		UK-2 FX-2	0.89	0.90	0.90
0.91		UK-2 FX-3	0.90	0.91	0.91
1.01		UK-2 FX-4	1.00	0.99	1.00
0.91			0.93	0.93	0.93

Table 9. Comparisons of models for UK-1 & 2 (continued).

0.85	UK-1 F-1	0.82	0.79	0.80
1.01	UK-1 F-2	0.94	0.90	0.92
0.96	UK-1 F-3	0.90	0.99	0.94
0.74	UK-1 F-4	0.77	0.73	0.75
0.60	UK-1 F-5	0.70	0.74	0.71
0.90	UK-1 F-6	1.05	1.05	1.05
0.93	UK-1 F-7	1.25	1.23	1.24
0.90	UK-1 F-8	1.32	1.30	1.30
0.86		0.97	0.97	0.96
0.87	UK-2 F-1	0.81	0.79	0.80
1.03	UK-2 F-2	0.95	0.95	0.94
1.01	UK-2 F-3	0.95	0.95	0.95
1.00	UK-2 F-4	0.92	0.90	0.91
0.98		0.91	0.90	0.90
0.96		1.00	1.00	1.00

Table 10. Navy model comparison for MILL RACE maps.

NAVY MODEL COMPARISON FOR MILL RACE MAPS 29DEC81

X(M)	Y(M)	Z(M)	MOD A	MOD D	D/A
2	0	0	21.27	19.65	0.92
	4		20.58	18.20	0.88
	8		4.60	4.34	0.94
	0	3	22.76	32.83	1.44
	4		22.01	31.20	1.42
	8		4.85	6.53	1.35
6	0	0	9.21	10.78	1.17
	4		7.85	9.23	1.18
	8		4.31	5.26	1.22
	0	3	9.52	14.06	1.48
	4		8.11	11.97	1.48
	8		4.42	6.49	1.47

Table 11. BRL model comparisons for MILL RACE maps.

BRL MODEL COMPARISONS FOR MILL RACE MAPS 29DEC81

X(M)	Y(M)	Z(M)	MOD A	MOD B	B/A
2	0	0	45.43	42.01	0.92
	4		8.19	8.70	1.06
	8		1.04	1.15	1.11
	0	3	48.75	45.08	0.92
	4		8.72	9.28	1.06
	8		1.07	1.18	1.10
6	0	0	12.21	11.27	0.92
	4		7.10	6.81	0.96
	8		2.43	2.42	1.00
	0	3	12.66	11.68	0.92
	4		7.33	7.03	0.96
	8		2.48	2.47	1.00

Table 12. UK-2 model comparisons for MILL RACE maps.

UK-2 MODEL COMPARISONS FOR MILL RACE MAPS 29DEC81

X(M)	Y(M)	Z(M)	MOD A	MOD C	MOD I	MOD I-	C/A	I/A	I-/A
2	0	0	31.22	23.56	24.00	24.00	0.75	0.77	0.77
	4		19.23	14.32	14.36	12.40	0.74	0.75	0.64
	8		2.14	1.82	1.93	1.43	0.85	0.90	0.67
	0	3	33.44	40.56	41.45	41.45	1.21	1.24	1.24
	4		20.56	24.56	25.05	20.92	1.19	1.22	1.02
	8		2.23	2.51	2.67	1.95	1.13	1.20	0.87
6	0	0	10.53	10.85	10.70	10.70	1.03	1.02	1.02
	4		8.10	8.20	8.15	7.85	1.01	1.01	0.97
	8		3.69	3.65	3.65	3.41	0.99	0.99	0.92
	0	3	11.20	14.36	14.17	14.17	1.28	1.27	1.27
	4		8.36	10.62	10.56	10.13	1.27	1.26	1.21
	8		3.78	4.41	4.41	4.09	1.17	1.17	1.08

Table 13. UK-1 model comparisons for MILL RACE maps.

UK-1 MODEL COMPARISONS FOR MILL RACE MAPS 29DEC81

X(M)	Y(M)	Z(M)	MOD A	MOD S1	MOD S2	S1/A	S2/A
2	-10	0	6.95	5.23	5.21	0.75	0.75
	-5		21.95	16.45	16.33	0.75	0.74
	0		18.18	13.20	10.50	0.73	0.58
	5		31.59	23.80	17.46	0.75	0.55
	10		7.41	5.49	5.26	0.74	0.71
	-10	3	7.39	8.32	8.30	1.13	1.12
	-5		23.48	28.66	28.51	1.22	1.21
	0		19.39	22.18	17.98	1.14	0.93
	5		33.82	41.08	30.25	1.21	0.89
	10		7.86	8.65	8.35	1.10	1.06
6	-10	0	5.19	5.08	4.90	0.98	0.94
	-5		8.61	8.47	7.76	0.98	0.90
	0		10.15	10.34	7.98	1.02	0.79
	5		11.49	11.36	8.49	0.99	0.74
	10		6.23	6.97	5.16	1.12	0.83
	-10	3	5.34	6.43	6.23	1.20	1.17
	-5		8.88	10.89	10.06	1.23	1.13
	0		10.44	13.15	10.10	1.26	0.97
	5		11.88	14.89	11.07	1.25	0.93
	10		6.40	7.86	6.54	1.23	1.02

should insist on more calibration of the TRS unit to be used.

3-5 A NOTE ON THE MILL RACE DATA.

Comparison of experimental measurements with theoretical predictions or model results should include a presentation of the experimental data. Since the data are still unpublished, a preliminary result for calorimeter F-4 exposed to the BRL unit on MILL RACE is shown as Figure 30.

Calorimeter F-2 exhibited a waveform similar to that shown in Figure 30 for F-4. Calorimeter F-1, on the other hand showed a significantly different waveform. Unfortunately, calorimeter F-3 failed.

All four calorimeters had been placed at the same range, 1.9 meters, from the nozzles on the ground zero side of the array. They also had been located at the same height of 2.0 meters. One calorimeter was placed in front of each of the four nozzles in an effort to record each nozzles' performance. Since the field of view of each calorimeter was not limited some contribution from the other nozzles was measured at each calorimeter (those that worked, that is).

The agreement of the BRL MILL RACE data with the model calculations was good (within ten percent) for calorimeters F-2 and F-4. Since these were the ones with similar waveforms, the agreement is encouraging. The fact that the agreement is poor for F-1 does not immediately lead to a conclusion. Did wind affect the results for this calorimeter? Is the model reliable? Until the the number of diagnostic calorimeters is increased on these tests, many questions will remain unanswered. If the variability of the experiment was substantially less, then it would be sufficient to use just a few diagnostic calorimeters. Since that is not the case, it should be our practice to use at least three calorimeters per nozzle.

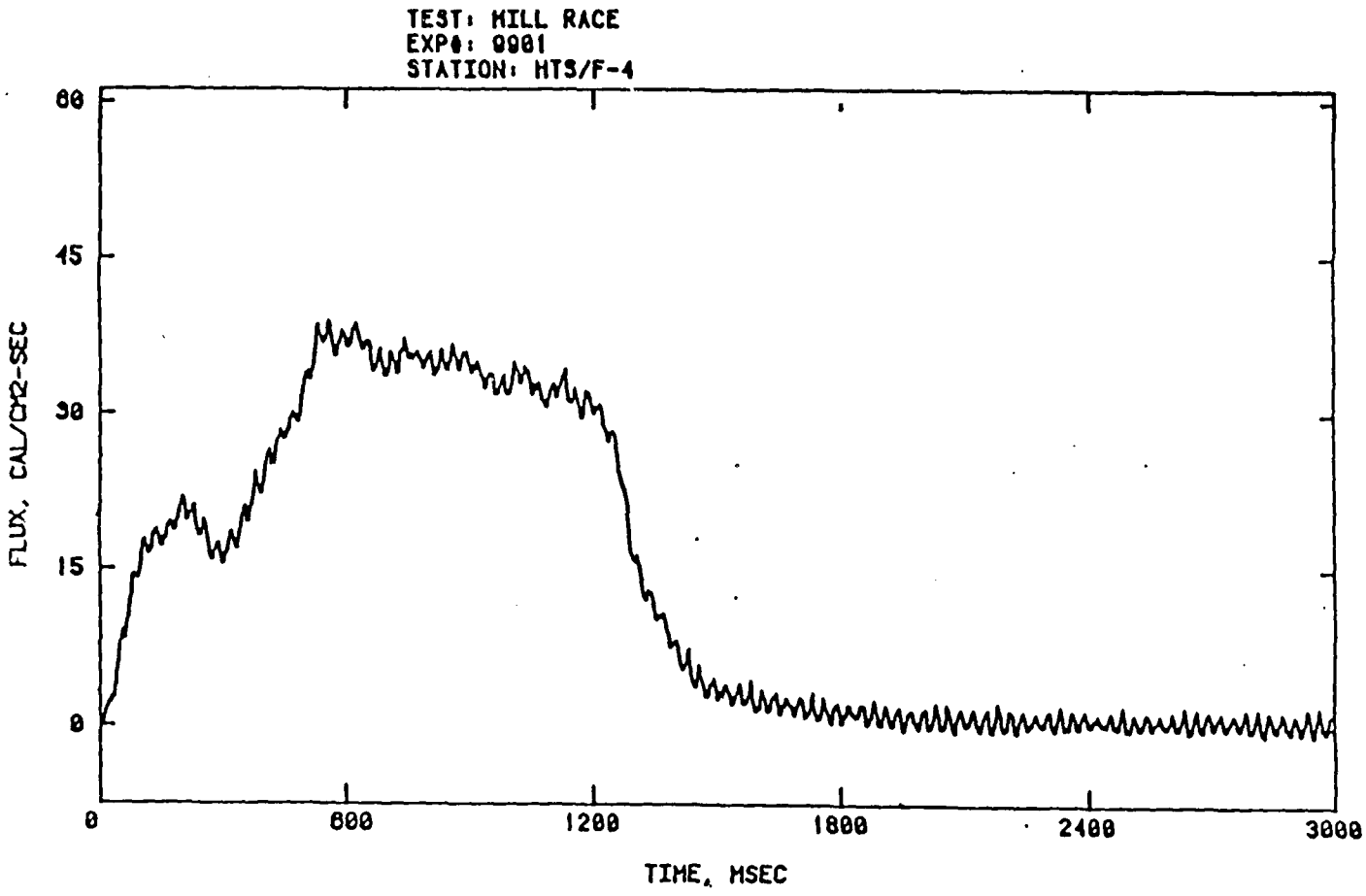

Figure 30. MILL RACE waveform: BRL calorimeter F-4.

SECTION 4

THE ALFGEE MODELS

This section presents the ALFGEE algorithms used in the modeling effort. For those readers interested in a brief introduction to the pertinent parts of radiation theory, we suggest a review of pages 183-188 in Reference 4. In addition, pages 36 and 82 of Reference 1 present the equations for calculating the flux from either an extended source or an ensemble of point sources. This review is recommended for those that wish to follow the ensuing discussion.

4-1 RADIATION FROM THE FLAMES.

The calculation of the radiant flux across a surface facing the flames is simply an integration over the sources of radiation, accounting for the effects of geometry. A surface integral is evaluated over an extended source. Addition of all the contributions from each source is performed for an ensemble of point sources.

An extended source can be approximated by a set of point sources, and then the flux computed as for an ensemble of point sources. The key is choosing where to place the points. This is not much different from numerically solving a surface integral. In fact, to obtain the same accuracy in both methods would require about the same amount of calculation. There is essentially no difference between treating the surface as point sources and as small surfaces when the extended source is opaque.

When certain symmetries exist it is possible to replace a surface integral with a single point. An example of this is radiation from an isotropic radiating sphere out to a collecting surface, which is outside of

the sphere and is facing the sphere. As long as the entire sphere that can be possibly visible to a collecting surface (depends on range) is visible to it, the received radiation would be the same as that from a point source placed at the center of the sphere.

For modeling purposes, we have chosen to approximate the extended source as a set of point sources placed on the axis of symmetry of the flame. The intent is to avoid integration over the width of the flame, thus keeping the amount of calculation at a minimum. This approach introduces small errors; these are unimportant because the model is ultimately calibrated to data. Hence, any bias introduced with height will tend to be removed with the subsequent calibration. This approach is an outgrowth of the earlier work on the bag source reported in Reference 1. Similarily, the criterion of how many point sources need to be distributed along this line was taken from this earlier work. An additional constant factor was included to ensure accuracy in unusual geometries.

Once it has been established how many points are needed to represent a flame (this is done for each field point), the source strength of the entire flame is distributed in proportion to the power-per-unit-length-model, which is described later. Since the number of points needed to represent each flame changes with field position, the source strength of each point source is normalized to the total from the ensemble.

Features such as normalization help ensure a continuity in the results when the collecting surface moves about in the illuminated field. For example, as the field point is moved toward the flames, the number of source points increases as the range decreases, yet the computed flux apparently exhibits no discontinuity. Naturally, these smooth transitions should not be important to the experimenter nor required by him. Nevertheless, they do help reduce noise in the computed results, which is useful when drawing contours.

The point sources are distributed along the centerline of a nozzle and span the height of the radiating part of the flame. The height of the flame is adjustable by the analyst. In early models, the resemblance of this

parameter to an actual flame height was coincidental. More recently, however, the best fits using the latest inverted cone model seem to yield a "flame height" parameter that appears to agree well with photographs.

4-2 ALFGEE COORDINATE SYSTEM.

Figure 31 presents the ALFGEE coordinate system used throughout this report. The ALFGEE coordinate system, formed by three Cartesian coordinates: x,y, and z, is right handed. The x-coordinate, commonly called the range, is usually the distance measured from the detector (or field point) where the irradiance is being calculated to the plane containing the nozzle centers of symmetry. The y-coordinate, commonly called the cross range, is usually the distance measured from the field point to the plane passing through the center of an even numbered array of nozzles that is perpendicular to the plane containing the nozzle centers of symmetry. Historically, the nozzles have been placed along the ground in a straight line. The z-coordinate, height, is normally measured to and above the ground plane.

Occasionally, the origin of the coordinate sytem will be changed, typically for an experimenter's convenience. This is readily accomplished, since the implementation of the algorithms has always included the flame coordinates.

The normal to the detecting surface is shown in Figure 31 as a unit vector, n. This normal is described by two angles, one is similar to and is called azimuth and the other is its elevation above the ground plane. The azimuth is specified by a rotation about the height axis, where an azimuth of zero is a normal pointed towards the negative x direction. The elevation is specified by a rotation about a line perpendicular to the normal and in an xy plane, ie. a plane of constant z.

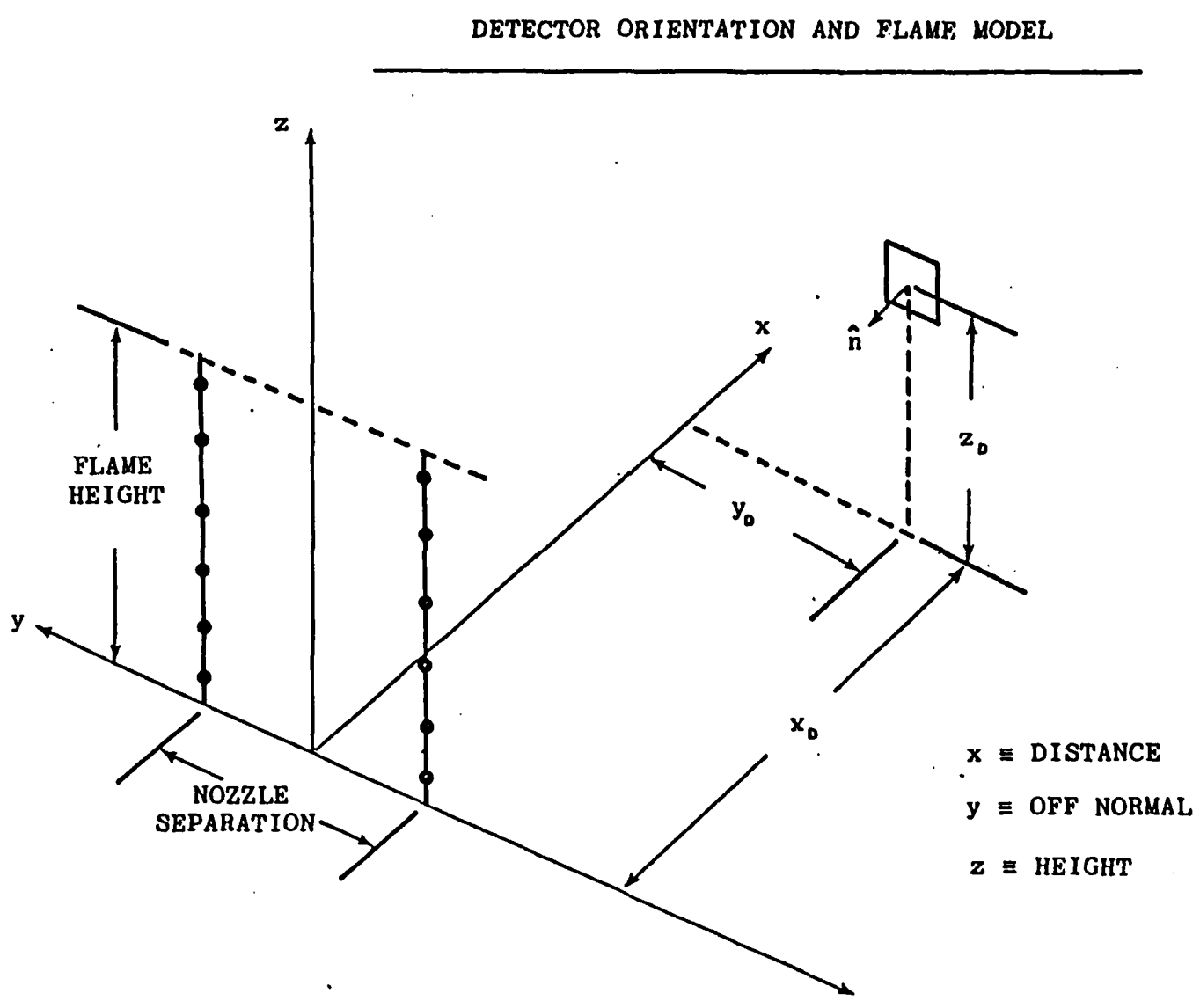

Figure 31. ALFGEE coordinate system.

4-3 TREATMENT OF GROUND REFLECTIONS (ALBEDO).

When the flames are close to other surfaces, some energy will be scattered by these other surfaces and may illuminate the collecting surface under consideration. Usually, the TRS nozzles are fired quite close to the ground.

Calculation of the scattered radiation would be more difficult, if done correctly, than the calculation of the direct radiation. This is because the ground is a diffuse reflector. Radiation incident upon the ground is scattered into the hemisphere of air above. This scattered radiation reaches the collecting surface if the scattering point is visible to the collector. Therefore, the incident flux on the ground should be calculated at many points on the ground, and then an integration over this large source performed for each collector location.

Again to reduce the amount of computation, certain approximations were made. Rather than perform the integration, we decided to treat the ground as a specular reflector with a reflection coefficient equal to the average albedo. This albedo is also a parameter that the analyst can adjust so calibration will again mitigate some of the errors associated with this approach. However, this model will not calculate any contribution from the ground for any collecting surface facing away from the flames. In that case, the model will clearly underpredict the received flux.

When the decision was made to proceed in this fashion, it was hoped that some experimental data would be available soon, to allow an assessment of the adequacy of this technique. Unfortunately, none of the recommended albedo experiments had been made by the time this effort was completed. Some attempts at a measurement have since been made (early 1983), but these are inconclusive. Meaningful measurements need to be made. Nevertheless, this approach seems to admit to reasonable modeling of the data. At some point when more reliance is placed on the modeling, it seems reasonable to resolve the remaining issues.

Finally, this approach used does not provide any angular dependence of the scattering by the ground. If the reflectivity of the ground changes as the angle of incidence (off the normal) changes as some authors have suggested, the albedo should depend on ground range from flame to collector.

4-4 STRENGTH OF A NOZZLE.

The model also includes another adjustable parameter that allows the analyst to modify the power of each flame and hence scale the output. This parameter has always been the last one adjusted when calibrating the model. Once a comparison has been made between a subset of the data base and the corresponding calculations for one set of parameters, the sum of the residuals can always be forced to be zero by multiplying the strength used in the calculations by the ratio of the sum of the measured values to the difference of the sum of the measured values and the sum of the residuals.

4-5 POWER PER UNIT HEIGHT.

One of the most important parts of the model is the distribution of the radiated power per unit height along the axis of the flame. Yet the modeling to date has relied on essentially no data to establish this basic relationship. An early cursory review of some photographic data indicated that there existed areas within the flame that radiated more energy per unit cross sectional area than other areas. Qualitatively, except for a small region very close to the nozzles, the brightness in the visible spectrum seemed to be a maximum near the nozzles, which decreased with height and cross sectional width. Whether the flame was radiating as a volume or as a surface could not be easily determined. However, if the flames were indeed opaque and were radiating from a relatively small region at the surface of the flame, the radiation clearly is not Lambertian.

In spite of this lack of data and in spite of our uncertainty as to the details of how these flames radiate, we chose to adopt a simple model based on

some qualitative interpretations of some photographic and video records. The measure of success in the early modeling efforts was the utility demonstrated by the model.

The model of the power per unit height chosen for the cylindrical representation included two adjustable coefficients. These coefficients provided a limited ability to adjust the distribution of energy along the flame axis to best fit the available data. One coefficient was normalized by the height of the radiating flame and separated the model into two regions. In the first region the normalized power per unit length was assummed to be a constant value, unity. In the second region the functional dependence chosen was a linear decrease with height. The second coefficient was the net difference from unity of the power per unit length at a normalized height of one. Thus, if the first coefficient equals one (or the second equals zero), the functional form would be a constant. If the first equals zero, and the second is set to one, the functional form would be linear with the maximum at the nozzle, decreasing to zero at the normalized flame height of one.

During the development of the inverted cone model, it was decided, after much consideration of the experience gained by calibrating to the various data, that a more realistic model should include the width of the flame at each source point. For the cylindrical model this of course cannot make any difference. The model that evolved was similar to the original one except that the constant region was removed and an additional linear region was added above the radiating flame. This was accomplished without increasing the number of coefficients by requiring the power per unit length to decrease to zero at the top of the second region. An alternate approach would have been to add a third region, but this would have required one more adjustable parameter in the model.

4-6 FLAME-FLAME OBSCURATION.

The very early models did not reduce the received flux when one flame obscurred the view of another. If a flame was completely shadowed by another

flame, its contribution to the flux was calculated as if the closer flame were transparent to the radiation from it. Initially, this approximation worked because in use the flames only infrequently obscurred one another, or the obscurred surface area was small. Eventually, however, as more nozzles were added to the flame arrays and more ground area was planned for experiments, it became clear that consideration of obscuration effects was essential.

In the cylindrical flame model, the geometry is straightforward. The original algorithms for computing this geometry work well so long as the flames do not touch. They lead to unphysical asymmetries in the results if the flames touch. This early approach included the assumption that the flames did not touch, to avoid some computations. For most of the early cases this was an adequate approximation.

To compute the radiation from any flame when obscuration effects are included, the effect of all the other flames on it must be considered. Every combination of flame pairs must be evaluated. In the ensuing discussion, one flame of the pair, at which radiation is being summed, is the radiating flame or radiator. The other possibly obscuring flame is called the obscurer. When the flames do not touch, only an obscurer closer than the radiator need be included. Those farther out cannot obscure even if they are different sizes.

Rather than computing the geometry for each combination of flame pairs, we can avoid half of the computations by sorting the flames. Then when the range to an obscurer exceeds that for a radiator, in order of range from the fixed point the rest of the obscurers for this radiator can be ignored.

When the development of the inverted cone model was started, the need for including intersecting flames was identified. Treating obscuration is more difficult, especially since the radius of the flames depends upon height in this model. Further, some symmetry is lost owing to the ground albedo. These lead to a substantial increase in computation. To reduce the computation, each inverted cone is approximated as a set of stacked disks. This simplification does not introduce appreciable error.

It has been assumed throughout the modeling effort that the models would be used for ensembles of identical flames. Each flame must be the same size and all the nozzles must be at the same height for the obscuration models to work correctly. When there exists a need to use these models for other arrangements of TRS units, or mixtures of different types of units, additional modeling effort will be required.

4-7 AN ERROR IN EARLY FLAME-FLAME OBSCURATION MODEL.

The implementation of the ALFGEE models, used for many of the calculations reported herein, contains a deficiency in the obscuration model. When flames touch, the obscuration algorithm does not accurately calculate the effects. Table 14 shows the results that are generated with this implementation. Note that for some results, the expected symmetry about y=0 is not produced. This effect is seen in the calculations for four nozzles. These calculations were performed for a particular MILL RACE experiment.

This particular defect existed in all obscuration models used throughout this effort. The results presented in this report, however, have not been affected thereby with the exception of the results in Table 14.

A listing of the implementation containing the error is included as Appendix E. This particular implementation was written by the author on an Apple II Plus microcomputer. It was written in Apple Pascal (version 1.1) for use on that machine. This listing is included to complete the presentation of the algorithms developed under this effort. These algorithms were implemented and tested for actual cases of interest.

Table 14. Comparison of different spacings in front of deckhouse.

RANGE OF 3.26 M

POSITION	6 FEET SPACING		9 FEET SPACING		12 FEET SPACING	
	2 NOZ	4 NOZ	2 NOZ	4 NOZ	2 NOZ	4 NOZ
-200	12.96	14.51	12.98	14.30	12.75	13.88
-150	14.79	16.09	14.25	15.37	13.36	14.32
-100	16.30	17.39	15.11	16.06	13.60	14.42
-50	17.27	18.20	15.57	16.38	13.62	14.32
0	17.60	18.40	15.72	16.41	13.60	14.21
50	17.27	17.96	15.57	16.18	13.62	14.15
100	16.30	16.89	15.11	15.64	13.60	14.06
150	14.79	15.31	14.25	14.71	13.36	13.77
200	12.96	13.41	12.98	13.38	12.75	13.11

SECTION 5

TRS - AIR BLAST INTERFERENCE

This section presents the limited work that was done to address some of the TRS-air blast interference issues. This work consisted of an initial look at how far out from the TRS units blowoff effects might be seen on event MILL RACE. These calculations were performed to estimate how much ground area can respond to the incident thermal radiation. To properly assess the effect on the air blast will require large and long running two and three dimensional calculations.

In addition, some simple one dimensional HULL-type calculations were performed to determine the magnitude of the effect a hot flame has on overpressure when air blast propagates through it. These calculations showed a small effect, which is contrary to the MISERS BLUFF result. This difference is attributed to the sizable effect expected from particulates in the flame. Unfortunately, computer related problems precluded us from performing further calculations.

5-1 BLOWOFF.

When thermal radiation is rapidly deposited into the ground, it can lead to an effect known as blowoff. The deposited energy does not have sufficient time to conduct away from the irradiated surface. For blowoff to occur, the temperature in the ground must quickly increase to the boiling point of water and some steam can be generated from any free water. Additional energy can raise the temperature further to where water and carbon dioxide bound to crystalline material can be explosively released. This rapid release of gases can drag up particulates, which are subsequently heated, and that appear as "blowoff" material. The importance of this material is in how

it affects air blast propagating through it. The nuclear air blast precursor is a good example.

The whole blowoff process is extremely complicated and not well understood even after considerable research. It is known that the amount of energy that it takes per unit area of soil to cause blowoff depends on many factors such as soil type, flux, and incident angle to name a few.

Nonetheless, for NTS type soils, similar to WSMR soils, and for nuclear weapon flux levels (for tens of Kiloton devices) an approximate value of six (6) calories per square centimeter has been used (Reference 5) and seems to be an appropriate value for our purposes for estimating incipient blowoff. This criterion is called the blowoff threshold.

5-2 POTENTIAL BLOWOFF ON MILL RACE.

Figures 32 through 37 present contours of equal peak flux incident on the ground calculated posttest for the MILL RACE event. The expected blowoff area is determined by this peak flux multiplied by the burn time to give fluence. Where the fluence exceeds the blowoff threshold, blowoff can occur. Each figure is drawn to the same scale to allow comparison. The dimensions are in meters and the flux is in calories per square centimeter per second.

As an example, Figure 32, shows the flux perpendicular to the ground from the BRL MILL RACE four nozzle array. The letter N shows the location of each nozzle along the y-axis. If the burn time is one second and the blowoff threshold is 6 calories per square centimeter, then contour 5 encloses the blowoff area. Contour 5 crosses the x axis at about 3.7 meters and crosses the y axis at about 3.8 meters. The contours look almost circular about the origin.

The results for Figure 32 were based on the cylindrical model calibrated to the BRL source. The data were not generated for negative y values because of the symmetry on either side of the x axis.

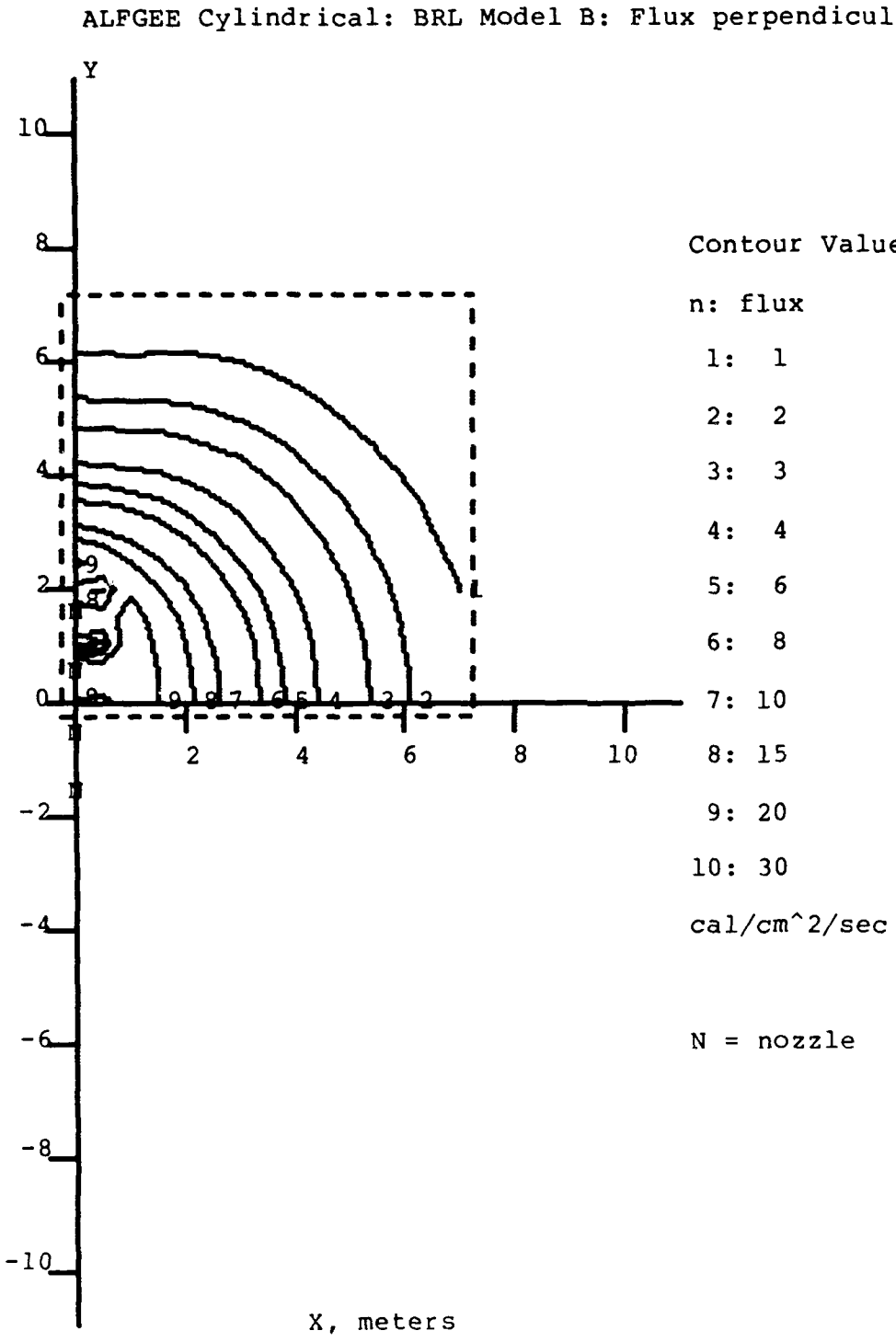

Figure 32. Flux on ground contours: BRL model B

AD-A168 707 ESTIMATING RADIATED THERMAL ENVIRONMENTS FROM ALUMINUM-LOX (LIQUID OXYGEN..(U) SCIENCE AND ENGINEERING ASSOCIATES INC SALEM MA B S CHAMBERS

UNCLASSIFIED 15 DEC 84 SEA-62-00-0:01 DNA-TR-85-3 F/G 20/13 NL

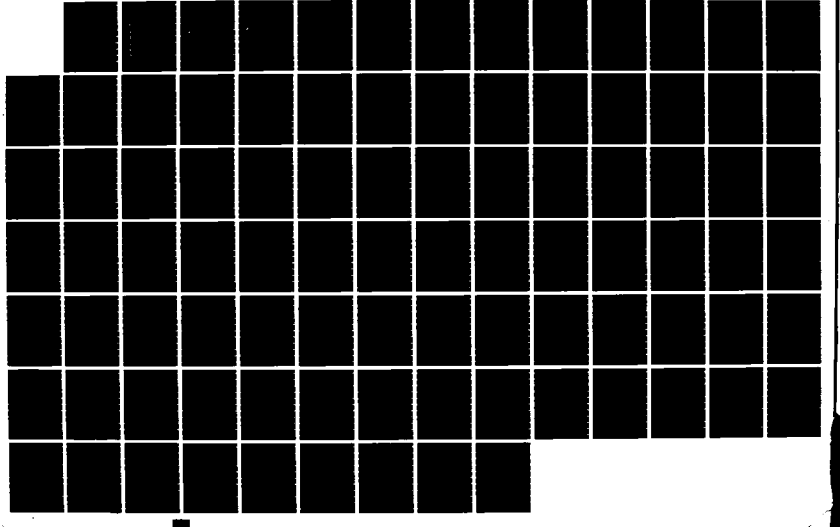

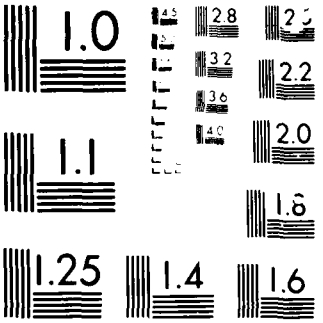
1.0
1.1
1.25
1.4
1.6
2.0
2.2
2.8
3.2
3.6
4.0

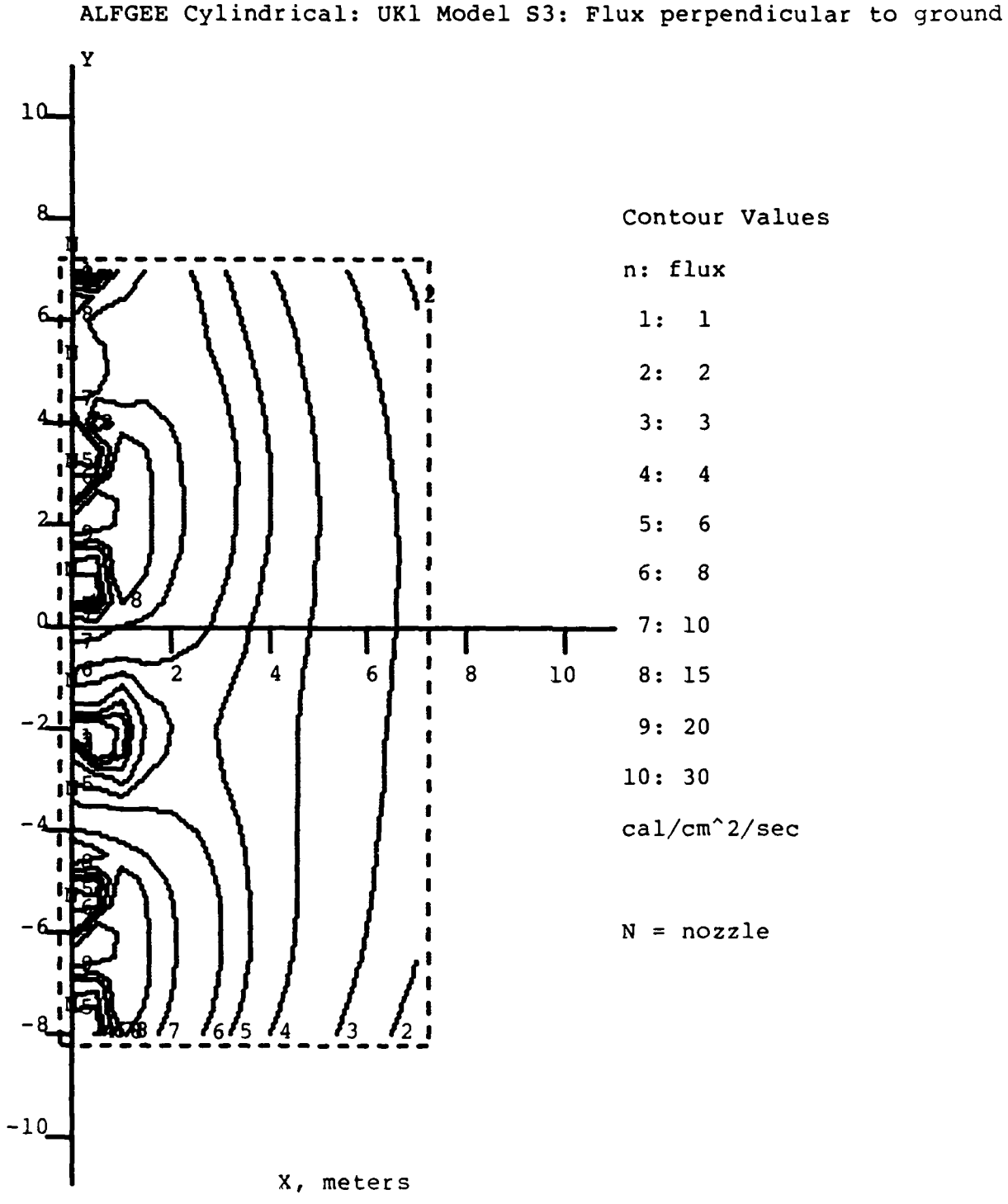

Figure 53. Flux on ground contours: UK-1 model S3.

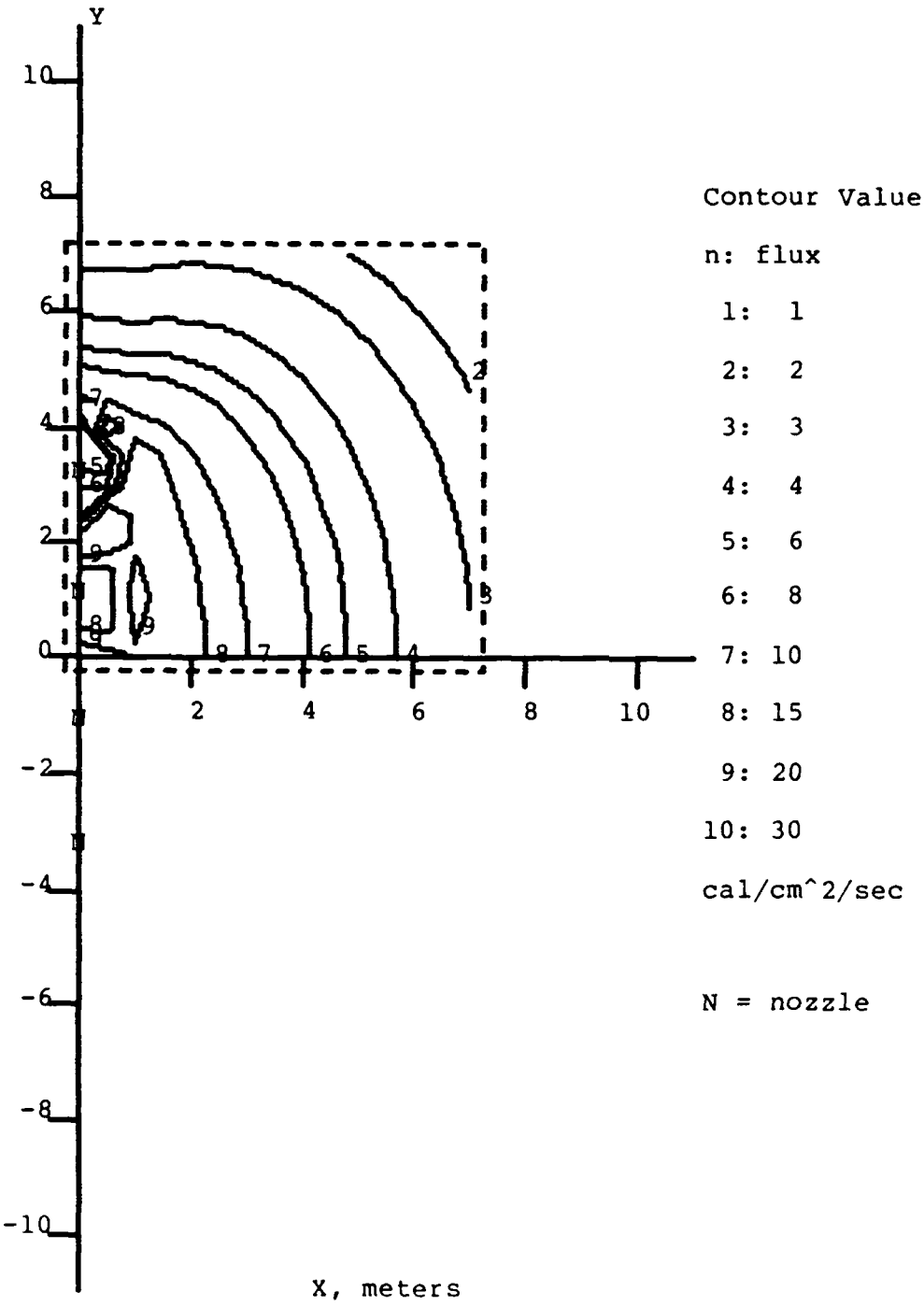

Figure 34. Flux on ground contours: UK2 model C.

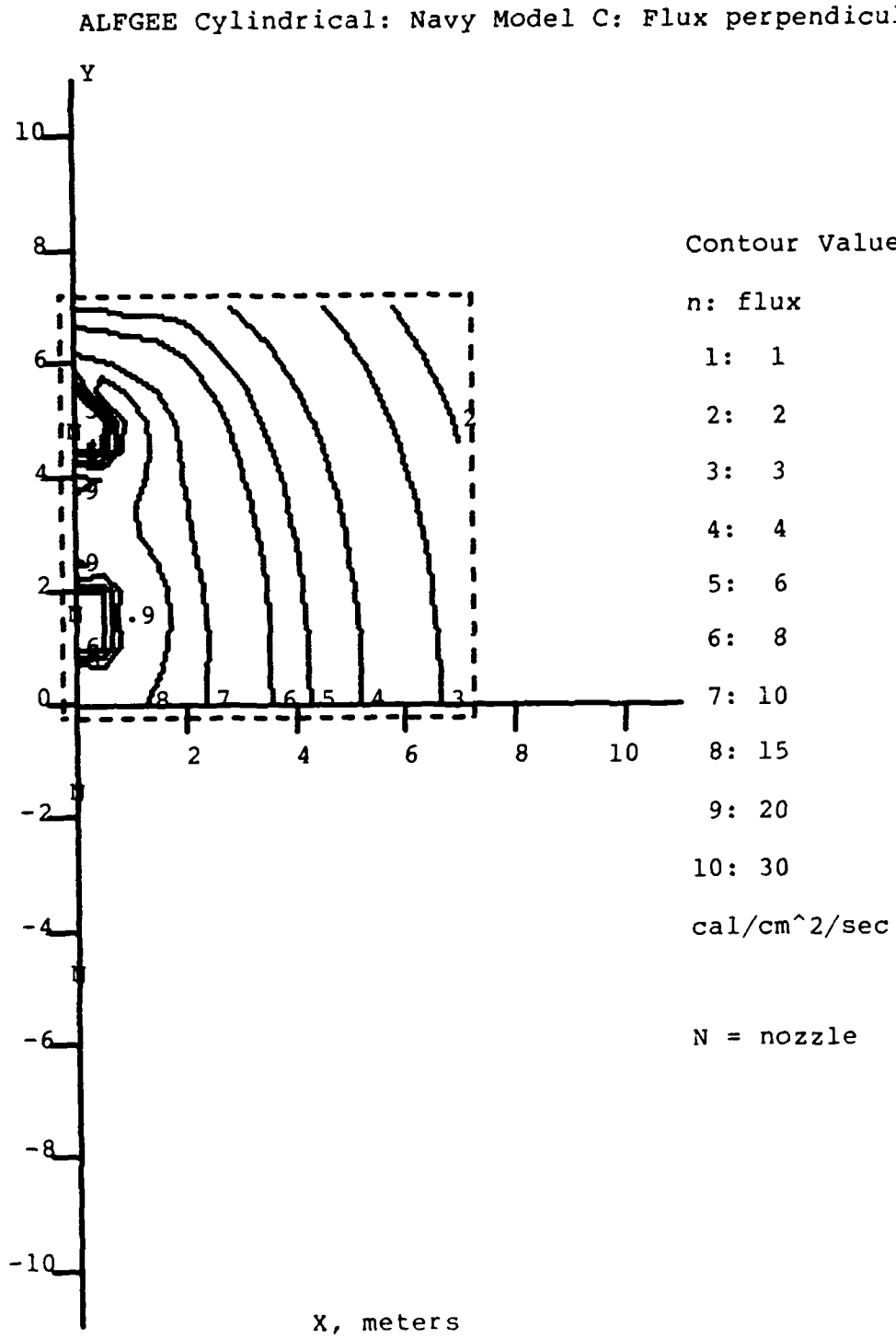

Figure 55. Flux on ground contours: Navy model C.

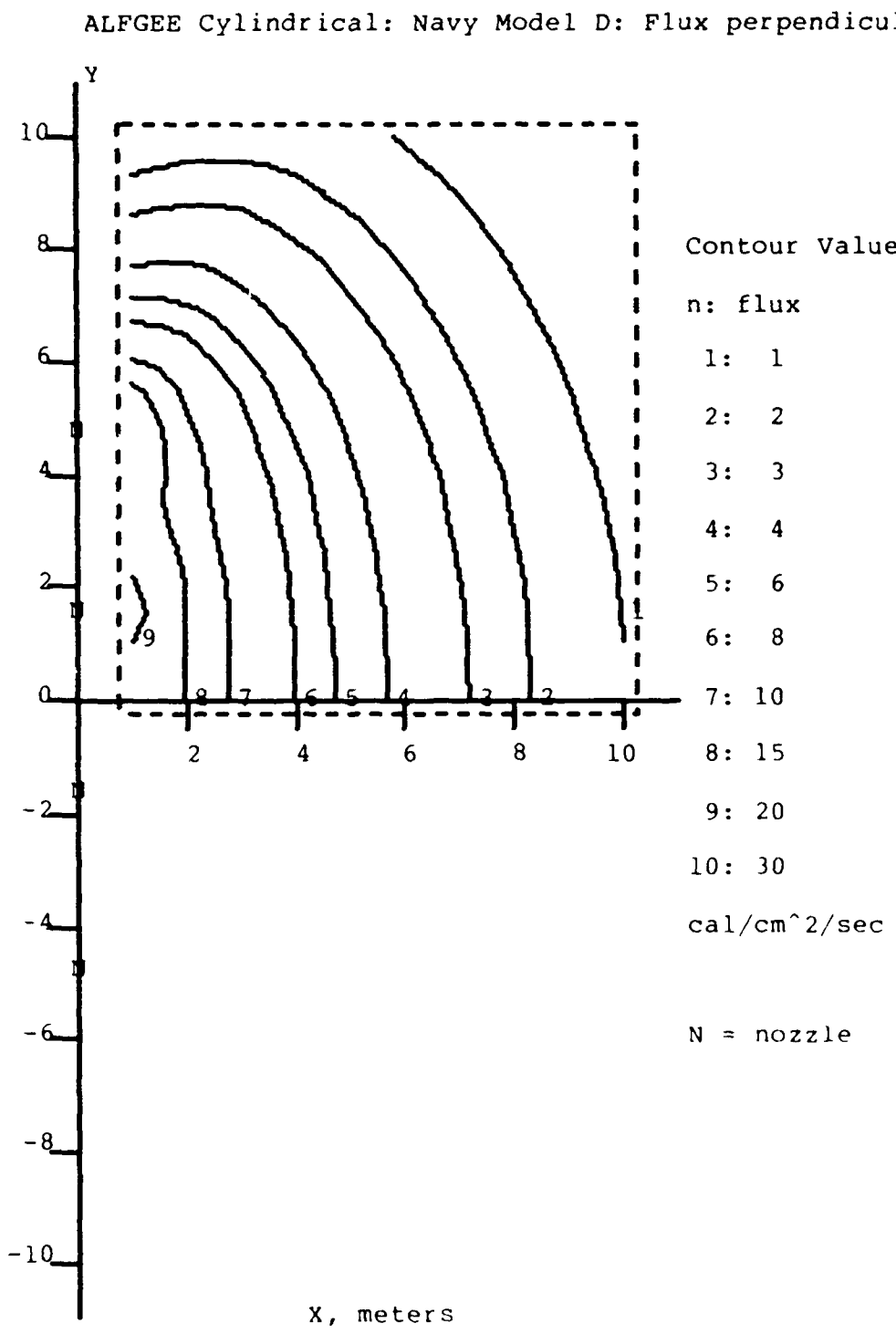

Figure 56. Flux on ground contours - Navy model D.

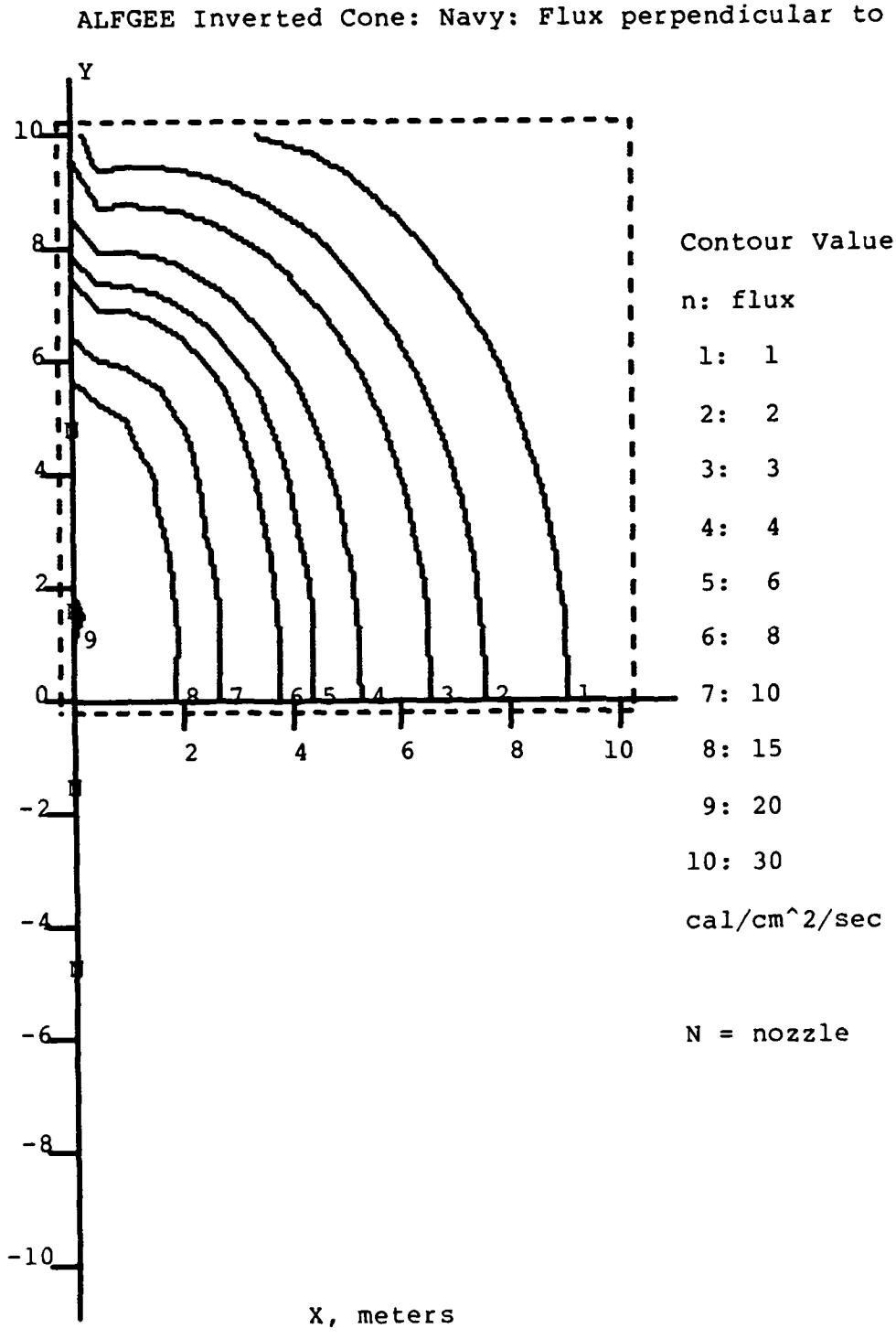

Figure 37. Flux on ground contours: Navy inverted cone.

Figure 33, on the other hand, shows that symmetry did not exist during MILL RACE. The UK-1 nozzles 3 and 4 did not ignite, and nozzle 7 burned unreliably. Adjusting the output for these three nozzles removes the symmetry, thus both positive and negative y values were computed and plotted.

Knowing the burn time for an array, the contour plots can be used to estimate the area of blowoff, given any blowoff threshold for burn times similar to those used in MILL RACE. The burn times for each nozzle array are: Navy 2.4 seconds; BRL 1.1 seconds; UK-2 1.0 seconds; and UK-1 2.0 seconds (Reference 3). By way of example, desert soil at NTS can start to blowoff at about 6 calories per square centimeter. The burn time for the eight nozzle UK-1 MILL RACE array was 2 seconds. The above blowoff criterion then corresponds to a flux of 3 calories per square centimeter per second, which is contour 3. The extent along the x axis is about 6.6 meters. The burn time, on the other hand, for the four nozzle UK-2 MILL RACE array was only one second. Therefore, contour 5 represents the blowoff threshold. It extends out to about 4.7 meters.

The area that exceeds the blowoff threshold for UK-1 greatly exceeds that for UK-2 because the burn time is twice as long and there are one to two more nozzles burning.

5-3 ONE DIMENSIONAL FLAME CALCULATIONS.

Table 15 summarizes the cases run to investigate the influence that a slab of hot air, sandwiched between cold ambient air, would have on air blast propagating through this layer.

Three incident overpressures were considered: 3, 7, and 10 psi. The case number (first column in the table) is the overpressure multiplied by 100. Two flame widths were briefly looked at. They were one and two meters and are indicated by the second column. The third column shows the ratio of the flame internal energy to ambient. The temperature ratio is not shown and depends on the equation of state. The corresponding flame temperature is approximately

Table 15. Table of HULL-1D results for propagation through hot thin flame.

TABLE OF HULL-1D RESULTS FOR PROPAGATION THROUGH HOT THIN FLAME

OBSERVER -->			110	115	120	125	130	135	140	145	150	155	160
CASE	#	X											
300	0.00	0.00	2.78	2.77	2.77	2.77	2.77	2.77	2.77	2.76	2.76	2.76	2.76
300	21.00	10.00	2.71	2.72	2.72	2.72	2.71	2.71	2.71	2.71	2.71	2.71	2.71
300	21.00	5.00	2.72	2.72	2.72	2.72	2.72	2.72	2.72	2.72	2.72	2.72	2.72
300	21.00	2.00	2.73	2.73	2.73	2.73	2.73	2.73	2.73	2.73	2.73	2.73	2.73
300	21.00	1.10	2.77	2.77	2.77	2.77	2.77	2.77	2.77	2.76	2.76	2.76	2.76
300	11.00	2.00	2.77	2.77	2.77	2.77	2.76	2.76	2.76	2.76	2.76	2.76	2.76
300	0.00	0.00	0.00	0.00	0.00	0.00	0.00	0.00	0.00	0.00	0.00	0.00	0.00
300	21.00	10.00	-2.20	-2.09	-2.06	-1.99	-1.95	-1.88	-1.88	-1.81	-1.77	-1.74	-1.67
300	21.00	5.00	-2.05	-1.95	-1.91	-1.88	-1.81	-1.77	-1.74	-1.66	-1.67	-1.59	-1.56
300	21.00	2.00	-1.59	-1.48	-1.48	-1.41	-1.37	-1.30	-1.27	-1.23	-1.19	-1.12	-1.09
300	21.00	1.10	-0.04	0.00	-0.04	-0.04	0.00	0.00	0.00	0.04	0.00	0.04	0.04
300	11.00	2.00	-0.25	-0.22	-0.22	-0.18	-0.18	-0.14	-0.14	-0.11	-0.11	-0.07	-0.04
700	0.00	0.00	6.48	6.48	6.47	6.46	6.46	6.45	6.45	6.44	6.43	6.43	6.42
700	21.00	10.00	6.30	6.31	6.31	6.31	6.31	6.31	6.30	6.30	6.30	6.30	6.30
700	21.00	5.00	6.31	6.32	6.32	6.32	6.32	6.32	6.32	6.31	6.31	6.31	6.31
700	21.00	2.00	6.35	6.35	6.35	6.35	6.35	6.35	6.34	6.34	6.34	6.34	6.34
700	21.00	1.10	6.47	6.47	6.47	6.46	6.46	6.45	6.44	6.44	6.43	6.43	6.42
700	11.00	1.10	6.48	6.48	6.47	6.46	6.46	6.45	6.45	6.44	6.43	6.43	6.42
700	0.00	0.00	0.00	0.00	0.00	0.00	0.00	0.00	0.00	0.00	0.00	0.00	0.00
700	21.00	10.00	-2.75	-2.61	-2.49	-2.40	-2.34	-2.26	-2.19	-2.13	-2.05	-1.99	-1.92
700	21.00	5.00	-2.61	-2.44	-2.32	-2.23	-2.17	-2.08	-2.02	-1.96	-1.88	-1.82	-1.76
700	21.00	2.00	-2.10	-1.98	-1.89	-1.81	-1.73	-1.64	-1.57	-1.49	-1.43	-1.34	-1.28
700	21.00	1.10	-0.14	-0.03	-0.03	-0.05	-0.05	-0.02	-0.02	-0.02	-0.02	-0.02	0.00
700	11.00	1.10	-0.02	-0.02	-0.02	-0.02	-0.02	0.00	0.00	0.00	0.02	0.02	0.02

Table 15. Table of HULL-1D results for propagation through hot thin flame (continued).

TABLE OF HULL-1D RESULTS FOR PROPAGATION THROUGH HOT THIN FLAME (CONTINUED)

OBSERVER -->			110	115	120	125	130	135	140	145	150	155	160
CASE	#	X											
1000	0.00	0.00	9.21	9.20	9.19	9.17	9.16	9.15	9.14	9.13	9.12	9.11	9.09
1000	21.00	10.00	8.93	8.94	8.94	8.94	8.94	8.94	8.94	8.93	8.93	8.93	8.92
1000	21.00	5.00	8.95	8.96	8.97	8.97	8.96	8.96	8.96	8.95	8.95	8.95	8.94
1000	21.00	1.10	9.19	9.20	9.19	9.18	9.16	9.15	9.14	9.13	9.12	9.11	9.10
1000	11.00	10.00	9.11	9.11	9.11	9.10	9.10	9.09	9.09	9.08	9.08	9.07	9.06
1000	5.00	10.00	9.21	9.20	9.19	9.18	9.17	9.16	9.15	9.14	9.13	9.11	9.10
1000	21.00	2.00	9.00	9.00	9.00	9.00	9.00	9.00	9.00	9.00	8.99	8.99	8.99
1000	0.00	0.00	0.00	0.00	0.00	0.00	0.00	0.00	0.00	0.00	0.00	0.00	0.00
1000	21.00	10.00	-3.02	-2.81	-2.63	-2.50	-2.41	-2.33	-2.23	-2.15	-2.06	-1.97	-1.88
1000	21.00	5.00	-2.86	-2.58	-2.40	-2.27	-2.18	-2.10	-2.00	-1.92	-1.83	-1.74	-1.65
1000	21.00	1.10	-0.18	-0.01	0.01	0.02	0.02	0.01	0.02	0.02	0.02	0.03	0.03
1000	11.00	10.00	-1.08	-0.91	-0.84	-0.76	-0.70	-0.63	-0.57	-0.51	-0.46	-0.40	-0.34
1000	5.00	10.00	-0.01	0.03	0.02	0.05	0.07	0.05	0.08	0.08	0.09	0.09	0.11
1000	21.00	2.00	-2.30	-2.11	-1.98	-1.86	-1.77	-1.67	-1.56	-1.46	-1.36	-1.25	-1.15

between 2500 and 3000 degrees Kelvin, although the results are not too sensitive to the temperature in this range.

The results are shown for various observer locations beyond the flame. Two blocks of data are shown for each overpressure. The first (top) block is the overpressure at the corresponding observer location. The second block is the percentage differences. The first line in each block is the free air case, ie. no flame is present. This is the baseline case against which every other case is compared. The distance from the center of the flame to observer 110 is 10.

The largest change observed was for 10 psi and this change was only three percent for distances close to the flame. Thus the induced effect due to the presence of just a hot air layer is small for the flame widths considered for overpressures less than 10 psi.

It is our hypothesis that the TRS flame must have some matter inside them that does not contribute significantly to the pressure. Otherwise, it would be expected that the bright hot flame would produce associated air blast, as was seen in early TRS bag designs. Whether solid particulates are formed or liquid droplets (molten aluminum oxide, for example) remains to be determined. In either case, it is expected that once sufficient particulates or droplets have been formed with a resultant material density of the order of the air density, then the flow will be affected significantly by these small pieces of matter through, at least, aerodynamic drag. Therefore, to establish the non-interference of TRS flames, additional one dimensional calculations with interactive particles, that can numerically simulate either solid particulates or liquid droplets, will need to be performed.

5-4 ADDITIONAL AIR BLAST INTERFERENCE WORK.

It was shown in the previous section that the induced effect on air blast due to the presence of just a hot air layer is small for the flame widths considered for overpressures less than 10 psi. In order to establish

the non-interference of TRS flames, additional one dimensional calculations with interactive particles will need to be performed.

Another effect that needs to be addressed is the induced three dimensional flow as a result of the three dimensional character of the TRS flame-air blast interaction. Such an investigation was outside of the scope of this effort.

The current practice in the field is to mitigate any air blast interference problems by firing the flames early enough to allow the complete burn of the flame as well as its rise out of the way before air blast arrival. Although this is felt to be a reasonable approach for reducing the direct influence of the flame on the local peak overpressure, the effect of the combustion products on air blast further down range and on the rest of the local air blast waveform has not been established. The most significant problem introduced by this approach to air blast interference mitigation may well be the possibly artificial delay introduced in the arrival of the air blast relative to thermal exposure. Considerable analysis may be required for each weapon system thusly exposed on a combined air blast / thermal test.

SECTION 6

CONCLUSIONS

This section presents the conclusions drawn in the area of estimating the radiated thermal environments from aluminum-liquid oxygen (Al-LOX) thermal radiation simulators (TRS). Some conclusions were also drawn in the area of TRS-air blast interference, however these were significantly limited.

6-1 MODEL DEVELOPMENT.

Most importantly, this effort produced models to calculate flame TRS generated peak flux that represent those same environments in the field. The inverted cone model is the best developed so far when flame obscuration and an accurate treatment of view angle are included. This model produces results that are in closest agreement with the data up through MILL RACE.

It is now possible to use one calibration of the inverted cone model to represent all cases. Consequently, the data base may now be of sufficient size to allow certain statistical inferences to be made about the inherent variability of the flame TRS in use in the field.

Model development was evolutionary. First we tried to provide a tool for interpolation based on simple physical principles. Next, refinements were developed in the representation of flame geometry, and a more accurate treatment of flame-flame obscuration. While model development was ongoing, the model was exercised for TRS development work, pre-MILL RACE nozzle checkout, experiment site layout, and experiment interpolation and analysis.

Some of the early data were affected to an unknown extent by calorimeter stand tip-back. This effect was more serious on the late time

flux data for much of the early calorimeter data. The current practice is to use heavier poles at the TRS sites; these are much less suseptible to thermal stress deformation.

We conclude that a substantially more exhaustive and a more careful effort to obtain accurate calorimeter data needs to be conducted. Further, more thorough data interpretation and analysis is required. At least four different individuals have read the "peak" flux off of oscilliscope traces that have been entered into the DNA data base. Now that these data are being recorded digitally, the detailed temporal waveforms can be made available for more meaningful data analysis. There has been no consistent approach applied to evaluation of the available data. In some cases data was withheld as not being representative.

The TRS development to date has been directed toward improving the flame generation. Little emphasis has been applied toward evaluating reliability or repeatability. We strongly recommend that one design be fixed for future use in the DNA HE program, and that this design be calibrated under realistic field conditions. Such calibration should be done using many more calorimeters than have been used in the past. While it is recognized that funding limitations tend to preclude having enough of what is needed, the calibration of the DNA thermal simulation "workhorse" should be viewed as the foundation of the nuclear thermal effects simulation program.

6-2 TRS-AIR BLAST INTERFERENCE.

In the area of TRS-Air Blast interference, the results are less clear. The conducted effort is largely incomplete, and additional work is required to resolve the issues. Calculations indicate that incipient blowoff of ground material was probable on MILL RACE. Other calculations have indicated that incipient ground blowoff is probable for the normal one second burn at the DNA TRS site at KAFB. Additional burn time would extend the blowoff area. What looks like the "steam porch" phase of ground blowoff has been seen in the photographs taken at the TRS site.

It was also concluded that modeling a TRS flame as merely a hot clean flame, i.e. one containing no particulates, will not accurately simulate results from MISERS BLUFF. During MISERS BLUFF the overpressure was reduced on one of the targets placed immediately behind the TRS units. Numerical calculations performed for overpressures up to 10 psi and for flame widths up to two meters wide demonstrated that other effects will need to be considered. Additional work is recommended to quantitatively understand the influence of particulates on the effect seen during MISERS BLUFF.

Finally, much difficulty in accessing the DNA-provided computational facilities at KAFB made it very difficult to continue the investigation of TRS-air blast interference.

SECTION 7

RECOMMENDATIONS

This section presents recommendations that resulted from performance of the work.

We recommend that additional work be performed to quantitatively understand the influence of particulates in the effect seen during MISERS BLUFF.

Our recommendations in the area of TRS modeling is that much more experimental and some modeling work needs to be done. In the area of TRS-airblast interference, our recommendation is to determine how well the current interference mitigation techniques will find acceptance in the nuclear survivability and vulnerability community.

A substantially more exhaustive and a more careful effort to obtain calorimeter data needs to be done. This recommendation is made with the knowledge that the data base essentially doubled during September 1982 when DNA and SAI conducted a Calibration Program at the DNA TRS site at Kirtland AFB. Even with those data, significant additional data under more controlled conditions is necessary if the community expects to place great reliance on modeled results.

More thorough data interpretation and analysis is recommended. At least four different individuals have read the "peak" flux off of oscilliscope traces that have been entered into the DNA data base. Now that these data are being recorded digitally, the detailed temporal waveforms could be made available for more meaningful data analysis. There has been no consistent approach applied to evaluating these data.

The TRS development to date has been geared to improving the flame generation. Little emphasis has been given to evaluating reliability or repeatability. We strongly recommend that a design be frozen for future use on the DNA HE program, and that that design be calibrated under realistic field conditions.

Finally, we regretably observe that much difficulty in accessing the DNA-provided computational facilities at KAFB made it virtually impossible to continue the investigation of TRS-air blast interference. It is recommended that DNA, not a contractor, more closely monitor difficulties that contractors are having when using the government furnished equipment. Whether this would lead to any improvement in throughput is debatable; nevertheless, we feel it is important to improve this communication of the problems we have been having, so that DNA management might have better information available when decisions are made.

SECTION 8

REFERENCES

1. Chambers, B. and Hasdal, J., "Estimates of Thermal Radiation Environments for Planning a Thermal Simulation on a HE Test," Science Applications, Inc., DNA 5073F, March 1979.

2. Kitchens, C. W. Jr., Lottero, R. E., Mark, A., and Teel, G. D., "Blast Wave Modifications during Combined Thermal Blast Simulation Testing," ARBRL-TR-02352, U.S. Army Ballistics Research Laboratory Technical Report, Aberdeen Proving Ground, MD, (July 1981).

3. Bousek, R., "Thermal Radiation Source" in "Proceedings of the MILL RACE PRELIMINARY RESULTS SYMPOSIUM 16-18 March 1982," Volume I, POR 7073-1, Field Command Defense Nuclear Agency, (July 1982).

4. Chandrasekhar, S., An Introduction to the Study of Stellar Structure, Dover Publications, Inc., New York, NY, 1958.

5. Ganong, G., and Whitaker, William A., "The Nuclear Blast Precursor," Volume I, Air Force Weapons Laboratory, report unpublished.

APPENDIX A

ANALYSIS OF CALORIMETER POLE BENDING

This appendix presents results from an analysis of the influence of the bending of the pipe, that holds the fixtures that in turn hold the calorimeters, on received thermal flux. The bending of a pipe, commonly called a calorimeter stand, is due to thermal stress that results from asymmetrical thermal loads. The effects can be significant. For this reason, the calorimeter stands were replaced with larger pipe, which will not be so easily bent.

The analysis consisted of inspecting the sensitivity of the flux to the changes of a pole's position as a result of irradiation. To simplify the analysis, the case considered was for uniform illumination of one side of the pole, causing it to tip back with a shape identical to an arc on a circle. This shape change causes the calorimeter's range to increase, its height to decrease, and its normal's elevation to increase.

The result is that each of the three above changes will reduce the received flux as the bending increases. The dominant effect, considering the change in geometry relationships, is the effect on range. For every centimeter the pole is tipped back at the calorimeter, the flux was reduced 0.4%. During the early testing, we estimate that this effect could have been of the order of 10 percent for later times. This is another reason for choosing to model the early peak flux, rather than the fluence. Recent data are not affected by this phenomenon due to larger pipe size. Table 16 summarizes the type of results generated.

Table 16. TRS sensitivity study entry form.

SCIENCE APPLICATIONS, INC. TRS SENSITIVITY STUDY ENTRY FORM: 17-JAN-81

THIS TEMPLATE IS USED TO CALCULATE EFFECT OF BEAM BENDING ON PEAK FLUX.

TRS FLAME EVENT D- 44 & 45 ENTERED 17-JAN-81

CALORIMETER: # FX- 1

SENSITIVITIES (% PER CM OR DEGREES)

RANGE X	.409
HEIGHT Z	.063
ELEVATION E	.269

ORIGINAL VALUES

RANGE X	304
HEIGHT Z	228
ELEVATION E	0

CHANGE IN ELEVATION AND FLUX

ELEVATION (DEG)	% IN FLUX
5	4.048490
10	8.045141
15	11.97481
20	15.82266
25	19.57428
30	23.21570
35	26.73351

APPENDIX B

TRS PEAK FLUX DATA: PRIOR TO MILL RACE

This appendix presents peak flux data taken on various two and four nozzles burns performed on the current DNA TRS nozzles at the KAFB site prior to the testing of the MILL RACE nozzles. This appendix documents where each calorimeter was located, as well as different interpretations of the "peak" flux's value.

Three tables are included. The first, Table 17, documents events D-15 through D-45, where data of some significance existed. Comparisons were made with an early calibration of the right cylinder model in this table. During the period of time when these data were being recorded, numerous adjustments were made to the operating parameters for the nozzles, and therefore, the variability in the data is considerable.

The second table, Table 18, presents the data taken during the Pentolite series. Comparisons were also made with an early calibration of the right cylinder model in this table. These data are interesting because more calorimeters were available on each shot.

Finally, Table 19, re-documents some of the events in the series D-34 through D-45. However, here comparisons were made with an early calibration of the inverted cone model. On the average, the inverted cone model improved agreement with the data.

Table 17. TRS data entry forms: events D-15 to D-45: cylinder.

SCIENCE APPLICATIONS, INC. TRS DATA ENTRY FORM: 1/3/81

TRS FLAME EVENT D- 15 ENTERED 17-JAN-81

COMMENT > WIND: NA MPH EARLY 2-NOZZLE BURNS

NOZZLE # --->		1	2						
AL KG/SEC/NOZ (EST)		NA	NA						
CALORIMETER	X CM	Y CM	Z CM	FLUX (JD)	FLUX (RM)	RM/JD	MODEL	%DF (JD)	%DF (RM)
FX-1	-183	53	152	39.60	NA	NA	41.62	5	NA
FX-2	365	53	304	8.70	NA	NA	14.54	67	NA
FX-3	183	53	304	27.30	NA	NA	34.97	28	NA
FX-4	183	53	152	38.80	NA	NA	41.62	7	NA

SCIENCE APPLICATIONS, INC. TRS DATA ENTRY FORM: 1/3/81

TRS FLAME EVENT D- 16 ENTERED 17-JAN-81

COMMENT > WIND: NA MPH EARLY 2-NOZZLE BURNS

NOZZLE # --->		1	2						
AL KG/SEC/NOZ (EST)		NA	NA						
CALORIMETER	X CM	Y CM	Z CM	FLUX (JD)	FLUX (RM)	RM/JD	MODEL	%DF (JD)	%DF (RM)
FX-1	-183	53	152	41.30	NA	NA	41.62	1	NA
FX-2	365	53	304	11.30	NA	NA	14.54	29	NA
FX-3	183	53	304	23.60	NA	NA	34.97	48	NA
FX-4	183	53	152	41.00	NA	NA	41.62	2	NA

Table 17. TRS data entry forms: events D-15 to D-45: cylinder (continued).

SCIENCE APPLICATIONS, INC. TRS DATA ENTRY FORM: 1/3/81

TRS FLAME EVENT D- 17 ENTERED 17-JAN-81

COMMENT > WIND: NA MPH EARLY 2-NOZZLE BURNS

NOZZLE # ---> 1 2
AL KG/SEC/NOZ(EST) NA NA

CALORIMETER	X CM	Y CM	Z CM	FLUX (JD)	FLUX (RM)	RM/JD	MODEL	%DF(JD)	%DF(RM)
FX-1	-183	53	152	43.00	NA	NA	41.62	-3	NA
FX-2	365	53	304	11.30	NA	NA	14.54	29	NA
FX-3	183	53	304	23.60	NA	NA	34.97	48	NA
FX-4	183	53	152	41.00	NA	NA	41.62	2	NA

SCIENCE APPLICATIONS, INC. TRS DATA ENTRY FORM: 1/3/81

TRS FLAME EVENT D- 18 ENTERED 17-JAN-81

COMMENT > WIND: NA MPH EARLY 2-NOZZLE BURNS

NOZZLE # ---> 1 2
AL KG/SEC/NOZ(EST) NA NA

CALORIMETER	X CM	Y CM	Z CM	FLUX (JD)	FLUX (RM)	RM/JD	MODEL	%DF(JD)	%DF(RM)
FX-1	-183	53	152	39.60	NA	NA	41.62	5	NA
FX-2	365	53	304	10.40	NA	NA	14.54	40	NA
FX-3	183	53	304	23.60	NA	NA	34.97	48	NA
FX-4	183	53	152	38.80	NA	NA	41.62	7	NA

Table 17. TRS data entry forms: events D-15 to D-45. cylinder (continued).

SCIENCE APPLICATIONS, INC. TRS DATA ENTRY FORM: 1/3/81

TRS FLAME EVENT D- 19 ENTERED 17-JAN-81

COMMENT > WIND: NA MPH EARLY 2-NOZZLE BURNS

NOZZLE # --->		1	2						
AL KG/SEC/NOZ(EST)		NA	NA						
CALORIMETER	X CM	Y CM	Z CM	FLUX (JD)	FLUX (RM)	RM/JD	MODEL	%DF(JD)	%DF(RM)
FX-1	-183	53	152	41.30	NA	NA	41.62	1	NA
FX-2	365	53	304	12.20	NA	NA	14.54	19	NA
FX-3	183	53	304	30.90	NA	NA	34.97	13	NA
FX-4	183	53	152	40.30	NA	NA	41.62	3	NA

SCIENCE APPLICATIONS, INC. TRS DATA ENTRY FORM: 1/3/81

TRS FLAME EVENT D- 20 ENTERED 17-JAN-81

COMMENT > WIND: NA MPH EARLY 2-NOZZLE BURNS

NOZZLE # --->		1	2						
AL KG/SEC/NOZ(EST)		4.80	4.80						
CALORIMETER	X CM	Y CM	Z CM	FLUX (JD)	FLUX (RM)	RM/JD	MODEL	%DF(JD)	%DF(RM)
FX-1	-183	53	152	41.30	NA	NA	41.62	1	NA
FX-2	365	53	304	16.10	NA	NA	14.54	-10	NA
FX-3	183	53	304	34.50	NA	NA	34.97	1	NA
FX-4	183	53	152	44.80	NA	NA	41.62	-7	NA

Table 17. TRS data entry forms: events D-15 to D-45: cylinder (continued).

SCIENCE APPLICATIONS, INC. TRS DATA ENTRY FORM: 1/3/81

TRS FLAME EVENT D- 21 ENTERED 17-JAN-81

COMMENT > WIND: NA MPH EARLY 2-NOZZLE BURNS

NOZZLE # --->	1	2
AL KG/SEC/NOZ(EST)	4.80	4.80

CALORIMETER	X CM	Y CM	Z CM	FLUX (JD)	FLUX (RM)	RM/JD	MODEL	%DF(JD)	%DF(RM)
FX-1	-183	53	152	43.00	NA	NA	41.62	-3	NA
FX-2	365	53	304	13.00	NA	NA	14.54	12	NA
FX-3	183	53	304	30.90	NA	NA	34.97	13	NA
FX-4	183	53	152	41.80	NA	NA	41.62	0	NA

SCIENCE APPLICATIONS, INC. TRS DATA ENTRY FORM: 1/3/81

TRS FLAME EVENT D- 21 ENTERED 17-JAN-81

COMMENT > WIND: NA MPH EARLY 2-NOZZLE BURNS

NOZZLE # --->	1	2
AL KG/SEC/NOZ(EST)	4.80	4.80

CALORIMETER	X CM	Y CM	Z CM	FLUX (JD)	FLUX (RM)	RM/JD	MODEL	%DF(JD)	%DF(RM)
FX-1	-183	53	152	43.00	NA	NA	41.62	-3	NA
FX-2	365	53	304	13.00	NA	NA	14.54	12	NA
FX-3	183	53	304	30.90	NA	NA	34.97	13	NA
FX-4	183	53	152	41.80	NA	NA	41.62	0	NA

Table 17. TRS data entry forms: events D-15 to D-45: cylinder (continued).

SCIENCE APPLICATIONS, INC. TRS DATA ENTRY FORM: 1/3/81

TRS FLAME EVENT D- 23 ENTERED 17-JAN-81

COMMENT > WIND: NA MPH EARLY 2-NOZZLE BURNS

NOZZLE # --->		1	2						
AL KG/SEC/NOZ(EST)		4.70	4.70						
CALORIMETER	X CM	Y CM	Z CM	FLUX (JD)	FLUX (RM)	RM/JD	MODEL	%DF(JD)	%DF(RM)
FX-1	122	66	228	57.80	NA	NA	58.73	2	NA
FX-2	365	53	304	13.90	NA	NA	14.54	5	NA
FX-3	183	53	304	32.70	NA	NA	34.97	7	NA
FX-4	183	53	152	43.30	NA	NA	41.62	-4	NA

SCIENCE APPLICATIONS, INC. TRS DATA ENTRY FORM: 1/3/81

TRS FLAME EVENT D- 24 ENTERED 17-JAN-81

COMMENT > WIND: NA MPH EARLY 2-NOZZLE BURNS

NOZZLE # --->		1	2						
AL KG/SEC/NOZ(EST)		4.90	4.90						
CALORIMETER	X CM	Y CM	Z CM	FLUX (JD)	FLUX (RM)	RM/JD	MODEL	%DF(JD)	%DF(RM)
FX-1	122	66	228	66.10	NA	NA	58.73	-11	NA
FX-2	365	53	304	15.60	NA	NA	14.54	-7	NA
FX-3	183	53	304	38.20	NA	NA	34.97	-8	NA
FX-4	183	53	152	44.80	NA	NA	41.62	-7	NA

Table 17. TRS data entry forms: events D-15 to D-45: cylinder (continued).

SCIENCE APPLICATIONS, INC. TRS DATA ENTRY FORM: 1/3/81

TRS FLAME EVENT D- 25 ENTERED 17-JAN-81

COMMENT > WIND: NA MPH EARLY 2-NOZZLE BURNS

NOZZLE # --->	1	2
AL KG/SEC/NOZ(EST)	4.80	4.80

CALORIMETER	X CM	Y CM	Z CM	FLUX (JD)	FLUX (RM)	RM/JD	MODEL	%DF(JD)	%DF(RM)
FX-1	122	66	228	57.80	NA	NA	58.73	2	NA
FX-2	365	53	304	14.80	NA	NA	14.54	-2	NA
FX-3	183	53	304	32.70	NA	NA	34.97	7	NA
FX-4	183	53	152	37.30	NA	NA	41.62	12	NA

SCIENCE APPLICATIONS, INC. TRS DATA ENTRY FORM: 1/3/81

TRS FLAME EVENT D- 26 ENTERED 17-JAN-81

COMMENT > WIND: NA MPH EARLY 2-NOZZLE BURNS

NOZZLE # --->	1	2
AL KG/SEC/NOZ(EST)	5.00	5.00

CALORIMETER	X CM	Y CM	Z CM	FLUX (JD)	FLUX (RM)	RM/JD	MODEL	%DF(JD)	%DF(RM)
FX-1	122	66	228	57.80	NA	NA	58.73	2	NA
FX-2	365	53	304	14.40	NA	NA	14.54	1	NA
FX-3	183	53	304	33.60	NA	NA	34.97	4	NA
FX-4	183	53	152	37.30	NA	NA	41.62	12	NA

Table 17. TRS data entry forms: events D-15 to D-45: cylinder (continued).

SCIENCE APPLICATIONS, INC. TRS DATA ENTRY FORM: 1/3/81

TRS FLAME EVENT D- 27 ENTERED 17-JAN-81

COMMENT > WIND: NA MPH EARLY 2-NOZZLE BURNS

NOZZLE # --->	1	2
AL KG/SEC/NOZ (EST)	5.00	5.00

CALORIMETER	X CM	Y CM	Z CM	FLUX (JD)	FLUX (RM)	RM/JD	MODEL	%DF(JD)	%DF(RM)
FX-1	122	66	228	29.50	NA	NA	58.73	99	NA
FX-2	365	53	304	8.70	NA	NA	14.54	67	NA
FX-3	183	53	304	20.90	NA	NA	34.97	67	NA
FX-4	183	53	152	22.30	NA	NA	41.62	87	NA

SCIENCE APPLICATIONS, INC. TRS DATA ENTRY FORM: 1/3/81

TRS FLAME EVENT D- 28 ENTERED 17-JAN-81

COMMENT > WIND: NA MPH EARLY 2-NOZZLE BURNS

NOZZLE # --->	1	2
AL KG/SEC/NOZ (EST)	5.20	5.20

CALORIMETER	X CM	Y CM	Z CM	FLUX (JD)	FLUX (RM)	RM/JD	MODEL	%DF(JD)	%DF(RM)
FX-1	122	66	228	57.80	NA	NA	58.73	2	NA
FX-2	365	53	304	15.70	NA	NA	14.54	-7	NA
FX-3	183	53	304	36.60	NA	NA	34.97	-4	NA
FX-4	183	53	152	44.80	NA	NA	41.62	-7	NA

Table 17. TRS data entry forms: events D-15 to D-45: cylinder (continued).

SCIENCE APPLICATIONS, INC. TRS DATA ENTRY FORM: 1/3/81

TRS FLAME EVENT D- 29 ENTERED 17-JAN-81

COMMENT > WIND: NA MPH EARLY 2-NOZZLE BURNS

NOZZLE # --->	1	2
AL KG/SEC/NOZ (EST)	5.10	5.10

CALORIMETER	X CM	Y CM	Z CM	FLUX (JD)	FLUX (RM)	RM/JD	MODEL	%DF (JD)	%DF (RM)
FX-1	122	66	228	57.80	NA	NA	58.73	2	NA
FX-2	365	53	304	13.90	NA	NA	14.54	5	NA
FX-3	183	53	304	32.70	NA	NA	34.97	7	NA
FX-4	183	53	152	41.80	NA	NA	41.62	0	NA

SCIENCE APPLICATIONS, INC. TRS DATA ENTRY FORM: 1/3/81

TRS FLAME EVENT D- 30 ENTERED 17-JAN-81

COMMENT > WIND: NA MPH EARLY 2-NOZZLE BURNS

NOZZLE # --->	1	2
AL KG/SEC/NOZ (EST)	5.10	5.10

CALORIMETER	X CM	Y CM	Z CM	FLUX (JD)	FLUX (RM)	RM/JD	MODEL	%DF (JD)	%DF (RM)
FX-1	122	66	228	57.80	NA	NA	58.73	2	NA
FX-2	365	53	304	13.10	NA	NA	14.54	11	NA
FX-3	183	53	304	34.50	NA	NA	34.97	1	NA
FX-4	183	53	152	41.80	NA	NA	41.62	0	NA

Table 17. TRS data entry forms: events D-15 to D-45: cylinder (continued).

SCIENCE APPLICATIONS, INC. TRS DATA ENTRY FORM: 1/3/81

TRS FLAME EVENT D- 31 ENTERED 17-JAN-81

COMMENT > WIND: NA MPH EARLY 2-NOZZLE BURNS

NOZZLE # --->	1	2
AL KG/SEC/NOZ (EST)	5.10	5.10

CALORIMETER	X CM	Y CM	Z CM	FLUX (JD)	FLUX (RM)	RM/JD	MODEL	%DF(JD)	%DF(RM)
FX-1	122	66	228	66.10	NA	NA	58.73	-11	NA
FX-2	365	53	304	17.40	NA	NA	14.54	-16	NA
FX-3	183	53	304	43.50	NA	NA	34.97	-20	NA
FX-4	183	53	152	35.50	NA	NA	41.62	17	NA

SCIENCE APPLICATIONS, INC. TRS DATA ENTRY FORM: 1/3/81

TRS FLAME EVENT D- 32 ENTERED 6-JAN-81

COMMENT > WIND: 0 MPH 2 NOZZLE BURN

NOZZLE # --->	1	2	3	4
AL KG/SEC/NOZ (EST)	0.00	0.00	4.10	4.10

CALORIMETER	X CM	Y CM	Z CM	FLUX (JD)	FLUX (RM)	RM/JD	MODEL	%DF(JD)	%DF(RM)
FX-1	122	278	229	67.70	61.10	0.90	58.63	-13	-4
FX-2	366	267	305	17.70	17.00	0.96	14.48	-18	-15
FX-3	183	267	305	43.60	40.00	0.92	34.85	-20	-13
FX-4	183	267	152	43.30	41.80	0.97	41.53	-4	-1

Table 17. TRS data entry forms: events D-15 to D-45: cylinder (continued).

SCIENCE APPLICATIONS, INC. TRS DATA ENTRY FORM: 1/3/81

TRS FLAME EVENT D- 33 ENTERED 6-JAN-81

COMMENT > WIND: 3 MPH 2 NOZZLE BURN

NOZZLE # --->	1	2	3	4
AL KG/SEC/NOZ(EST)	0.00	0.00	4.70	4.70

CALORIMETER	X CM	Y CM	Z CM	FLUX (JD)	FLUX (RM)	RM/JD	MODEL	%DF(JD)	%DF(RM)
FX-1	122	278	229	62.00	57.80	0.93	58.63	-5	1
FX-2	366	267	305	17.40	16.30	0.94	14.48	-17	-11
FX-3	183	267	305	38.20	35.90	0.94	34.85	-9	-3
FX-4	183	267	152	41.80	41.00	0.98	41.53	-1	1

SCIENCE APPLICATIONS, INC. TRS DATA ENTRY FORM: 1/3/81

TRS FLAME EVENT D- 34 ENTERED 6-JAN-81

COMMENT > WIND: 3 MPH 4 NOZZLE BURN

NOZZLE # --->	1	2	3	4
AL KG/SEC/NOZ(EST)	5.10	5.10	4.10	4.10

CALORIMETER	X CM	Y CM	Z CM	FLUX (JD)	FLUX (RM)	RM/JD	MODEL	%DF(JD)	%DF(RM)
FX-1	152	172	229	70.20	62.00	0.88	70.87	1	14
FX-2	366	160	305	29.60	27.00	0.91	26.39	-11	-2
FX-3	183	160	305	50.00	49.10	0.98	54.83	10	12
FX-4	183	160	152	59.70	58.20	0.97	64.46	8	11

Table 17. TRS data entry forms: events D-15 to D-45: cylinder (continued).

SCIENCE APPLICATIONS, INC. TRS DATA ENTRY FORM: 1/3/81

TRS FLAME EVENT D- 35 ENTERED 6-JAN-81

COMMENT > WIND: NA MPH 4 NOZZLE ATTEMPT

NOZZLE # --->		1	2	3	4				
AL KG/SEC/NOZ (EST)		0.00	0.00	4.40	4.40				
CALORIMETER	X CM	Y CM	Z CM	FLUX (JD)	FLUX (RM)	RM/JD	MODEL	%DF (JD)	%DF (RM)
FX-1	366	0	229	NA	NA	NA	9.18	NA	NA
FX-2	366	107	229	NA	NA	NA	12.57	NA	NA
FX-3	366	213	229	18.20	NA	NA	15.10	-17	NA
FX-4	366	320	229	16.40	NA	NA	15.10	-8	NA

SCIENCE APPLICATIONS, INC. TRS DATA ENTRY FORM: 1/3/81

TRS FLAME EVENT D- 36 ENTERED 6-JAN-81

COMMENT > WIND: NA MPH 4 NOZZLE BURN

NOZZLE # --->		1	2	3	4				
AL KG/SEC/NOZ (EST)		4.10	4.10	5.10	5.10				
CALORIMETER	X CM	Y CM	Z CM	FLUX (JD)	FLUX (RM)	RM/JD	MODEL	%DF (JD)	%DF (RM)
FX-1	366	0	229	NA	NA	NA	24.28	NA	NA
FX-2	366	107	229	NA	NA	NA	27.68	NA	NA
FX-3	366	213	229	40.00	NA	NA	27.68	-31	NA
FX-4	366	320	229	20.90	NA	NA	24.28	16	NA

Table 17. TRS data entry forms: events D-15 to D-45: cylinder (continued).

SCIENCE APPLICATIONS, INC. TRS DATA ENTRY FORM: 1/3/81

TRS FLAME EVENT D- 38 ENTERED 16-JAN-81

COMMENT > WIND: 15 MPH 4 NOZ BURN. WIND BLEW FROM NOZ 4-->1

NOZZLE # --->		1	2	3	4				
AL KG/SEC/NOZ (EST)		NA	NA	NA	NA				
CALORIMETER	X CM	Y CM	Z CM	FLUX (JD)	FLUX (RM)	RM/JD	MODEL	%DF (JD)	%DF (RM)
FX-1	183	0	229	NA	14.00	NA	48.60	NA	247
FX-2	183	107	229	NA	21.00	NA	60.06	NA	186
FX-3	183	213	229	NA	27.00	NA	60.06	NA	122
FX-4	183	320	229	NA	29.00	NA	48.60	NA	68

SCIENCE APPLICATIONS, INC. TRS DATA ENTRY FORM: 1/3/81

TRS FLAME EVENT D- 39 ENTERED 6-JAN-81

COMMENT > WIND: 0 MPH 4 NOZZLE BURN

NOZZLE # --->		1	2	3	4				
AL KG/SEC/NOZ (EST)		NA	NA	NA	NA				
CALORIMETER	X CM	Y CM	Z CM	FLUX (JD)	FLUX (RM)	RM/JD	MODEL	%DF (JD)	%DF (RM)
FX-1	366	0	229	NA	23.50	NA	24.28	NA	3
FX-2	366	107	229	NA	27.40	NA	27.68	NA	1
FX-3	366	213	229	NA	27.70	NA	27.68	NA	0
FX-4	366	320	229	NA	20.80	NA	24.28	NA	17

Table 17. TRS data entry forms: events D-15 to D-45: cylinder (continued).

SCIENCE APPLICATIONS, INC. TRS DATA ENTRY FORM: 1/3/81

TRS FLAME EVENT D- 40 ENTERED 6-JAN-81

COMMENT > WIND: 0 MPH 4 NOZZLE BURN

NOZZLE # --->	1	2	3	4
AL KG/SEC/NOZ (EST)	NA	NA	NA	NA

CALORIMETER	X CM	Y CM	Z CM	FLUX (JD)	FLUX (RM)	RM/JD	MODEL	%DF(JD)	%DF(RM)
FX-1	183	0	229	NA	41.30	NA	48.60	NA	18
FX-2	183	107	229	NA	52.20	NA	60.06	NA	15
FX-3	183	427	229	NA	21.40	NA	29.12	NA	36
FX-4	183	533	229	NA	8.76	NA	15.02	NA	71

SCIENCE APPLICATIONS, INC. TRS DATA ENTRY FORM: 1/3/81

TRS FLAME EVENT D- 43 ENTERED 16-JAN-81

COMMENT > WIND: NA MPH 4 NOZ BURN. WIND BLEW FROM NOZ 1-->4 BACK TO FRONT(45)

NOZZLE # --->	1	2	3	4
AL KG/SEC/NOZ (EST)	NA	NA	NA	NA

CALORIMETER	X CM	Y CM	Z CM	FLUX (JD)	FLUX (RM)	RM/JD	MODEL	%DF(JD)	%DF(RM)
FX-1	274	320	229	NA	37.20	NA	33.63	NA	-10
FX-2	274	213	229	NA	40.90	NA	39.88	NA	-2
FX-3	274	107	229	NA	30.90	NA	39.88	NA	29
FX-4	274	0	229	NA	20.90	NA	33.63	NA	61

Table 17. TRS data entry forms: events D-15 to D-45: cylinder (continued).

SCIENCE APPLICATIONS, INC. TRS DATA ENTRY FORM: 1/3/81

TRS FLAME EVENT D- 44 ENTERED 16-JAN-81

COMMENT > WIND: NA MPH 4 NOZ BURN

NOZZLE # --->	1	2	3	4
AL KG/SEC/NOZ (EST)	NA	NA	NA	NA

CALORIMETER	X CM	Y CM	Z CM	FLUX (JD)	FLUX (RM)	RM/JD	MODEL	%DF (JD)	%DF (RM)
FX-1	304	152	229	31.90	NA	NA	35.90	13	NA
FX-2	NA	NA	NA	NA	NA	NA	NA	NA	NA
FX-3	182	213	203	58.20	NA	NA	61.82	6	NA
FX-4	182	107	203	NA	NA	NA	61.82	NA	NA

SCIENCE APPLICATIONS, INC. TRS DATA ENTRY FORM: 1/3/81

TRS FLAME EVENT D- 45 ENTERED 16-JAN-81

COMMENT > WIND: NA MPH 4 NOZ BURN

NOZZLE # --->	1	2	3	4
AL KG/SEC/NOZ (EST)	NA	NA	NA	NA

CALORIMETER	X CM	Y CM	Z CM	FLUX (JD)	FLUX (RM)	RM/JD	MODEL	%DF (JD)	%DF (RM)
FX-1	304	152	229	29.90	NA	NA	35.90	20	NA
FX-2	NA	NA	NA	NA	NA	NA	NA	NA	NA
FX-3	182	213	203	NA	NA	NA	61.82	NA	NA
FX-4	182	107	203	55.20	NA	NA	61.82	12	NA

Table 18. TRS data entry forms: pentolite series: cylinder.

SCIENCE APPLICATIONS, INC. TRS DATA ENTRY FORM:5/11/81

TRS FLAME EVENT D-PENT-2 ENTERED 5/11/81

COMMENT > WIND: NA MPH

NOZZLE # --->			1	2	3	4				
AL KG/SEC/NOZ(EST)			NA	NA	NA	NA				
CALORIMETER	X CM	(+/-)	Y CM	Z CM	FLUX (RT.SD)	FLUX (LF.SD)	LF/RT	MODEL	%DF(RT)	%DF(LF)
FX-2/3	200		53	200	43.00	52.00	1.21	53.75	25	3
FX-1/4	200		160	200	41.00	41.00	1.00	41.84	2	2
FX-6	350		0	200	NA	24.00	NA	29.63	NA	23
FX-5/7	350		160	200	20.00	22.00	1.10	24.41	22	11
FX-9/10	500		53	200	10.00	NA	NA	17.38	74	NA
FX-8/11	500		160	200	NA	12.00	NA	15.53	NA	29

NOTE: NEGATIVE VALUES OF Y ARE ON RIGHT SIDE (IE. RT.SD)

Table 18. TRS data entry forms: Pentolite series: cylinder (continued).

SCIENCE APPLICATIONS, INC. TRS DATA ENTRY FORM:5/11/81

TRS FLAME EVENT D-PENT-3,4,5 ENTERED 5/11/81

COMMENT > WIND: NA MPH

NOZZLE # --->			1	2	3	4				
AL KG/SEC/NOZ (EST)			NA	NA	NA	NA				
CALORIMETER	X CM	(-/+) Y CM	Z CM	FLUX (RT.SD)	FLUX (LF.SD)	LF/RT	MODEL	%DF(RT)	%DF(LF)
PENT-3									
FX-2/3	200	107	200	46.00	41.00	0.89	49.34	7	20
FX-1/4	200	320	200	16.00	11.00	0.69	16.40	3	49
FX-6	350	0	200	NA	25.00	NA	29.63	NA	19
FX-5/7	350	320	200	14.00	12.00	0.86	14.24	2	19
FX-9/10	500	107	200	7.00	15.00	2.14	16.66	138	11
FX-8/11	500	320	200	10.00	10.00	1.00	10.95	10	10
PENT-4									
FX-2/3	200	107	200	48.00	52.00	1.08	49.34	3	-5
FX-1/4	200	320	200	13.00	13.00	1.00	16.40	26	26
FX-6	350	0	200	NA	30.00	NA	29.63	NA	-1
FX-5/7	350	320	200	13.00	14.00	1.08	14.24	10	2
FX-9/10	500	107	200	7.00	19.00	2.71	16.66	138	-12
FX-8/11	500	320	200	10.00	11.00	1.10	10.95	10	0
PENT-5									
FX-2/3	200	107	200	43.00	52.00	1.21	49.34	15	-5
FX-1/4	200	320	200	17.00	19.00	1.12	16.40	-4	-14
FX-6	350	0	200	NA	29.00	NA	29.63	NA	2
FX-5/7	350	320	200	16.00	17.00	1.06	14.24	-11	-16
FX-9/10	500	107	200	6.00	16.00	2.67	16.66	178	4
FX-8/11	500	320	200	10.00	12.00	1.20	10.95	10	-9

NOTE: NEGATIVE VALUES OF Y ARE ON RIGHT SIDE (IE. RT.SD)

Table 19. TRS data entry forms: events D-34 to D-45: inverted.

SCIENCE APPLICATIONS, INC. TRS DATA ENTRY FORM: 1/3/81

TRS FLAME EVENT D- 34 ENTERED 26-JAN-81

COMMENT > WIND: 3 MPH 4 NOZZLE BURN

NOZZLE # --->			1	2	3	4				
AL KG/SEC/NOZ (EST)			5.10	5.10	4.10	4.10				
CALORIMETER	X CM	Y CM	Z CM	FLUX (JD)	FLUX (RM)	RM/JD	MODEL	%DF (JD)	%DF (RM)	
FX-1	152	172	229	70.20	62.00	0.88	65.99	-6	6	
FX-2	366	160	305	29.60	27.00	0.91	25.96	-12	-4	
FX-3	183	160	305	50.00	49.10	0.98	51.80	4	5	
FX-4	183	160	152	59.70	58.20	0.97	60.98	2	5	

SCIENCE APPLICATIONS, INC. TRS DATA ENTRY FORM: 1/3/81

TRS FLAME EVENT D- 35 ENTERED 26-JAN-81

COMMENT > WIND: NA MPH 4 NOZZLE ATTEMPT

NOZZLE # --->			1	2	3	4				
AL KG/SEC/NOZ (EST)			0.00	0.00	4.40	4.40				
CALORIMETER	X CM	Y CM	Z CM	FLUX (JD)	FLUX (RM)	RM/JD	MODEL	%DF (JD)	%DF (RM)	
FX-1	366	0	229	NA	NA	NA	8.42	NA	NA	
FX-2	366	107	229	NA	NA	NA	12.12	NA	NA	
FX-3	366	213	229	18.20	NA	NA	15.07	-17	NA	
FX-4	366	320	229	16.40	NA	NA	15.07	-8	NA	

Table 19. TRS data entry forms: events D-34 to D-45: inverted (continued).

SCIENCE APPLICATIONS, INC. TRS DATA ENTRY FORM: 1/3/81

TRS FLAME EVENT D- 36 ENTERED 26-JAN-81

COMMENT > WIND: NA MPH 4 NOZZLE BURN

NOZZLE # --->	1	2	3	4
AL KG/SEC/NOZ (EST)	4.10	4.10	5.10	5.10

CALORIMETER	X CM	Y CM	Z CM	FLUX (JD)	FLUX (RM)	RM/JD	MODEL	%DF (JD)	%DF (RM)
FX-1	366	0	229	NA	NA	NA	23.04	NA	NA
FX-2	366	107	229	NA	NA	NA	27.16	NA	NA
FX-3	366	213	229	40.00	NA	NA	27.16	-32	NA
FX-4	366	320	229	20.90	NA	NA	23.04	10	NA

SCIENCE APPLICATIONS, INC. TRS DATA ENTRY FORM: 1/3/81

TRS FLAME EVENT D- 38 ENTERED 26-JAN-81

COMMENT > WIND: 15 MPH 4 NOZ BURN. WIND BLEW FROM NOZ 4-->1

NOZZLE # --->	1	2	3	4
AL KG/SEC/NOZ (EST)	NA	NA	NA	NA

CALORIMETER	X CM	Y CM	Z CM	FLUX (JD)	FLUX (RM)	RM/JD	MODEL	%DF (JD)	%DF (RM)
FX-1	183	0	229	NA	14.00	NA	43.85	NA	213
FX-2	183	107	229	NA	21.00	NA	56.69	NA	170
FX-3	183	213	229	NA	27.00	NA	56.69	NA	110
FX-4	183	320	229	NA	29.00	NA	43.85	NA	51

Table 19. TRS data entry forms: events D-34 to D-45. Inverted (continued).

SCIENCE APPLICATIONS, INC. TRS DATA ENTRY FORM: 1/3/81

TRS FLAME EVENT D- 39 ENTERED 26-JAN-81

COMMENT > WIND: 0 MPH 4 NOZZLE BURN

NOZZLE # --->	1	2	3	4
AL KG/SEC/NOZ (EST)	NA	NA	NA	NA

CALORIMETER	X CM	Y CM	Z CM	FLUX (JD)	FLUX (RM)	RM/JD	MODEL	%DF(JD)	%DF(RM)
FX-1	366	0	229	NA	23.50	NA	23.04	NA	-2
FX-2	366	107	229	NA	27.40	NA	27.16	NA	-1
FX-3	366	213	229	NA	27.70	NA	27.16	NA	-2
FX-4	366	320	229	NA	20.80	NA	23.04	NA	11

SCIENCE APPLICATIONS, INC. TRS DATA ENTRY FORM: 1/3/81

TRS FLAME EVENT D- 40 ENTERED 26-JAN-81

COMMENT > WIND: 0 MPH 4 NOZZLE BURN

NOZZLE # --->	1	2	3	4
AL KG/SEC/NOZ (EST)	NA	NA	NA	NA

CALORIMETER	X CM	Y CM	Z CM	FLUX (JD)	FLUX (RM)	RM/JD	MODEL	%DF(JD)	%DF(RM)
FX-1	183	0	229	NA	41.30	NA	43.85	NA	6
FX-2	183	107	229	NA	52.20	NA	56.69	NA	9
FX-3	183	427	229	NA	21.40	NA	23.61	NA	10
FX-4	183	533	229	NA	8.76	NA	10.84	NA	24

Table 19. TRS data entry forms: events D-34 to D-45: inverted (continued).

SCIENCE APPLICATIONS, INC. TRS DATA ENTRY FORM: 1/3/81

TRS FLAME EVENT D- 43 ENTERED 26-JAN-81

COMMENT > WIND: NA MPH 4 NOZ BURN. WIND BLEW FROM NOZ 1-->4 BACK TO FRONT(45)

NOZZLE # --->	1	2	3	4				
AL KG/SEC/NOZ(EST)	NA	NA	NA	NA				
CALORIMETER	X CM	Y CM	Z CM	FLUX (JD)	FLUX (RM)	RM/JD	MODEL	%DF(JD)	%DF(RM)
FX-1	274	320	229	NA	37.20	NA	31.21	NA	-16
FX-2	274	213	229	NA	40.90	NA	38.60	NA	-6
FX-3	274	107	229	NA	30.90	NA	38.60	NA	25
FX-4	274	0	229	NA	20.90	NA	31.21	NA	49

SCIENCE APPLICATIONS, INC. TRS DATA ENTRY FORM: 1/3/81

TRS FLAME EVENT D- 44 ENTERED 26-JAN-81

COMMENT > WIND: NA MPH 4 NOZ BURN

NOZZLE # --->	1	2	3	4				
AL KG/SEC/NOZ(EST)	NA	NA	NA	NA				
CALORIMETER	X CM	Y CM	Z CM	FLUX (JD)	FLUX (RM)	RM/JD	MODEL	%DF(JD)	%DF(RM)
FX-1	304	152	229	31.90	NA	NA	34.94	10	NA
FX-2	NA	NA	NA	NA	NA	NA	NA	NA	NA
FX-3	182	213	203	58.20	NA	NA	58.11	0	NA
FX-4	182	107	203	NA	NA	NA	58.11	NA	NA

Table 19. TRS data entry forms: events D-34 to D-45: inverted (continued).

SCIENCE APPLICATIONS, INC. TRS DATA ENTRY FORM: 1/3/81

TRS FLAME EVENT D- 45 ENTERED 26-JAN-81

COMMENT > WIND: NA MPH 4 NOZ BURN

NOZZLE # --->	1	2	3	4
AL KG/SEC/NOZ (EST)	NA	NA	NA	NA

CALORIMETER	X CM	Y CM	Z CM	FLUX (JD)	FLUX (RM)	RM/JD	MODEL	%DF(JD)	%DF(RM)
FX-1	304	152	229	29.90	NA	NA	34.94	17	NA
FX-2	NA	NA	NA	NA	NA	NA	NA	NA	NA
FX-3	182	213	203	NA	NA	NA	58.11	NA	NA
FX-4	182	107	203	55.20	NA	NA	58.11	5	NA

APPENDIX C

A MODEL COMPARED WITH DATA BASE

This appendix presents a comparison of the available peak flux data with one calibration to the inverted cone model. Two tables are included; both list the same data, but in two different orders. One is sorted by event, Table 20, and is almost chronological. The other, Table 21, is sorted by the ratio of model results to measured results. The model used was the inverted cone. These lists illustrate how the differences are statistically dispersed.

Table 20. Event sort of model comparison with data base.

X	Z	R	CALOR	EVENT
-182.90	152.40	1.11	FX-1	D15
365.80	304.80	0.54	FX-2	D15
182.90	304.80	0.69	FX-3	D15
182.90	152.40	1.09	FX-4	D15
-182.90	152.40	1.21	FX-1	D17
365.80	304.80	0.82	FX-2	D17
182.90	304.80	0.76	FX-3	D17
182.90	152.40	1.13	FX-4	D17
-182.90	152.40	1.16	FX-1	D19
365.80	304.80	0.75	FX-2	D19
182.90	304.80	0.78	FX-3	D19
182.90	152.40	1.13	FX-4	D19
-182.90	152.40	1.16	FX-1	D20
365.80	304.80	1.00	FX-2	D20
182.90	304.80	0.88	FX-3	D20
182.90	152.40	1.26	FX-4	D20
-182.90	152.40	1.21	FX-1	D21
365.80	304.80	0.80	FX-2	D21
182.90	304.80	0.78	FX-3	D21
182.90	152.40	1.17	FX-4	D21
121.90	228.60	1.11	FX-1	D23
365.80	304.80	0.86	FX-2	D23
182.90	304.80	0.83	FX-3	D23
182.90	152.40	1.22	FX-4	D23
121.90	228.60	1.27	FX-1	D24
365.80	304.80	0.96	FX-2	D24
182.90	304.80	0.97	FX-3	D24
182.90	152.40	1.26	FX-4	D24
121.90	228.60	1.11	FX-1	D25
365.80	304.80	0.91	FX-2	D25
182.90	304.80	0.83	FX-3	D25
182.90	152.40	1.05	FX-4	D25
121.90	228.60	1.11	FX-1	D26
365.80	304.80	0.89	FX-2	D26
182.90	304.80	0.85	FX-3	D26
182.90	152.40	1.05	FX-4	D26
121.90	228.60	1.11	FX-1	D28
365.80	304.80	0.97	FX-2	D28
182.90	304.80	0.93	FX-3	D28
182.90	152.40	1.26	FX-4	D28
121.90	228.60	1.11	FX-1	D29
365.80	304.80	0.86	FX-2	D29
182.90	304.80	0.83	FX-3	D29
182.90	152.40	1.17	FX-4	D29
121.90	228.60	1.11	FX-1	D30
365.80	304.80	0.81	FX-2	D30
182.90	304.80	0.88	FX-3	D30
182.90	152.40	1.17	FX-4	D30
121.90	228.60	1.27	FX-1	D31
365.80	304.80	1.08	FX-2	D31
182.90	304.80	1.10	FX-3	D31
182.90	152.40	1.00	FX-4	D31

Table 20. Event sort of model comparison with data base (continued).

121.90	228.60	1.30	FX-1	D32
365.80	304.80	1.09	FX-2	D32
182.90	304.80	1.11	FX-3	D32
182.90	152.40	1.22	FX-4	D32
121.90	228.60	1.19	FX-1	D33
365.80	304.80	1.08	FX-2	D33
182.90	304.80	0.97	FX-3	D33
182.90	152.40	1.17	FX-4	D33
365.80	228.60	1.18	FX-3	D35
365.80	228.60	1.07	FX-4	D35
152.40	228.60	1.24	FX-1	D34
365.80	304.50	1.25	FX-2	D34
182.90	304.50	1.05	FX-3	D34
182.90	152.40	1.25	FX-4	D34
365.80	228.60	1.16	FX-1	D39
365.80	228.60	1.18	FX-2	D39
365.80	228.60	1.18	FX-3	D39
365.80	228.60	1.02	FX-4	D39
182.90	228.60	1.00	FX-1	D40
182.90	228.60	1.06	FX-2	D40
182.90	228.60	0.86	FX-3	D40
182.90	228.60	0.74	FX-4	D40
274.30	228.60	1.30	FX-1	D43
274.30	228.60	1.21	FX-2	D43
274.30	228.60	0.91	FX-3	D43
274.30	228.60	0.73	FX-4	D43
304.80	228.60	1.06	FX-1	D44
182.90	203.00	1.19	FX-3	D44
304.80	228.60	0.99	FX-1	D45
182.90	203.00	1.13	FX-4	D45
200.00	200.00	1.09	FX-1	PENT-2
200.00	200.00	0.95	FX-2	PENT-2
200.00	200.00	1.15	FX-3	PENT-2
200.00	200.00	1.09	FX-4	PENT-2
350.00	200.00	0.95	FX-5	PENT-2
350.00	200.00	0.97	FX-6	PENT-2
350.00	200.00	1.04	FX-7	PENT-2
500.00	200.00	0.92	FX-11	PENT-2
200.00	200.00	0.95	FX-1	PENT-3
200.00	200.00	1.08	FX-2	PENT-3
200.00	200.00	0.96	FX-3	PENT-3
200.00	200.00	0.66	FX-4	PENT-3
350.00	200.00	1.06	FX-5	PENT-3
350.00	200.00	1.01	FX-6	PENT-3
350.00	200.00	0.91	FX-7	PENT-3
500.00	200.00	1.04	FX-8	PENT-3
500.00	200.00	1.09	FX-10	PENT-3
500.00	200.00	1.04	FX-11	PENT-3
200.00	200.00	0.77	FX-1	PENT-4
200.00	200.00	1.12	FX-2	PENT-4
200.00	200.00	1.22	FX-3	PENT-4
200.00	200.00	0.77	FX-4	PENT-4
350.00	200.00	0.98	FX-5	PENT-4
350.00	200.00	1.22	FX-6	PENT-4
350.00	200.00	1.06	FX-7	PENT-4
500.00	200.00	1.04	FX-8	PENT-4
500.00	200.00	1.38	FX-10	PENT-4

Table 20. Event sort of model comparison with data base (continued).

500.00	200.00	1.14	FX-11	PENT-4
200.00	200.00	1.01	FX-1	PENT-5
200.00	200.00	1.01	FX-2	PENT-5
200.00	200.00	1.22	FX-3	PENT-5
200.00	200.00	1.13	FX-4	PENT-5
350.00	200.00	1.21	FX-5	PENT-5
350.00	200.00	1.17	FX-6	PENT-5
350.00	200.00	1.29	FX-7	PENT-5
500.00	200.00	1.04	FX-8	PENT-5
500.00	200.00	1.16	FX-10	PENT-5
500.00	200.00	1.25	FX-11	PENT-5
300.00	317.50	1.22	FX-1	UK1-PRE
300.00	317.50	1.26	FX-2	UK1-PRE
300.00	317.50	1.25	FX-3	UK1-PRE
269.00	317.50	1.30	CAL-4	UK1-PRE
183.00	317.50	1.14	CAL-6	UK1-PRE
300.00	317.50	1.03	FX-4	UK1-PRE
589.00	317.50	1.24	CAL-1	UK1-PRE
511.00	317.50	1.20	CAL-2	UK1-PRE
511.00	317.50	1.28	CAL-3	UK1-PRE
589.00	317.50	1.29	CAL-5	UK1-PRE
0.00	317.50	0.57	CAL-1	NAV-PRE
244.00	317.50	1.05	CAL-2	NAV-PRE
589.00	317.50	1.08	CAL-3	NAV-PRE
244.00	317.50	1.15	CAL-4	NAV-PRE
244.00	317.50	1.08	CAL-5	NAV-PRE
244.00	317.50	0.81	CAL-6	NAV-PRE
244.00	317.50	1.07	FX-1	NAV-PRE
589.00	317.50	1.07	FX-2	NAV-PRE
589.00	317.50	1.12	FX-3	NAV-PRE
244.00	317.50	1.00	FX-4	NAV-PRE
274.00	335.00	0.95	CAL-1	UK2-PRE
274.00	122.00	0.99	CAL-2	UK2-PRE
274.00	335.00	1.01	CAL-3	UK2-PRE
274.00	122.00	1.05	CAL-4	UK2-PRE
274.00	335.00	1.01	CAL-5	UK2-PRE
274.00	122.00	0.96	CAL-6	UK2-PRE
274.00	122.00	0.89	CAL-7	UK2-PRE
274.00	229.00	0.88	FX-1	UK2-PRE
274.00	229.00	0.93	FX-2	UK2-PRE
274.00	229.00	0.95	FX-3	UK2-PRE
274.00	229.00	1.03	FX-4	UK2-PRE
183.00	172.00	1.22	CAL-1	BRL-PRE
183.00	265.00	1.09	CAL-2	BRL-PRE
183.00	357.00	1.08	CAL-3	BRL-PRE
183.00	357.00	1.20	CAL-4	BRL-PRE
183.00	357.00	1.13	CAL-5	BRL-PRE
183.00	265.00	1.04	CAL-6	BRL-PRE
183.00	172.00	1.11	CAL-7	BRL-PRE
183.00	265.00	1.06	FX-1	BRL-PRE
183.00	200.00	1.22	FX-2	BRL-PRE
183.00	172.00	1.16	FX-3	BRL-PRE
183.00	200.00	1.17	FX-4	BRL-PRE
180.30	116.20	0.82	F-1	UK-1 MR
271.80	166.40	0.94	F-2	UK-1 MR
261.60	139.10	1.03	F-3	UK-1 MR
596.90	229.90	0.81	F-4	UK-1 MR

Table 20. Event sort of model comparison with data base (continued).

591.80	230.50	0.81	F-5	UK-1 MR
467.40	168.90	1.15	F-6	UK-1 MR
576.60	229.90	1.36	F-7	UK-1 MR
576.60	229.20	1.42	F-8	UK-1 MR
268.00	179.10	0.83	F-1	UK-2 MR
269.20	179.10	0.98	F-2	UK-2 MR
269.90	189.90	1.00	F-3	UK-2 MR
259.10	179.10	0.94	F-4	UK-2 MR
-190.50	200.70	1.67	F-1	BRL MR
-190.50	200.70	1.07	F-2	BRL MR
-190.50	200.70	1.00	F-3	BRL MR
276.90	92.70	0.87	F-1	NAVY MR
576.60	207.00	1.11	F-2	NAVY MR
576.60	171.40	1.04	F-3	NAVY MR
271.80	92.70	0.65	F-4	NAVY MR

Table 21. Ratio sort of model comparison with data base.

X	Z	R	CALOR	EVENT
365.80	304.80	0.54	FX-2	D15
0.00	317.50	0.57	CAL-1	NAV-PRE
271.80	92.70	0.65	F-4	NAVY MR
200.00	200.00	0.66	FX-4	PENT-3
182.90	304.80	0.69	FX-3	D15
274.30	228.60	0.73	FX-4	D43
182.90	228.60	0.74	FX-4	D40
365.80	304.80	0.75	FX-2	D19
182.90	304.80	0.76	FX-3	D17
200.00	200.00	0.77	FX-1	PENT-4
200.00	200.00	0.77	FX-4	PENT-4
182.90	304.80	0.78	FX-3	D21
182.90	304.80	0.78	FX-3	D19
365.80	304.80	0.80	FX-2	D21
365.80	304.80	0.81	FX-2	D30
244.00	317.50	0.81	CAL-6	NAV-PRE
591.80	230.50	0.81	F-5	UK-1 MR
596.90	229.90	0.81	F-4	UK-1 MR
365.80	304.80	0.82	FX-2	D17
180.30	116.20	0.82	F-1	UK-1 MR
182.90	304.80	0.83	FX-3	D25
182.90	304.80	0.83	FX-3	D23
182.90	304.80	0.83	FX-3	D29
268.00	179.10	0.83	F-1	UK-2 MR
182.90	304.80	0.85	FX-3	D26
365.80	304.80	0.86	FX-2	D23
365.80	304.80	0.86	FX-2	D29
182.90	228.60	0.86	FX-3	D40
276.90	92.70	0.87	F-1	NAVY MR
182.90	304.80	0.88	FX-3	D20
182.90	304.80	0.88	FX-3	D30
274.00	229.00	0.88	FX-1	UK2-PRE
365.80	304.80	0.89	FX-2	D26
274.00	122.00	0.89	CAL-7	UK2-PRE
365.80	304.80	0.91	FX-2	D25
274.30	228.60	0.91	FX-3	D43
350.00	200.00	0.91	FX-7	PENT-3
500.00	200.00	0.92	FX-11	PENT-2
182.90	304.80	0.93	FX-3	D28
274.00	229.00	0.93	FX-2	UK2-PRE
271.80	166.40	0.94	F-2	UK-1 MR
259.10	179.10	0.94	F-4	UK-2 MR
200.00	200.00	0.95	FX-2	PENT-2
350.00	200.00	0.95	FX-5	PENT-2
200.00	200.00	0.95	FX-1	PENT-3
274.00	335.00	0.95	CAL-1	UK2-PRE
274.00	229.00	0.95	FX-3	UK2-PRE
365.80	304.80	0.96	FX-2	D24
200.00	200.00	0.96	FX-3	PENT-3
274.00	122.00	0.96	CAL-6	UK2-PRE
182.90	304.80	0.97	FX-3	D24

Table 21. Ratio sort of model comparison with data base (continued).

365.80	304.80	0.97	FX-2	D28
182.90	304.80	0.97	FX-3	D33
350.00	200.00	0.97	FX-6	PENT-2
350.00	200.00	0.98	FX-5	PENT-4
269.20	179.10	0.98	F-2	UK-2 MR
304.80	228.60	0.99	FX-1	D45
274.00	122.00	0.99	CAL-2	UK2-PRE
365.80	304.80	1.00	FX-2	D20
182.90	152.40	1.00	FX-4	D31
182.90	228.60	1.00	FX-1	D40
244.00	317.50	1.00	FX-4	NAV-PRE
269.90	189.90	1.00	F-3	UK-2 MR
-190.50	200.70	1.00	F-3	BRL MR
350.00	200.00	1.01	FX-6	PENT-3
200.00	200.00	1.01	FX-1	PENT-5
200.00	200.00	1.01	FX-2	PENT-5
274.00	335.00	1.01	CAL-3	UK2-PRE
274.00	335.00	1.01	CAL-5	UK2-PRE
365.80	228.60	1.02	FX-4	D39
300.00	317.50	1.03	FX-4	UK1-PRE
274.00	229.00	1.03	FX-4	UK2-PRE
261.60	139.10	1.03	F-3	UK-1 MR
350.00	200.00	1.04	FX-7	PENT-2
500.00	200.00	1.04	FX-8	PENT-3
500.00	200.00	1.04	FX-11	PENT-3
500.00	200.00	1.04	FX-8	PENT-4
500.00	200.00	1.04	FX-8	PENT-5
183.00	265.00	1.04	CAL-6	BRL-PRE
576.60	171.40	1.04	F-3	NAVY MR
182.90	152.40	1.05	FX-4	D25
182.90	152.40	1.05	FX-4	D26
182.90	304.50	1.05	FX-3	D34
244.00	317.50	1.05	CAL-2	NAV-PRE
274.00	122.00	1.05	CAL-4	UK2-PRE
182.90	228.60	1.06	FX-2	D40
304.80	228.60	1.06	FX-1	D44
350.00	200.00	1.06	FX-5	PENT-3
350.00	200.00	1.06	FX-7	PENT-4
183.00	265.00	1.06	FX-1	BRL-PRE
365.80	228.60	1.07	FX-4	D35
244.00	317.50	1.07	FX-1	NAV-PRE
589.00	317.50	1.07	FX-2	NAV-PRE
-190.50	200.70	1.07	F-2	BRL MR
365.80	304.80	1.08	FX-2	D31
365.80	304.80	1.08	FX-2	D33
200.00	200.00	1.08	FX-2	PENT-3
589.00	317.50	1.08	CAL-3	NAV-PRE
244.00	317.50	1.08	CAL-5	NAV-PRE
183.00	357.00	1.08	CAL-3	BRL-PRE
182.90	152.40	1.09	FX-4	D15
365.80	304.80	1.09	FX-2	D32
200.00	200.00	1.09	FX-1	PENT-2
200.00	200.00	1.09	FX-4	PENT-2
500.00	200.00	1.09	FX-10	PENT-3
183.00	265.00	1.09	CAL-2	BRL-PRE
182.90	304.80	1.10	FX-3	D31
-182.90	152.40	1.11	FX-1	D15

Table 21. Ratio sort of model comparison with data base (continued).

121.90	228.60	1.11	FX-1	D23
121.90	228.60	1.11	FX-1	D25
121.90	228.60	1.11	FX-1	D26
121.90	228.60	1.11	FX-1	D28
121.90	228.60	1.11	FX-1	D29
121.90	228.60	1.11	FX-1	D30
182.90	304.80	1.11	FX-3	D32
183.00	172.00	1.11	CAL-7	BRL-PRE
576.60	207.00	1.11	F-2	NAVY MR
200.00	200.00	1.12	FX-2	PENT-4
589.00	317.50	1.12	FX-3	NAV-PRE
182.90	152.40	1.13	FX-4	D17
182.90	152.40	1.13	FX-4	D19
182.90	203.00	1.13	FX-4	D45
200.00	200.00	1.13	FX-4	PENT-5
183.00	357.00	1.13	CAL-5	BRL-PRE
500.00	200.00	1.14	FX-11	PENT-4
183.00	317.50	1.14	CAL-6	UK1-PRE
200.00	200.00	1.15	FX-3	PENT-2
244.00	317.50	1.15	CAL-4	NAV-PRE
467.40	168.90	1.15	F-6	UK-1 MR
-182.90	152.40	1.16	FX-1	D19
-182.90	152.40	1.16	FX-1	D20
365.80	228.60	1.16	FX-1	D39
500.00	200.00	1.16	FX-10	PENT-5
183.00	172.00	1.16	FX-3	BRL-PRE
182.90	152.40	1.17	FX-4	D21
182.90	152.40	1.17	FX-4	D29
182.90	152.40	1.17	FX-4	D30
182.90	152.40	1.17	FX-4	D33
350.00	200.00	1.17	FX-6	PENT-5
183.00	200.00	1.17	FX-4	BRL-PRE
365.80	228.60	1.18	FX-3	D35
365.80	228.60	1.18	FX-2	D39
365.80	228.60	1.18	FX-3	D39
121.90	228.60	1.19	FX-1	D33
182.90	203.00	1.19	FX-3	D44
511.00	317.50	1.20	CAL-2	UK1-PRE
183.00	357.00	1.20	CAL-4	BRL-PRE
-182.90	152.40	1.21	FX-1	D21
-182.90	152.40	1.21	FX-1	D17
274.30	228.60	1.21	FX-2	D43
350.00	200.00	1.21	FX-5	PENT-5
182.90	152.40	1.22	FX-4	D23
182.90	152.40	1.22	FX-4	D32
200.00	200.00	1.22	FX-3	PENT-4
350.00	200.00	1.22	FX-6	PENT-4
200.00	200.00	1.22	FX-3	PENT-5
300.00	317.50	1.22	FX-1	UK1-PRE
183.00	172.00	1.22	CAL-1	BRL-PRE
183.00	200.00	1.22	FX-2	BRL-PRE
152.40	228.60	1.24	FX-1	D34
589.00	317.50	1.24	CAL-1	UK1-PRE
365.80	304.50	1.25	FX-2	D34
182.90	152.40	1.25	FX-4	D34
500.00	200.00	1.25	FX-11	PENT-5
300.00	317.50	1.25	FX-3	UK1-PRE

Table 21. Ratio sort of model comparison with data base (continued).

182.90	152.40	1.26	FX-4	D20
182.90	152.40	1.26	FX-4	D24
182.90	152.40	1.26	FX-4	D28
300.00	317.50	1.26	FX-2	UK1-PRE
121.90	228.60	1.27	FX-1	D24
121.90	228.60	1.27	FX-1	D31
511.00	317.50	1.28	CAL-3	UK1-PRE
350.00	200.00	1.29	FX-7	PENT-5
589.00	317.50	1.29	CAL-5	UK1-PRE
121.90	228.60	1.30	FX-1	D32
274.30	228.60	1.30	FX-1	D43
269.00	317.50	1.30	CAL-4	UK1-PRE
576.60	229.90	1.36	F-7	UK-1 MR
500.00	200.00	1.38	FX-10	PENT-4
576.60	229.20	1.42	F-8	UK-1 MR
-190.50	200.70	1.67	F-1	BRL MR

APPENDIX D

TRS CALORIMETER LOCATIONS: MILL RACE

This appendix documents the locations of the calorimeters on MILL RACE. Four arrays of nozzles were fielded. Three arrays consisted of four nozzles each, and one array consisted of eight nozzles.

Table 22. TRS data entry forms: MILL RACE.

SAI MILL RACE TRS DATA ENTRY FORM 9-DEC-81 B. CHAMBERS

BRL MILL RACE CALORIMETER	COORDINATES IN INCHES X	Y	Z	COORDINATES IN CMS X	Y	Z
F-1	-75.00	-140.00	79.00	-190.50	-355.60	200.66
F-2	-75.00	-93.00	79.00	-190.50	-236.22	200.66
F-3	-75.00	-47.00	79.00	-190.50	-119.38	200.66
F-4	-75.00	0.00	79.00	-190.50	0.00	200.66
NOZZLES						
1	0.00	-6.00	0.00	0.00	-15.24	0.00
2	0.00	-48.00	0.00	0.00	-121.92	0.00
3	0.00	-90.00	0.00	0.00	-228.60	0.00
4	0.00	-132.00	0.00	0.00	-335.28	0.00

COMMENTS:
DISTANCES WERE RECORDED BY COL. BOUSEK, DNAFC

Table 22. TRS data entry forms: MILL RACE (continued).

SAI MILL RACE TRS DATA ENTRY FORM 9-DEC-81 B. CHAMBERS

UK-1

MILL RACE CALORIMETER	COORDINATES IN INCHES X	Y	Z	COORDINATES IN CMS X	Y	Z
F-1	71.00	37.00	45.75	180.34	93.98	116.21
F-2	107.00	131.00	65.50	271.78	332.74	166.37
F-3	103.00	229.25	54.75	261.62	582.30	139.07
F-4	235.00	93.00	90.50	596.90	236.22	229.87
F-5	233.00	276.75	90.75	591.82	702.95	230.51
F-6	184.00	377.25	66.50	467.36	958.22	168.91
F-7	227.00	496.50	90.50	576.58	1261.11	229.87
F-8	227.00	650.75	90.25	576.58	1652.91	229.24
NOZZLES						
1	0.00	73.00	0.00	0.00	185.42	0.00
2	0.00	157.00	0.00	0.00	398.78	0.00
3	0.00	241.00	0.00	0.00	612.14	0.00
4	0.00	325.00	0.00	0.00	825.50	0.00
5	0.00	409.00	0.00	0.00	1038.86	0.00
6	0.00	493.00	0.00	0.00	1252.22	0.00
7	0.00	577.00	0.00	0.00	1465.58	0.00
8	0.00	661.00	0.00	0.00	1678.94	0.00

COMMENTS:
DISTANCES MEASURED BY COL. BOUSEK, DNAFC

Table 22. TRS data entry forms: MILL RACE (continued).

SAI MILL RACE TRS DATA ENTRY FORM 9-DEC-81 B. CHAMBERS

UK-2 COORDINATES IN INCHES COORDINATES IN CMS

MILL RACE CALORIMETER	X	Y	Z	X	Y	Z
F-1	105.50	-329.50	70.50	267.97	-836.93	179.07
F-2	106.00	-203.50	70.50	269.24	-516.89	179.07
F-3	106.25	-145.50	74.75	269.88	-369.57	189.87
F-4	102.00	0.00	70.50	259.08	0.00	179.07
NOZZLES						
1	0.00	-18.00	0.00	0.00	-45.72	0.00
2	0.00	-102.00	0.00	0.00	-259.08	0.00
3	0.00	-186.00	0.00	0.00	-472.44	0.00
4	0.00	-270.00	0.00	0.00	-685.80	0.00

COMMENTS:
DISTANCES MEASURED BY COL. BOUSEK, DNAFC

Table 22. TRS data entry forms: MILL RACE (continued).

SAI MILL RACE TRS DATA ENTRY FORM 9-DEC-81 B. CHAMBERS

NAVY

MILL RACE CALORIMETER	COORDINATES IN INCHES X	Y	Z	COORDINATES IN CMS X	Y	Z
F-1	109.00	0.00	36.50	276.86	0.00	92.71
F-2	227.00	111.00	81.50	576.58	281.94	207.01
F-3	227.00	322.00	67.50	576.58	817.88	171.45
F-4	107.00	385.00	36.50	271.78	977.90	92.71
NOZZLES						
1	0.00	26.00	0.00	0.00	66.04	0.00
2	0.00	152.00	0.00	0.00	386.08	0.00
3	0.00	278.00	0.00	0.00	706.12	0.00
4	0.00	404.00	0.00	0.00	1026.16	0.00

COMMENTS:

DISTANCES WERE RECORDED BY COL. BOUSEK, DNAFC

APPENDIX E

ALFGEE LISTINGS

This appendix presents listings of an implementation of the ALFGEE algorithms on an Apple II microcomputer system. The language used is Pascal and the operating system is Apple Pascal Version 1.1. These are derivatives of the UCSD II.1 Pascal system.

The implementation is in seven files. These are given in the usual Pascal ordering, where entities are defined before being used (or referenced). The main program is contained on the last file.

Your attention is directed to an earlier section (4.7), where it is stated that this implementation *will not* provide correct results for touching flames. Further, the default values for the model parameters, contained herein, are outdated.

```
{$S+}
UNIT circle_intersection;
INTERFACE
USES transcend; {Copyright 1979,1980 Apple Computer, Inc. & UC Regents}

  FUNCTION acos(x: REAL):REAL;
  FUNCTION cintersection (xl, yl, rl, xn, yn, rn: REAL;
                          VAR d, xil, yil, xi2, yi2: REAL): BOOLEAN;
  IMPLEMENTATION

  FUNCTION acos;
  CONST pid2 = 1.570796327; epsilon = 1.0E-8;
  VAR y: REAL;

  BEGIN acos := 0.0;
    IF ABS(x) > 1.0 THEN EXIT(acos)
    ELSE IF ABS(x) < epsilon THEN acos := pid2 ELSE
      BEGIN
        y := 1.0 - SQR(x);
        IF y <> 0.0 THEN acos := pid2 - ATAN(x / SQRT(y))
        ELSE IF x > 0.0 THEN acos := 0.0 ELSE acos := pid2 + pid2
      END
  END;

  FUNCTION cintersection;
  CONST pi = 3.14159265;
  VAR alpha, theta: REAL;

  BEGIN
    cintersection := FALSE;
    rl := ABS(rl); rn := ABS(rn);
    d := SQRT(SQR(xn-xl)+SQR(yn-yl));
    IF (d > 0.0) AND (d <= rl + rn) THEN
      BEGIN
        IF xn=xl THEN theta := -pi/2.0 ELSE theta := ATAN((yn-yl)/(xn-xl));
        IF xn < xl THEN theta := theta + pi;
        alpha := acos((SQR(rl) - SQR(d) - SQR(rn))/(2.0*d*rn));
        xi2 := xn + rn * COS(theta+alpha);
        yi2 := yn + rn * SIN(theta+alpha);
        xil := xn + rn * COS(theta-alpha);
```

Figure 38. ALFGEE file: CINT.UNIT.TEXT.

```
        yil := yn + rn * SIN(theta-alpha);
        cintersection := TRUE;
      END;
  END;
BEGIN END.
```


Figure 38. ALFGEE file: CINT.UNIT.TEXT (continued).

```
{$S+} {$V-}

UNIT variables;
{ Version:  13-Apr-82 }
INTERFACE

CONST pi = 3.141592654; promptline =2;
      maxnobags = 100;  quesline = 22;
      dashes = '----------------------------------------';
      doshes = '-  ---   -------------  -------------';

VAR pr:TEXT; outdev:STRING;
    fourpi,degtorad,radtodeg:REAL;
    albedo,hgtacoeff,hgtbcoeff:REAL;
    nbags:INTEGER;
    widthofbag,heightofbag,bestguessbag,bagstrength:REAL;
    xbag,ybag,zbag,tbag,sbag:ARRAY[1..maxnobags] OF REAL;
    nx,ny,nz,nt,ne:INTEGER;
    ix,iy,iz,it,ie:INTEGER;
    dx,dy,dz,dt,de:REAL;
    nextloop:PACKED ARRAY [1..5] OF CHAR;
    xdist0,ydist0,zdist0,theta0,elev0:REAL;
    xdistf,ydistf,zdistf,thetaf,elevf:REAL;
    ignorekeys,debug:BOOLEAN;
    intlen,reallen: INTEGER;

  PROCEDURE dummy100;

  IMPLEMENTATION

  PROCEDURE dummy100;

  BEGIN
  END;

BEGIN
END.
```

Figure 39. ALFGEE file. TRS.VARS.TEXT

```
{$S+} {$V-}
UNIT trsinput;
{ Version: 13-Apr-82 }
INTERFACE
USES
transcend, {Copyright 1979,1980 Apple Computer, Inc. & UC Regents}
{$U TRS.VARS.CODE} variables;
TYPE soc=SET OF CHAR;
PROCEDURE get_an_x(a,j:INTEGER;s:STRING;k,l:INTEGER;VAR x:REAL);
PROCEDURE get_an_i(a,j:INTEGER;s:STRING;k,l:INTEGER;VAR x:INTEGER);
PROCEDURE get_an_b(a,j:INTEGER;s:STRING;k,l:INTEGER;VAR x:BOOLEAN);
PROCEDURE get_an_s(a,j:INTEGER;s:STRING;k,l:INTEGER;VAR x:STRING);
PROCEDURE promptat(l:INTEGER;s:STRING);
FUNCTION  getchar(s:soc): CHAR;
PROCEDURE readdata;
IMPLEMENTATION
   PROCEDURE promptat; BEGIN GOTOXY(0,l); WRITE(CHR(29)); WRITE(s); END;
   FUNCTION getchar;
   VAR ch: CHAR;
   BEGIN
     REPEAT WRITE(CHR(7)); READ(keyboard,ch); UNTIL ch IN s;
     WRITE(ch); getchar := ch;
   END;
PROCEDURE g(h,i:INTEGER); BEGIN GOTOXY(h,i); WRITE(CHR(29)); GOTOXY(h,i); END;
PROCEDURE get_an_x;BEGIN G(a,j);WRITE(s);g(k,l);READ(x);g(k,l);G(a,j);END;
PROCEDURE get_an_i;BEGIN G(a,j);WRITE(s);g(k,l);READ(x);g(k,l);G(a,j);END;
PROCEDURE get_an_b;
VAR c: STRING;
BEGIN G(a,j);
  WRITE(s);g(k,l);
  WRITE('Y(es or N(o ?'); READ(c); x := (c='Y') OR (c='y');
  g(k,l);G(a,j);
END;
PROCEDURE get_an_s;BEGIN G(a,j);WRITE(s);g(k,l);READ(x);g(k,l);G(a,j);END;
   PROCEDURE default;
   VAR i,j:INTEGER;
   BEGIN
      fourpi := 4.0 * pi;
      degtorad := pi / 180; radtodeg := 1 / degtorad;
      bagstrength := 1.0;
```

Figure 40. ALFGEE file: TRS.INPUTA.TEXT.

```
    bestguessbag := 0.0;
    widthofbag := 0.0;
    heightofbag := 0.0;
    albedo := 0.0;
    hgtacoeff := 0.0;
    hgtbcoeff := 0.0;
    nbags := 1; debug := FALSE;
    FOR i := 1 TO maxnobags DO
      BEGIN
        xbag[i] := 0.0; j := (i+1) DIV 2;
        ybag[i] := 0.0;
        zbag[i] := 0.0;
        tbag[i] := 0.0; sbag[i] := 1.0;
      END;
    xdist0 := 100; xdistf := 100; dx := 0.0; nx := 1;
    ydist0 := 0.0; ydistf := 0.0; dy := 0.0; ny := 1;
    zdist0 := 150.0; zdistf := 150.0; dz := 0.0; nz := 1;
    theta0 := 0.0; thetaf := 0.0; dt := 0.0; nt := 1;
    elev0 := 0.0; elevf := 0.0; de := 0.0; ne := 1;
    nextloop[1] := 'E';
    nextloop[2] := 'T';
    nextloop[3] := 'Z';
    nextloop[4] := 'Y';
    nextloop[5] := 'X';
    ignorekeys := FALSE;
END;
PROCEDURE menuhead;
BEGIN
    WRITE(CHR(11)); WRITELN; WRITELN(dashes);
    WRITELN(' #          description              value  ');
    WRITELN('---         -----------              -----  ');
END;
PROCEDURE menu2head;
BEGIN WRITELN; WRITELN(dashes);
    WRITELN('#  m    x (cm)       y (cm)       z (cm)    ');
    WRITELN('- -- ----------  ----------  ---------- ');
END;
PROCEDURE menu3head;
BEGIN WRITELN; WRITELN(dashes);
    WRITELN('#  mod    strength ( - )  burn time(sec)');
```

Figure 40. ALEGEE file: TRS.INPUTA.TEXT (continued).

```
   WRITELN(doshes);
END;
PROCEDURE menutail;
BEGIN
   WRITELN(dashes);
   WRITE('option #: [0 returns]    which one ?');
END;
PROCEDURE menu1;
CONST nbagspl = 10; lineoffset = 6;
VAR n1,ms,me,line:INTEGER;
BEGIN
   promptat(promptline,'trs: LEVEL 1 menu:       GENERAL options');
   menuhead;
   WRITELN(' 1 number of trs nozzles in array',nbags:3);
   WRITELN(' 2 trs nozzle characteristics');
   WRITELN(' 3 trs nozzle position selector');
   WRITELN(' 4 trs nozzle strength selector');
   WRITELN(' 5 detector position');
   WRITELN(' 6 detector orientation');
   WRITELN(' 7 output format specifications');
   WRITELN(' 8 specify loop order');
   WRITELN(' 9 RUN the case');
   WRITE  (' a (toggle)  ignore keypress ?  ');
   IF ignorekeys THEN WRITELN('YES') ELSE WRITELN('no');
   menutail;
END;
PROCEDURE menu2;
BEGIN
   promptat(promptline,'trs: LEVEL 2 menu:          OUTPUT specs');
   menuhead;
   WRITELN(' 1    console: should be output device');
   WRITELN(' 2    printer: should be output device');
   WRITELN(' 3    remout:  should be output device');
   WRITELN(' 4    a diskette file should be device');
   WRITELN;
   WRITELN('   outdev is ',outdev);
   WRITELN;
   WRITELN(' 5    debug print on');
   WRITELN(' 6    debug print off');
   WRITELN;
```

Figure 40. ALFGEE file: TRS.INPUTA.TEXT (continued).

```
   WRITE('   debug print is ');
   IF debug THEN WRITE('ON') ELSE WRITE('off');
   WRITELN;
   menutail;
END;
PROCEDURE prod3;
CONST w = 11; f = 1; li = 4;
VAR product: REAL;
BEGIN
   WRITELN;
   product := nx * ny; product := product * nz * nt;
   product := product * ne;
   WRITELN('number of cases is  = ',product:w:f);
   WRITELN('nx:',nx:li,'   ny:',ny:li,'   nz:',nz:li);
   WRITELN('na:',nt:li,'   ne:',ne:li);
   menutail;
END;
PROCEDURE menu3;
CONST w = 11; f = 1; li = 4;
BEGIN
   promptat(promptline,'trs: LEVEL 2 menu:     DETECTOR position');
   menuhead;
   WRITELN(' 1     xdist0: smallest x =',xdist0.w:f);
   WRITELN(' 2     xdistf: greatest x =',xdistf:w:f);
   WRITELN(' 3      dx: spacing in x  =',dx:w:f);
   WRITELN;
   WRITELN(' 4     ydist0: smallest y =',ydist0:w:f);
   WRITELN(' 5     ydistf: greatest y =',ydistf:w:f);
   WRITELN(' 6      dy: spacing in y  =',dy:w:f);
   WRITELN;
   WRITELN(' 7     zdist0: smallest z =',zdist0:w:f);
   WRITELN(' 8     zdistf: greatest z =',zdistf:w:f);
   WRITELN(' 9      dz: spacing in z  =',dz:w:f);
   prod3;
END;
PROCEDURE menu35;
CONST w = 10; f = 1; li = 4;
BEGIN
   promptat(promptline,'trs: LEVEL 2 menu:  DETECTOR orientation');
   menuhead;
```

Figure 40. ALFGEE file: TRS.INPUTA.TEXT (continued).

```
    WRITELN(' 1    azimuth0: smallest   =',theta0:w:f);
    WRITELN(' 2    azimuth:  greatest   =',thetaf:w:f);
    WRITELN(' 3    da:azimuth spacing   =',dt:w:f);
    WRITELN;
    WRITELN(' 4    elevation0:smallest  =',elev0:w:f);
    WRITELN(' 5    elevationf:greatest  =',elevf:w:f);
    WRITELN(' 6    de:elevation spacing =',de:w:f);
    prod3;
END;
PROCEDURE menu4;
CONST w = 12; f = 1; li = 5;
BEGIN
    promptat(promptline,'trs: LEVEL 2 menu:      trs NOZZLE specs');
    menuhead;
    WRITELN(' 1      relative strength =',bagstrength:w:f);
    WRITELN(' 2      absolute strength =',bestguessbag:w:f);
    WRITELN(' 3      flame diameter    =',widthofbag:w:f);
    WRITELN(' 4      flame height      =',heightofbag:w:f);
    WRITELN(' 5 (rel)hgt of luminosity =',hgtacoeff:w:f);
    WRITELN(' 6 (rel)strength at nozzle=',hgtbcoeff:w:f);
    WRITELN(' 7      ground albedo     =',albedo:w:f);
    menutail;
END;
PROCEDURE menu45;
CONST nbagspl = 10;
VAR nl,ms,me,line:INTEGER; ch:CHAR; s:STRING[1];
BEGIN
    promptat(promptline,'trs: LEVEL 2 menu:          NOZZLE lists');
    menuhead; s := ' ';
    IF nbags > 0 THEN
      BEGIN
        nl := (nbags - 1) DIV nbagspl + 1;
        ms := 1; me := 10;
        FOR line := 1 TO nl DO
          BEGIN
            IF nbags < me THEN me := nbags;
            IF line = 10 THEN ch := 'a'
              ELSE ch := CHR(ORD('0')+line);
            s[1] := ch;
            WRITELN(' ',s,'       nozzles   (',
```

Figure 40. ALFGEE file: TRS.INPUTA.TEXT (continued).

```
                    ms:2,' -',me:3,')       *     ');
            ms := me + 1; me := me + nbagspl;
          END;
      END;
   menutail;
END;
PROCEDURE menu5(ms,me:INTEGER);
VAR i,line:INTEGER; ch:CHAR; s:STRING[1];
BEGIN
   promptat(promptline,'trs: LEVEL 3 menu:  trs NOZZLE locations');
   WRITE(CHR(11));
   menu2head; s := ' ';
   FOR i := ms TO me DO
     BEGIN
       line := i - ms + 1;
       IF line = 10 THEN ch := 'a'
         ELSE ch := CHR(ORD('0')+line);
       s[1] := ch;
       WRITELN(s,i:3,xbag[i]:12:5,ybag[i]:12:5,zbag[i]:12:5);
     END;
   menutail;
END;
PROCEDURE menu6(ms,me:INTEGER);
VAR i,line:INTEGER; ch:CHAR; s:STRING[1];
BEGIN
   promptat(promptline,'trs: LEVEL 3 menu:  trs NOZZLE strengths');
   WRITE(CHR(11));
   menu3head; s := ' ';
   FOR i := ms TO me DO
     BEGIN
       line := i - ms + 1;
       IF line = 10 THEN ch := 'a'
         ELSE ch := CHR(ORD('0')+line);
       s[1] := ch;
       WRITELN(s,'  ',i:3,sbag[i]:14:5,tbag[i]:16:5);
     END;
   menutail;
END;
PROCEDURE menu7;
CONST w = 15; f = 1; li = 5;
```

Figure 40. ALFGEE file: TRS.INPUTA.TEXT (continued).

```
  BEGIN
     promptat(promptline,'trs: LEVEL 2 menu:          LOOP control');
     menuhead;
     WRITELN(' 1          outermost loop is over ',nextloop[1]);
     WRITELN(' 2          next                   ',nextloop[2]);
     WRITELN(' 3          next                   ',nextloop[3]);
     WRITELN(' 4          next                   ',nextloop[4]);
     WRITELN(' 5          innermost loop is over ',nextloop[5]);
     WRITELN;
     WRITELN('x,y,z,t,e should each only be used once!');
     menutail;
  END;
{$I TRS.INPUTB.TEXT}
```


Figure 40. ALFGEE file: TRS.INPUTA.TEXT (continued).

```
PROCEDURE readdata;
VAR successful,finished,question:BOOLEAN; selection:INTEGER; ch:CHAR;
   PROCEDURE readoutput;
   CONST n = 11;
   VAR s,disk,name:STRING;
       finished:BOOLEAN;
      PROCEDURE redo(VAR s:STRING);
      BEGIN
         CLOSE(pr,lock);
         outdev := s;
         REWRITE(pr,outdev);
      END;
   BEGIN
     finished := FALSE;
     REPEAT
       menu2; ch := getchar(['0'..'6']);
       selection := ORD(ch)-ORD('0');
       CASE selection OF
         0:finished := TRUE;
         1:BEGIN s := 'CONSOLE:'; redo(s) END;
         2:BEGIN s := 'PRINTER:'; redo(s) END;
         3:BEGIN s := 'REMOUT:'; redo(s) END;
         4:REPEAT
             promptat(promptline,' '); WRITE(CHR(11));
             successful := FALSE;
             promptat(n,'which disk for results ?  [i will add :]');
             WRITELN; disk := 'DEFAULT';
             READLN(disk);
             IF disk = 'DEFAULT' THEN successful := TRUE
             ELSE
               BEGIN
                 promptat(n+4,'what file name ?       [i will add .TEXT]');
                 WRITELN; name := 'OUTDEFAULT';
                 READLN(name);
                 name := CONCAT(disk,':',name,'.TEXT');
                 outdev := name;
                 {$I-}
                 CLOSE(pr,lock);
                 REWRITE(pr,outdev);
                 successful := IORESULT = 0;
```

Figure 41. ALFGEE file: TRS.INPUTB.TEXT.

```
            {$I+}
          END;
        UNTIL successful;
      5:debug := TRUE;
      6:debug := FALSE;
    END;
  UNTIL finished;
END;
PROCEDURE adjust(x0:REAL;VAR xf:REAL;VAR dx:REAL;VAR nx:INTEGER);
BEGIN
  IF dx <= 0.0 THEN dx := xf - x0;
  IF dx > 0.0 THEN
    BEGIN
      nx := ROUND((xf - x0)/dx);
      xf := x0 + nx * dx;
      nx := nx + 1
    END
  ELSE nx := 1;
END;
PROCEDURE readdetector;
VAR finished:BOOLEAN;
BEGIN
  finished := FALSE;
  REPEAT
    menu3; ch := getchar(['0'..'9']);
    selection := ORD(ch)-ORD('0');
    promptat(quesline,' '); WRITE(CHR(11));
    CASE selection OF
        0:finished := TRUE;
        1:BEGIN
            promptat(quesline,'xdist0 = ?'); READLN(xdist0);
            IF xdist0 > xdistf THEN xdistf := xdist0;
            nx := 1;
          END;
        2:BEGIN
            promptat(quesline,'xdistf = ?'); READLN(xdistf);
            IF xdistf > xdist0 THEN adjust(xdist0,xdistf,dx,nx);
          END;
        3:BEGIN
            promptat(quesline,'dx = ?'); READLN(dx);
```

Figure 41. ALFGEE file: TRS.INPUTB.TEXT (continued).

```
            adjust(xdist0,xdistf,dx,nx);
          END;
        4:BEGIN
            promptat(quesline,'ydist0 = ?'); READLN(ydist0);
            IF ydist0 > ydistf THEN ydistf := ydist0;
            ny := 1;
          END;
        5:BEGIN
            promptat(quesline,'ydistf = ?'); READLN(ydistf);
            IF ydistf > ydist0 THEN adjust(ydist0,ydistf,dy,ny);
          END;
        6:BEGIN
            promptat(quesline,'dy = ?'); READLN(dy);
            adjust(ydist0,ydistf,dy,ny);
          END;
        7:BEGIN
            promptat(quesline,'zdist0 = ?'); READLN(zdist0);
            IF zdist0 > zdistf THEN zdistf := zdist0;
            nz := 1;
          END;
        8:BEGIN
            promptat(quesline,'zdistf = ?'); READLN(zdistf);
            IF zdistf > zdist0 THEN adjust(zdist0,zdistf,dz,nz);
          END;
        9:BEGIN
            promptat(quesline,'dz = ?'); READLN(dz);
            adjust(zdist0,zdistf,dz,nz);
          END;
      END;
  UNTIL finished;
END;
PROCEDURE readorientation;
VAR finished:BOOLEAN;
BEGIN
  finished := FALSE;
  REPEAT
    menu35; ch := getchar(['0'..'6']);
    selection := ORD(ch)-ORD('0');
    promptat(quesline,' '); WRITE(CHR(11));
    CASE selection OF
```

Figure 41. ALFGEE file: TRS.INPUTB.TEXT (continued).

```
          0:finished := TRUE;
          1:BEGIN
              promptat(quesline,'azimuth0 = ?'); READLN(theta0);
              IF theta0 > thetaf THEN thetaf := theta0;
              nt := 1;
            END;
          2:BEGIN
              promptat(quesline,'azimuthf = ?'); READLN(thetaf);
              IF thetaf > theta0 THEN adjust(theta0,thetaf,dt,nt);
            END;
          3:BEGIN
              promptat(quesline,'da = ?'); READLN(dt);
              adjust(theta0,thetaf,dt,nt);
            END;
          4:BEGIN
              promptat(quesline,'elevation0 = ?'); READLN(elev0);
              IF elev0 > elevf THEN elevf := elev0;
              nt := 1;
            END;
          5:BEGIN
              promptat(quesline,'elevationf = ?'); READLN(elevf);
              IF elevf > elev0 THEN adjust(elev0,elevf,de,ne);
            END;
          6:BEGIN
              promptat(quesline,'de = ?'); READLN(de);
              adjust(elev0,elevf,de,ne);
            END;
        END;
    UNTIL finished;
END;
PROCEDURE readmodule;
VAR finished:BOOLEAN;
BEGIN
  finished := FALSE;
  REPEAT
    menu4; ch := getchar(['0'..'7']);
    selection := ORD(ch)-ORD('0');
    CASE selection OF
       0:finished := TRUE;
       1:REPEAT
```

Figure 41. ALEGEE file: TRS.INPUTB.TEXT (continued).

```
            promptat(quesline,'RELATIVE strength = ?');
            READLN(bagstrength);
          UNTIL bagstrength > 0.0;
        2:REPEAT
            promptat(quesline,'ABSOLUTE strength (cal) = ?');
            READLN(bestguessbag);
          UNTIL bestguessbag > 0.0;
        3:REPEAT
            promptat(quesline,'flame DIAMETER (cm) = ?');
            READLN(widthofbag);
          UNTIL widthofbag > 0.0;
        4:REPEAT
            promptat(quesline,'flame HEIGHT (cm) = ?');
            READLN(heightofbag);
          UNTIL heightofbag > 0.0;
        5:REPEAT
            promptat(quesline,'Luminosity limit ? (Rel hgt)');
            READLN(hgtacoeff);
          UNTIL (hgtacoeff >= 1.0);
        6:REPEAT
            promptat(quesline,'Power at nozzle ? (rel str)');
            READLN(hgtbcoeff);
          UNTIL (hgtbcoeff >= 0.0);
        7:REPEAT
            promptat(quesline,'ALBEDO of ground = ?');
            READLN(albedo);
          UNTIL ((albedo >= 0.0) AND (albedo <= 1.0));
      END;
  UNTIL finished;
END;
PROCEDURE looporder;
VAR finished,question:BOOLEAN; ch:CHAR;
BEGIN
  finished := FALSE;
  REPEAT
    menu7; ch := getchar(['0'..'5']);
    selection := ORD(ch)-ORD('0');
    IF selection > 0 THEN
      BEGIN
        promptat(quesline,'which for this LOOP ?       [x/y/z/t/e]');
```

Figure 41. ALEGEE file: TRS.INPUTB.TEXT (continued).

```
        ch := getchar(['X','Y','Z','T','E','x','y','z','t','e']);
        IF ch IN ['x','y','z','t','e'] THEN ch := CHR(ORD(ch)-32);
        nextloop[selection] := ch;
      END
    ELSE finished:= TRUE;
  UNTIL finished;
END;
PROCEDURE readmset(mset:INTEGER);
VAR finished,question:BOOLEAN; ch:CHAR;
    ms,me:INTEGER;
BEGIN
  finished := FALSE;
  me := mset * 10; ms := me - 9;
  IF me > nbags THEN me := nbags;
  IF me < ms THEN EXIT(readmset);
  REPEAT
    menu5(ms,me); ch := getchar(['0'..'9','A','a']);
    IF ch IN ['A','a'] THEN selection := 10
      ELSE selection := ORD(ch)-ORD('0');
    IF selection > me - ms + 1 THEN WRITE(CHR(7))
    ELSE IF selection > 0 THEN
      BEGIN
        promptat(quesline,'change x, y, or z ?   [x/y/z]');
        ch := getchar(['X','Y','Z','x','y','z']);
        promptat(quesline,'the value of ');
        WRITE(ch,' is = ?');
        CASE ch OF
          'X','x': READLN(xbag[(mset-1)*10+selection]);
          'Y','y': READLN(ybag[(mset-1)*10+selection]);
          'Z','z': READLN(zbag[(mset-1)*10+selection]);
        END;
      END
    ELSE finished:= TRUE;
  UNTIL finished;
END;
PROCEDURE readposition;
VAR finished:BOOLEAN;
BEGIN
  finished := FALSE;
  REPEAT
```

Figure 41. ALFGEE file: TRS.INPUTB.TEXT (continued).

```
    menu45; ch := getchar(['0'..'9','A','a']);
    IF ch IN ['A','a'] THEN selection := 10
      ELSE selection := ORD(ch)-ORD('0');
    CASE selection OF
       0:finished := TRUE;
       1,2,3,4,5,6,7,8,9,10:readmset(selection);
      END;
  UNTIL finished;
END;
PROCEDURE readmget(mset:INTEGER);
VAR finished,question:BOOLEAN; ch:CHAR;
    ms,me:INTEGER;
BEGIN
  finished := FALSE;
  me := mset * 10; ms := me - 9;
  IF me > nbags THEN me := nbags;
  IF me < ms THEN EXIT(readmget);
  REPEAT
    menu6(ms,me); ch := getchar(['0'..'9','A','a']);
    IF ch IN ['A','a'] THEN selection := 10
      ELSE selection := ORD(ch)-ORD('0');
    IF selection > me - ms + 1 THEN WRITE(CHR(7))
    ELSE IF selection > 0 THEN
      BEGIN
        promptat(quesline,'change s or t ?        [s/t]');
        ch := getchar(['S','T','s','t']);
        promptat(quesline,'the value of ');
        WRITE(ch,' is = ?');
        CASE ch OF
          'S','s': READLN(sbag[(mset-1)*10+selection]);
          'T','t': READLN(tbag[(mset-1)*10+selection]);
         END;
      END
    ELSE finished:= TRUE;
  UNTIL finished;
END;
PROCEDURE readstrength;
VAR finished:BOOLEAN;
BEGIN
  finished := FALSE;
```

Figure 41. ALEGEE file. TRS.INPUTB.TEXT (continued).

```
      REPEAT
        menu45; ch := getchar(['0'..'9','A','a']);
        IF ch IN ['A','a'] THEN selection := 10
          ELSE selection := ORD(ch)-ORD('0');
        CASE selection OF
           0:finished := TRUE;
           1,2,3,4,5,6,7,8,9,10:readmget(selection);
          END;
      UNTIL finished;
    END;
BEGIN
    finished := FALSE;
    REPEAT
       menu1; ch := getchar(['0'..'9','A','a']);
       IF ch IN ['0'..'9'] THEN selection := ORD(ch)-ORD('0')
                          ELSE selection := 10;
       CASE selection OF
         0:BEGIN
             promptat(promptline,'       <<<<< EXIT PROCEDURE >>>>>');
             WRITE(CHR(11)); WRITE(CHR(7)); UNITCLEAR(1);
             get_an_b(9,5,'are you ready to quit ?',15,10,finished);
             IF finished THEN
               BEGIN
                 PAGE(OUTPUT);
                 CLOSE(pr,LOCK);
                 EXIT(PROGRAM)
               END
           END;
         1:REPEAT
             promptat(quesline,'how many NOZZLES in the field ? ');
             READLN(nbags);
             IF nbags > maxnobags THEN
             BEGIN
                WRITE(CHR(7));
                get_an_b(0,quesline,
                      'number EXCEEDS allowable, max ok ?',-1,-1,question);
                IF question THEN nbags := maxnobags
             END;
           UNTIL (nbags > 0) AND (nbags <= maxnobags);
         2:readmodule;
```

Figure 41. ALEGEE file: TRS.INPUTB.TEXT (continued).

```
            3:readposition;
            4:readstrength;
            5:readdetector;
            6:readorientation;
            7:readoutput;
            8:looporder;
            9:finished := TRUE;
           10:ignorekeys := NOT ignorekeys;
           END;
      UNTIL finished;
  END;
BEGIN default END.
```


Figure 41. ALFGEE file: TRS.INPUTB.TEXT (continued).

```
{$S+} {$V-}
UNIT trs_stuff;
{ Version:  13-Apr-82 }
INTERFACE
USES
applestuff,transcend, {Copyright 1979, 1980 Apple Computer, Inc. & UC Regents}
{$U TRS.VARS.CODE} variables,
{$U TRS.INPUT.CODE} trsinput;
VAR
   codeversion, header, prheader, prtailer: STRING;
   xdist,ydist,zdist,theta,elev,flu:REAL;
   crflag,screen,diablo,decwriter:BOOLEAN;
   i,line,lastline,printline,remline: INTEGER;
   wlbag,wlrbag,rg2bag,rgbag,
   pbag,abag,bbag: ARRAY[1..maxnobags] OF REAL;
   kbag: ARRAY[1..maxnobags] OF INTEGER;
   PROCEDURE chkline (indicator:BOOLEAN);
   PROCEDURE heading;
   PROCEDURE start;
   PROCEDURE pause;
   FUNCTION  escape :BOOLEAN;
   PROCEDURE prheading;
  IMPLEMENTATION
   PROCEDURE heading;
   BEGIN
      WRITELN(pr,'     XDIST       YDIST       Height',
                 '     Azimuth    Elevation         Flux      ');
      chkline(FALSE);
      WRITELN(pr,'     (cm.)       (cm.)       (cm.)',
                 '       (deg)       (deg)      (cal/cm^2/sec) ');
      chkline(FALSE);
      WRITELN(pr,'     -----       -----       -----',
                 '        -----     ---------    -------------- ');
      chkline(FALSE);
   END;
   PROCEDURE start;
   VAR s: STRING;
   BEGIN
      PAGE(OUTPUT); outdev := 'CONSOLE:';
      REWRITE(pr,outdev);
```

Figure 42. ALFGEE file: TRS.UNIT.TEXT.

```
    PAGE(OUTPUT);
    s := CONCAT(header,codeversion);
    promptat(0,s);
    line := 1;
END;
PROCEDURE pause;
BEGIN
  WRITE('press <RETURN> to continue...');
  READLN;
  UNITCLEAR(1);
  line := 2;
  GOTOXY(0,line); WRITE(CHR(29));
END;
FUNCTION  escape;
VAR ch:CHAR;
BEGIN
  escape := FALSE;
  IF NOT ignorekeys THEN IF KEYPRESS THEN
    BEGIN
      READ(ch);
      IF ch = CHR(3) THEN
        BEGIN
          CLOSE(pr,lock);
          EXIT(PROGRAM);
        END;
      IF ch = CHR(27) THEN escape := TRUE;
      IF ch = CHR(13) THEN crflag := TRUE;
    END;
END;
PROCEDURE prheading;
VAR r:INTEGER;
BEGIN
   GOTOXY(0,1); WRITE(CHR(11));
   line := 2; GOTOXY(0,line);
   IF NOT screen THEN PAGE(pr);
   WRITELN(pr,prheader,prtailer,codeversion);
   WRITELN(pr);WRITELN(pr);
   WRITELN(pr,
          'Flame: #        X         Y         Z         T         S');
   line := line + 4;
```

Figure 42. ALFGEE file: TRS.UNIT.TEXT (continued).

```
    FOR n := 1 TO nbags DO
       BEGIN
          WRITELN(pr,n:8,xbag[n]:10:1,ybag[n]:10:1,zbag[n]:10:1,
                         tbag[n]:10:1,sbag[n]:10:1);
          chkline(FALSE);
       END;
    WRITELN(pr); chkline(FALSE);
    WRITELN(pr,' Relative Strength  = ',bagstrength:10:1);
    chkline(FALSE);
    WRITELN(pr,' Absolute Strength  = ',bestguessbag:10:1,' cal/sec');
    chkline(FALSE);
    WRITELN(pr,' Flame Diameter     = ',widthofbag:10:1,' cm.');
    chkline(FALSE);
    WRITELN(pr,' Flame Height       = ',heightofbag:10:1,' cm.');
    chkline(FALSE);
    WRITELN(pr,
    ' Luminosity Limit   = ',hgtacoeff:10:1,' (Rel to flame hgt)');
    chkline(FALSE);
    WRITELN(pr,
    ' "Power" at nozzle  = ',hgtbcoeff:10:1,' (Rel to power at flame hgt.)');
    chkline(FALSE);
    WRITELN(pr,' Ground Albedo      = ',albedo:10:1);
    chkline(FALSE);
    WRITELN(pr);
    chkline(FALSE);
    heading;
END;
PROCEDURE chkline;
BEGIN
    line := line + 1;
    IF screen THEN IF line >= lastline THEN
      BEGIN
        pause;
        IF indicator THEN heading;
      END
    ELSE IF diablo THEN
      BEGIN
        IF line >= printline THEN IF indicator THEN
          BEGIN
            line := 1; prheading;
```

Figure 42. ALFGEE file: TRS.UNIT.TEXT (continued).

```
            END;
          END
        ELSE IF decwriter THEN
          BEGIN
            IF line >= remline THEN IF indicator THEN
              BEGIN
                line := 1; prheading;
              END;
          END
    END;
BEGIN
    intlen := 5; reallen := 15; lastline := 22; printline := 56; remline := 76;
END.
```


Figure 42. ALFGEE file: TRS.UNIT.TEXT (continued).

```
{$S+} {$V-}
PROGRAM trsradiation;
{ Version: 13-Apr-82 }
                    {   TRS Radiation Program - FLAMES    }
USES
applestuff, transcend, {Copyright 1979,1980 Apple Computer, Inc.& UC Regents}
{$U CINT.UNIT.CODE} circle_intersection,
{$U TRS.VARS.CODE} variables,
{$U TRS.INPUT.CODE} trsinput,
{$U TRS.UNIT.CODE} trs_stuff;
   FUNCTION asin(x: REAL):REAL; FORWARD;
   SEGMENT PROCEDURE loops;
   VAR loopcount:INTEGER; lc:ARRAY[1..5] OF INTEGER;
       lll,il,i2,i3,i4,i5,nl,n2,n3,n4,n5:INTEGER;
       ch:CHAR;
      PROCEDURE calculate;
      CONST cangle = 90.0; safety = 9.0;
            mmax = 51;
            mmin = 15;
      VAR i,j,k,l,lmax,n,m:INTEGER;
          te,ee,se,ce,tt,st,ct:REAL;
          xj,yj,zj,sj,tj,rg,rg2,mp,si,wl,wlr,nwl,nwlr,zk,r,r2,ca:REAL;
          sip,zip:ARRAY[0..mmax] OF REAL;
          dz:REAL;
          thmax,thmin,thavgi,thavgf: REAL;
          PROCEDURE bagprint;
          CONST w = 10; d = 3;
          BEGIN
            WRITELN(pr);
            chkline(TRUE);
            WRITELN(pr,
              'Module #',j:d,
              ', with ',m:d,' pts. ',
              'Where k =',kbag[j]:d);
            chkline(TRUE);
          END;
          PROCEDURE powprint;
          CONST w = 10; d = 3;
          BEGIN
            WRITELN(pr,
```

Figure 43. ALFGEE file: LOX-FLAME.TEXT.

```
    ' i =',i:d,
    ' ca =',ca:w:d,
    ' nwlr =',nwlr:w:d,
    ' wlr =',wlr:w:d,
    ' tf =',thavgf,
    ' ti =',thavgi);
  chkline(TRUE);
END;
PROCEDURE sortprint;
CONST w = 10; d = 3;
VAR j: INTEGER;
BEGIN
  WRITELN(pr,'      x          y         wl        wlr  ',
             '     rg2        rg          a         b');
  chkline(TRUE);
  FOR j := 1 TO nbags DO
    BEGIN
      WRITELN(pr,  xbag[j]:w:d,   ybag[j]:w:d,
                  wlbag[j]:w:d, wlrbag[j]:w:d,
                 rg2bag[j]:w:d,  rgbag[j]:w:d,
                   abag[j]:w:d,   bbag[j]:w:d);
      chkline(TRUE);
    END;
END;
FUNCTION model (z:REAL):REAL;
VAR p: REAL;
BEGIN
  IF z <= 1.0 THEN
    BEGIN
      IF hgtbcoeff = 1.0 THEN p := 1.0
      ELSE p := 1.0 + (1.0 - z) * (hgtbcoeff - 1.0)
    END
  ELSE IF z < hgtacoeff THEN
    BEGIN
      IF hgtacoeff <= 1.0 THEN p := 0.0
      ELSE p := 1.0 + (1.0 - z) / (hgtacoeff - 1.0)
    END
  ELSE p := 0;

  IF z < 1.0 THEN model := p * z * (widthofbag/2.0)
```

Figure 43. ALEGEE file: LOX-FLAME.TEXT (continued).

```
   ELSE model := p * (widthofbag/2.0);
 END;
PROCEDURE selector;
TYPE item = RECORD key: REAL; index: INTEGER; END;
VAR kselect: ARRAY[1..maxnobags] OF item; i,j,k:INTEGER; x: item;
BEGIN
  FOR j := 1 TO nbags DO kselect[j].key := rgbag[j];
  FOR j := 1 TO nbags DO kselect[j].index := j;
  FOR i := 1 TO nbags - 1 DO
    BEGIN
      k := i; x := kselect[i];
        FOR j := i + 1 TO nbags DO
          IF kselect[j].key < x.key THEN
            BEGIN
              k := j; x := kselect[j];
            END;
          kselect[k] := kselect[i]; kselect[i] := x;
    END;
  FOR j := 1 TO nbags DO kbag[j] := kselect[j].index;
END;
PROCEDURE sortbags;
VAR w2,radius: REAL; j: INTEGER;
BEGIN
  radius := widthofbag / 2.0;
  FOR j := 1 TO nbags DO
    BEGIN
      xj := xbag[j]; yj := ybag[j];
      rg2 := SQR(xdist-xj)+SQR(ydist-yj); rg := SQRT(rg2);
      wl := (xdist - xj) * st + (ydist - yj) * ct;
      w2 := (ydist - yj) * st - (xdist - xj) * ct;
      wlr := wl * ce;
      wlbag[j] := wl; wlrbag[j] := wlr;
      rg2bag[j] := rg2; rgbag[j] := rg;
      abag[j] := radtodeg * asin(radius / rgbag[j]);
      bbag[j] := radtodeg * acos(wl / rgbag[j]);
      IF w2 < 0.0 THEN
        bbag[j] := -bbag[j];
    END;
END;
PROCEDURE modbagstrength (l: INTEGER);
```

Figure 43. ALFGEE file: LOX-FLAME.TEXT (continued).

```
VAR j, k, m, n: INTEGER;
    ratio,  satio,  angle, anglemax, anglemin,
    zint,   ztip,   zsource: REAL;
    dist, xil,yil,xi2,yi2: REAL;
    radius,
    tang_dist: REAL;
    intersect: BOOLEAN;
    sr, rr, deltaabag: REAL;
  PROCEDURE switch (VAR x1,x2: REAL);
  VAR t: REAL;
  BEGIN t := x1; x1 := x2; x2 := t; END;
  FUNCTION determinant (x1,y1,x2,y2,x3,y3: REAL): REAL;
  BEGIN determinant := x1*(y2-y3) + x2*(y3-y1) + x3*(y1-y2) END;
  FUNCTION sameside: BOOLEAN;
  VAR pos1,pos2: BOOLEAN;
  BEGIN
    pos1 :=
     (determinant(xbag[1],ybag[1],xbag[m],ybag[m],xil,yil) > 0.0);
    pos2 :=
     (determinant(xbag[1],ybag[1],xbag[m],ybag[m],xdist,ydist) > 0.0);
    sameside := (pos1 AND pos2);
  END;
  PROCEDURE inmod;
  VAR inter1dist, inter2dist, beta1, beta2: REAL;
    FUNCTION calcbeta (x,y,d: REAL): REAL;
    VAR w1,w2,beta: REAL;
    BEGIN
      w1 := (xdist - x) * st + (ydist - y) * ct;
      w2 := (ydist - y) * st - (xdist - x) * ct;
      beta := radtodeg * acos(w1 / d);
      IF w2 < 0.0 THEN beta := -beta;
      calcbeta := beta;
    END;
  BEGIN
    tang_dist  := SQRT(rg2bag[m]-SQR(sr));
    inter1dist := SQRT(SQR(xdist-xi1)+SQR(ydist-yi1));
    inter2dist := SQRT(SQR(xdist-xi2)+SQR(ydist-yi2));
    beta1 := calcbeta(xi1,yi1,inter1dist);
    beta2 := calcbeta(xi2,yi2,inter2dist);
    IF inter1dist < tang_dist THEN
```

Figure 43. ALFGEE file: LOX-FLAME.TEXT (continued).

```
      anglemin := bbag[m] - betal;
    IF inter2dist < tang_dist THEN
      anglemax := beta2 - bbag[m];
  END;
  PROCEDURE modangles;
  BEGIN
    angle := radtodeg * asin(sr / rgbag[m]);
    anglemax := angle; anglemin := angle;
    IF intersect THEN inmod;
    IF thmin > bbag[m] - anglemin THEN
      IF bbag[m] + anglemax > thmin THEN
        thmin := bbag[m] + anglemax;
    IF thmax < bbag[m] + anglemax THEN
      IF bbag[m] - anglemin < thmax THEN
        thmax := bbag[m] - anglemin;
  END;
BEGIN
  radius := widthofbag / 2.0;
  j := 0;
  REPEAT j := SUCC(j) UNTIL (l = kbag[j]) OR (j = nbags);
  ratio := 1.0; ztip := zbag[l];
  zsource := ABS(zk);
  IF zsource < ztip THEN ratio := 0.0
  ELSE IF zsource < heightofbag + ztip THEN
    ratio := (zsource - ztip)/heightofbag;
  rr := ratio * radius;
  deltaabag := radtodeg * asin(rr / rgbag[l]);
  thmin  := bbag[l] - deltaabag;
  thmax  := bbag[l] + deltaabag;
  thavgi := bbag[l];
  FOR n := 1 TO nbags DO
    BEGIN
      m := kbag[n];
      anglemin := 0.0; anglemax := 0.0;
      IF l <> m THEN
        BEGIN
          satio := 1.0; ztip := zbag[m];
          zint := ABS(zdist + (zk-zdist) * (rgbag[m] / rgbag[l]));
          IF zint < ztip THEN satio := 0.0
          ELSE IF zint < heightofbag + ztip THEN
```

Figure 43. ALFGEE file: LOX-FLAME.TEXT (continued).

```
                satio := (zint - ztip)/heightofbag;
              sr := satio * radius;
              intersect := cintersection(
              xbag[l],ybag[l],rr,xbag[m],ybag[m],sr,dist,xil,yil,xi2,yi2);
              IF (intersect AND (NOT sameside)) THEN
                BEGIN switch(xil,xi2); switch(yil,yi2);END;
              IF n <= j THEN modangles ELSE IF intersect THEN modangles;
            END;
        END;
      thavgf := 0.5 * (thmin + thmax);
      IF (thmax > thmin) AND (ratio > 0.0) THEN
        pbag[l] := sbag[l] * (thmax - thmin) / (deltaabag + deltaabag)
      ELSE pbag[l] := 0.0;
    END;
BEGIN
    IF albedo > 0.0 THEN lmax := 2 ELSE lmax := l;
    tt := (theta + cangle) * degtorad; st := SIN(tt); ct := COS(tt);
    ee := elev * degtorad; se := SIN(ee); ce := COS(ee);
    flu := 0.0; sortbags;selector;
    FOR j := l TO nbags DO
      BEGIN
        xj := xbag[j]; yj := ybag[j]; zj := zbag[j];
        tj := tbag[j];
        rg2 := rg2bag[j]; rg := rgbag[j];
        wl := wlbag[j]; wlr := wlrbag[j];
        mp := (safety * heightofbag) / rg + l;
        m := TRUNC(mp); IF m > mmax THEN m := mmax;
                        IF m < mmin THEN m := mmin;
        dz := heightofbag/m; zip[0] := -0.5 * dz + zj;
        FOR i := l TO m DO zip[i] := zip[i-l] + dz;
        si := bagstrength;
        sip[0] := 0.0;
        FOR i := l TO m DO
          BEGIN
            sip[i] := model( (zip[i] - zj)/heightofbag);
            sip[0] := sip[0] + sip[i];
          END;
        FOR i := l TO m DO sip[i] := si * sip[i]/sip[0];
        FOR i := l TO m DO
          BEGIN
```

Figure 43. ALFGEE file: LOX-FLAME.TEXT (continued).

```
                zk := zip[i];
                FOR l := 1 TO lmax DO
                  BEGIN
                    IF l > 1 THEN zk := -zk;
                    r2 := rg2 + SQR(zdist - zk);
                    r  := SQRT(r2);
                    modbagstrength(j);
                    si := sip[i] * pbag[j];
                    nwlr := wlr;
                    IF thavgi <> thavgf THEN
                      BEGIN
                        te := (thavgf-theta) * degtorad;
                        nwl := rg * (COS(te) * st + SIN(te) * ct);
                        nwlr := nwl * ce;
                      END;
                    ca := (nwlr - (zdist - zk) * se)/r;
                    IF l > 1 THEN ca := ca * albedo;
                    IF ca > 0.0 THEN flu := flu + si * ca / r2;
                  END;
              END;
          END;
        flu := flu * bestguessbag / fourpi;
    END;
BEGIN
  FOR loopcount := 1 TO 5 DO
    BEGIN
      ch := nextloop[loopcount];
      CASE ch OF
          'X':lc[loopcount] := nx;
          'Y':lc[loopcount] := ny;
          'Z':lc[loopcount] := nz;
          'T':lc[loopcount] := nt;
          'E':lc[loopcount] := ne;
       END;
    END;
  nl := lc[1]; n2 := lc[2]; n3 := lc[3]; n4 := lc[4]; n5 := lc[5];
  FOR i1 := 1 TO nl DO
  BEGIN
    FOR i2 := 1 TO n2 DO
    BEGIN
```

Figure 43. ALFGEE file: LOX-FLAME.TEXT (continued).

```
FOR i3 := 1 TO n3 DO
BEGIN
  FOR i4 := 1 TO n4 DO
  BEGIN
    FOR i5 := 1 TO n5 DO
    BEGIN
      FOR loopcount := 1 TO 5 DO
        BEGIN
          CASE loopcount OF
            1:lll := i1;
            2:lll := i2;
            3:lll := i3;
            4:lll := i4;
            5:lll := i5;
           END;
          ch := nextloop[loopcount];
          CASE ch OF
             'X':ix := lll;
             'Y':iy := lll;
             'Z':iz := lll;
             'T':it := lll;
             'E':ie := lll;
           END;
        END;
      elev  := elev0  + (ie - 1) * de;
      theta := theta0 + (it - 1) * dt;
      zdist := zdist0 + (iz - 1) * dz;
      ydist := ydist0 + (iy - 1) * dy;
      xdist := xdist0 + (ix - 1) * dx;
      IF NOT screen THEN
        BEGIN
          GOTOXY(0,9);
          WRITE('ie=',ie:3,' it=',it:3,
                ' iz=',iz:3,' iy=',iy:3,' ix=',ix:3);
          WRITE(CHR(29));
        END;
      calculate;
      WRITELN(pr,xdist:10:1,ydist:12:1,zdist:12:1,
                 theta:12:1,elev:12:1,flu:16:2);
      chkline(TRUE);
```

Figure 43. ALFGEE file: LOX-FLAME.TEXT (continued).

```
                IF escape THEN EXIT(loops);
              END;
            END;
          END;
        END;
      END;
    END;
    FUNCTION asin;
    CONST pid2 = 1.570796327; epsilon = 1.0E-6;
    VAR y: REAL;
    BEGIN
      asin := 0.0; IF ABS(x) > 1.0 THEN EXIT(asin)
      ELSE IF ABS(x) < epsilon THEN asin := 0.0 ELSE
        BEGIN
          y := 1.0 - SQR(x);
          IF y <> 0.0 THEN asin := ATAN(x / SQRT(y))
          ELSE IF x > 0.0 THEN asin := pid2 ELSE asin := -pid2
        END
    END;
BEGIN {$N+} {$R applestuff,transcend,circle_intersection,variables,trs_stuff}
    codeversion := 'BSC(14.3)';
    header := '>Pascal[1.1]   DNA A1-LOX TRS  ';
    prheader := 'Pascal(1.1)  DNA A1-LOX TRS Inverted Cone Flame ';
    prtailer := 'with Obscuration ';
    lastline := 22; printline := 54; remline := 76;
    start;
    REPEAT
      GOTOXY(0,2); WRITE(CHR(11)); crflag := FALSE;
      REPEAT
        readdata;
        screen := (outdev = 'CONSOLE:'); diablo := (outdev = 'PRINTER:');
        decwriter := (outdev = 'REMOUT:');
        prheading;
        IF NOT screen THEN
          BEGIN
            GOTOXY(0,1); WRITE(CHR(11)); GOTOXY(0,7);
            WRITE('ne=',ne:3,' na=',nt:3,' nz=',nz:3,' ny=',ny:3,' nx=',nx:3);
            WRITE(CHR(29));
          END;
        loops;
```

Figure 43. ALFGEE file: LOX-FLAME.TEXT (continued).

```
        IF screen THEN pause ELSE
          BEGIN
            GOTOXY(0,7); WRITE(CHR(29)); GOTOXY(0,9); WRITE(CHR(29));
          END;
      UNTIL crflag
  UNTIL EOF
END.
```


Figure 43. ALFGEE file: LOX-FLAME.TEXT (continued).

DISTRIBUTION LIST

DEPARTMENT OF DEFENSE

Defense Intelligence Agency
ATTN: RTS-2A, Tech Lib
ATTN: RTS-2B

Defense Nuclear Agency
ATTN: NAWE
ATTN: STSP
4 cys ATTN: STTI-CA

Defense Technical Information Center
12 cys ATTN: DD

Field Command, Defense Nuclear Agency
ATTN: FCPR
ATTN: FCT
ATTN: FCTEI
ATTN: FCTT
ATTN: FCTT, W. Summa
ATTN: FCTXE

Under Secy of Defense for Rsch & Engrg
ATTN: Engr Tech, J. Persh

DEPARTMENT OF THE ARMY

BMD Advanced Technology Center
ATTN: ATC-O, F. Hoke
ATTN: BMDATC-D, M. Capps
ATTN: ICRDABH-X

BMD Program Office
ATTN: DACS-BMT
ATTN: DACS-BMZ

BMD Systems Command
ATTN: BMDSC-HW

Harry Diamond Laboratories
ATTN: DELHD-DTSO, 00103
ATTN: DELHD-NW-P
ATTN: DELHD-NW-RA, L. Belliveau, 22100
ATTN: DELHD-TA-L, 81100, Tech Lib

US Army Ballistic Research Lab
ATTN: DRDAR-BLA-S, Tech Lib
ATTN: DRDAR-BLT

US Army Engr Waterways Exper Station
ATTN: Library
ATTN: WESSE

US Army Foreign Science & Tech Ctr
ATTN: DRXST-SD

US Army Material Command
ATTN: DRXAM-TL, Tech Lib

US Army Mobility Equip R&D Command
ATTN: DRDME-WC, Tech Lib

US Army Nuclear & Chemical Agency
ATTN: Library

US Army Tank Automotive R&D Command
ATTN: DRDTA-UL, Tecn Lib

DEPARTMENT OF THE ARMY (Continued)

US Army White Sands Missile Range
ATTN: STEWS-TE-N

USA Missile Command
ATTN: DRSMI

DEPARTMENT OF THE NAVY

David Taylor Naval Ship R & D Center
ATTN: Tech Info Ctr, Code 522.1

Naval Research Laboratory
ATTN: Code 2627, Tech Lib

Naval Surface Weapons Center
ATTN: Code X211, Tech Lib

Naval Surface Weapons Center
ATTN: Tech Library & Info Svcs Br

Naval Weapons Center
ATTN: Code 266, C. Austin
ATTN: Code 3263, J. Bowen
ATTN: Code 343, FKA6A2, Tech Svcs

Naval Weapons Evaluation Facility
ATTN: Code 10, Tech Lib

Space & Naval Warfare Systems Command
ATTN: PME 117-21

Strategic Systems Programs, PM-1
ATTN: NSP-43, Tech Lib

DEPARTMENT OF THE AIR FORCE

Aeronautical Systems Division
ATTN: ASD/ENSSA

Air Force Institute of Technology
ATTN: Library

Air Force Weapons Laboratory
ATTN: NTE

Foreign Technology Division
ATTN: NIIS Library

Strategic Air Command
ATTN: DOCSD
ATTN: DOWE
ATTN: INAO
ATTN: NRI/STINFO

DEPARTMENT OF ENERGY

Department of Energy
Albuquerque Operations Office
ATTN: Technical Library

University of California
Lawrence Livermore National Lab
ATTN: Technical Info Dept Library

Oak Ridge National Laboratory
ATTN: Central Rsch Library

DEPARTMENT OF ENERGY (Continued)

Sandia National Laboratories
ATTN: Div 1531, P. Adams
ATTN: Tech Lib 3141

Los Alamos National Laboratory
ATTN: MS P364, Reports Library

OTHER GOVERNMENT AGENCY

Federal Emergency Management Agency
ATTN: Ofc of Rsch/NP, D. Benson

DEPARTMENT OF DEFENSE CONTRACTORS

California Research & Technology, Inc
ATTN: F. Sauer

Kaman Tempo
ATTN: DASIAC

DEPARTMENT OF DEFENSE CONTRACTORS (Continued)

Kaman Tempo
ATTN: DASIAC
ATTN: J. Shoutens
ATTN: W. Chan

Nichols Research Corp, Inc
ATTN: N. Byrn

Science Applications International Corp
ATTN: Technical Library

Science Applications International Corp
ATTN: W. Chadsey

Science & Engineering Associates, Inc
2 cys ATTN: B. Chambers III

Science Applicaitons International Crop
ATTN: G. Binninger

END

DTIC

7-86